11-2018

Development of Hydroxyapatite-Polymer Sorbents for the Removal of Heavy Metal Ions from Waste Waters

Eleanora Charnetskaya

United Arab Emirates University

College of Science

Department of Chemistry

DEVELOPMENT OF HYDROXYAPATITE-POLYMER SORBENTS FOR THE REMOVAL OF HEAVY METAL IONS FROM WASTE WATERS

Eleanora Charnetskaya

This thesis is submitted in partial fulfillment of the requirements for the degree of Master of Science in Chemistry

Under the Supervision of Prof. Yaser E. Greish

November 2018

Declaration of Original Work

I, Eleanora Charnetskaya, the undersigned, a graduate student at the United Arab Emirates University (UAEU), and the author of this thesis entitled *"Development of Hydroxyapatite-Polymer Sorbents for the Removal of Heavy Metal Ions from Waste Waters"*, hereby, solemnly declare that this thesis is my own original research work that has been done and prepared by me under the supervision of Prof. Yaser E. Greish, in the College of Science at UAEU. This work has not previously been presented or published or formed the basis for the award of any academic degree, diploma or a similar title at this or any other university. Any materials borrowed from other sources (whether published or unpublished) and relied upon or included in my thesis have been properly cited and acknowledged in accordance with appropriate academic conventions. I further declare that there is no potential conflict of interest with respect to the research, data collection, authorship, presentation and/or publication of this thesis.

Student's Signature  Date 15.11.2018

This Master Thesis is accepted by:

Dean of the College of Science: Professor Ahmed Murad

Signature 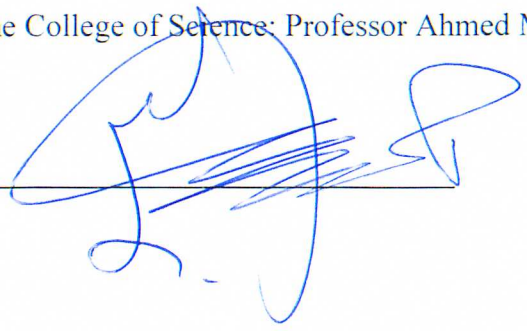 Date 6/12/2018

Acting Dean of the College of Graduate Studies: Professor Ali Al-Marzouqi

Signature 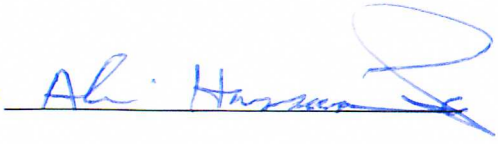 Date 16/12/2018

Copy 7 of 8

Advisory Committee

1) Advisor: Yaser E. Greish

Title: Professor

Department of Chemistry

College of Science

2) Co-advisor: Abdel-Hamid I. Mourad

Title: Professor

Department of Mechanical Engineering

College of Engineering

3) Co-advisor: Eisa A. AlMatroushi

Title: Associate Professor

Department of Chemical and Petroleum Engineering

College of Engineering

Approval of the Master Thesis

This Master Thesis is approved by the following Examining Committee Members:

1) Advisor (Committee Chair): Yaser E. Greish

   Title: Professor

   Department of Chemistry

   College of Science

   Signature _____ Date 15/11/2018

2) Member: Basim Abu-Jdayil

   Title: Professor

   Department of Chemical and Petroleum Engineering

   College of Engineering

   Signature _____ Date 15/11/2018

3) Member (External Examiner): Dr. Kyrikai Polychronopolo

   Title: Associate Professor

   Department of Mechanical Engineering

   Institution: Khalifa University (UAE)

   Signature _____ Date 15/11/2018

This Master Thesis is accepted by:

Dean of the College of Science: Professor Ahmed Murad

Signature _____ Date _____

Acting Dean of the College of Graduate Studies: Professor Ali Al-Marzouqi

Signature _____ Date _____

Copy ____ of ____

Abstract

Water pollution due to the presence of soluble metal ions is one of the greatest challenges to environmental scientists. Different methods have been explored to the removal of these soluble ions. Among these methods, elimination by sorption into/onto solid materials has been considered one of the successful approaches. Sorbent materials usually chemically interact with soluble ions and eliminate them by bond formation between the ions and the sorbent molecules. On the other hand, soluble ions can be also exchanged with inorganic sorbents in which other environmentally friendly ions can exchange with the soluble metal ions. In the current study, the sorption of metal ions through chemical adsorption and ion exchange mechanisms were explored. Apatitic calcium phosphate solid sorbents with various Ca/P molar ratios were synthesized and characterized after being prepared and after thermal treatment at 800^{o}C. Additionally, a stoichiometric HAp with a Ca/P molar ratio of 1.67 was also evaluated in three forms, synthetic, commercial in the μm scale and commercial in the nm scale, as a component in a composite with cellulose acetate fibrous sorbents. In this regard, the proportion of the stoichiometric HAp powders was maintained at 5 and 10% by weight. All sorbents were evaluated for their efficiency to remove Cd^{2+} ions, as a model soluble metallic ion pollutant, from a simulated aqueous media. A batch study was utilized in this regard where the effect of varying the pH of the medium, the weight of the sorbent material, the initial concentration of the sorbate (Cd^{2+}) ions and the contact time between the sorbent and the sorbate solution were thoroughly studied and evaluated. Results showed the high crystallinity of the prepared and purchased calcium phosphate sorbents and the homogeneity of distribution of the stoichiometric apatitic sorbent particulates within the fibrous membrane of CA. An optimization was carried out for the sorption process where an optimum pH of 5.5 was selected in all experiments in the presence of 0.1 g of the sorbent material and 1 mmol of the sorbate ions for a maximum of 3 contact hours. Comparatively, pure calcium phosphate sorbents were found more efficient than CA fibrous sorbents containing a maximum of 10 wt% of the stoichiometric apatite particulates. In addition, the relatively lower affinity of the CA fibrous membrane towards Cd^{2+} ions is based on its chemical structure, where the ester and -OH functional groups of the CA is inferior in its

interaction with Cd^{2+} ions, compared with the exchange mechanism between the Cd^{2+} ion in solution and the Ca^{2+} ions within the apatite structure.

Keywords: Hydroxyapatite, calcium-deficiency, thermal treatment, nanoparticles, heavy metal ions, nanofibers, waste water treatment.

Title and Abstract (in Arabic)

تطوير مواد ماصة من الهيدروكسى أباتيت واللدائن لازالة أيونات المعادن الثقيلة من مياه الصرف الصحى

الملخص

أن تلوث المياه بأيونات معدنيه ذائبه هي واحده من التحديات التي تواجه البحث العلمي. فنتيجه لذوبان هذه الأيونات المعدنيه يجعل من الصعب التعرف عليها، وفي نفس الوقت تشكل خطرا علي الحياه البيئيه.

هناك طرق مختلفه تم أستخدامها لأزاله هذه المعادن، ومن ضمن هذه الطرق هي أزالتها عن طريق أمتصاصها فوق مواد أخري صلبه وهي من الطرق الناجحه. المواد التي أستخدمت في أمتصاصها غالبا تتفاعل مع الأيونات المعدنيه وتتحد معها مكونه روابط كيميائيه، و من الناحيه الأخري، فأن هذه المعادن الذائبه يمكن أن تتحول الي مواد أخري غير مضره للبيئه عن طريق التبادل الأيوني الكيميائي.

و في هذه الدراسه، أمتصاص الأيونات المعدنيه كان من خلال أدمصاص كيميائي و تبادل أيوني. تم أستخدام ماده صلبه من كالسيوم فوسفات اباتايت كماده ماصه بنسب مختلفه من الكالسيوم / الفوسفات تم تخليقها و تصنيفها بعد تحضيرها ومعالجتها حراريا في درجه 800 درجه مئويه، بلأضافه الي تحضيرها في نطاق الميكرو والنانو مع ألياف السيليلوزأسيتات الماصه، وتم أختبار الماده الماصه المحضره لفاعليتها في أزاله أيونات الكادميوم كمثال للمعادن المتأينه الذائبه الملوثه للبيئه، وتم أختبارها في درجات حموضه مختلفه، و أوزان مختلفه للماده الماصه، و أيضا تغيير تركيزالكادميوم و الوقت المستغرق لعمليه الأمتصاص. وكل هذه العوامل تم دراستها و أختبارها.

مفاهيم البحث الرئيسية: هيدروكسياباتيت ، نقص الكالسيوم ، المعالجة الحرارية ، الحبيبات النانويه ، أيونات المعادن الثقيلة ، ألياف النانو ، معالجه المياه الملوثة

Acknowledgments

I express my gratitude to United Arab Emirates University, which provided me with all resources and expanded my scientific horizons.

I would like to thank the chair and all members of the Department of Chemistry at the United Arab Emirates University for assisting me all over my studies and research.

My special gratitude goes to my advisor Prof. Yaser Greish who gave me the opportunity to work in his research laboratory and participate in international conferences to meet and talk with scientists from different parts of the world about their research works and findings and to my co-advisor Prof. Abdel-Hamid I. Mourad from Department of Mechanical Engineering. I would like to express my gratitude to Dr. Eisa Al Matrushi from College of Engineering, my former PI of our research project for the chance to work as a research assistant and MSc student in the project.

Thanks to Prof. Basim Abu-Jdayil and Dr. Kyriaki Polychronopolo for agreeing to be members of Examining Committee.

This thesis would be impossible to complete without kind help and support of my husband and patience of my children along this journey.

Dedication

To my remarkable self

Table of Contents

List of Tables

List of Figures

List of Abbreviations

HAp	Hydroxyapatite
CA	Cellulose acetate
BET	Brunauer-Emmett-Teller
ICP-OES	Inductively Coupled Plasma - Optical Emission Spectrometry

Chapter 1: Introduction

1.1 Overview

Water is the most valuable natural resource existing on our planet. Contamination of water is a common problem faced today because of the toxic effect to the health of human being and other livings. Treatment of all types of waters is a crucial concern to the scientists around the world. Freshwater comprises 3% of the total water on earth but a small percentage (0.01%) of this freshwater is available for direct human use (Hinrichsen, D. Tacio, H., 2002). The importance of availability of good quality drinking water cannot be underestimated. Around 1.1 billion people in the world have very limited access to the safe drinking water; 2.5 billion people have no access to basic sanitation, and more than 5 million people die each year from diseases related to consuming contaminated water (Azizullah, Khattak, Richter, & Häder, 2011).

1.2 Water Pollution

Intensive industrialization in past decades has resulted in pollution of the natural water resources with different types of pollutants (Sajid, Nazal, Ihsanullah, Baig, & Osman, 2018). Water pollutants can be briefly classified into following major categories that include organic pollutants like oil and pesticides, pathogens (bacteria, viruses and protozoa), nutrients and agriculture runoff (nitrates, phosphate), and inorganic pollutants (acids, salts and toxic metals). All these substances, if they exceed a threshold value, are deleterious and cause severe health problems in humans and other organisms in the ecosystem (Azizullah et al., 2011). Examples of these pollutants will be outlined in the following sections.

1.2.1 Organic Pollutants

Oxygen demanding wastes such as domestic and municipal sewage, wastewater from food processing industries, canning industries, paper and pulp mills, tanneries etc. have considerable concentration of biodegradable organic compounds, which undergo degradation and decomposition by aerobic bacteria consuming dissolved in water oxygen (DO), thus causing its level to decrease. It will be a serious issue affecting aquatic life, if DO falls below safe limit. It should be mentioned that the decrease in the DO is used as an index of pollution. In addition to these pollutants, synthetic organic compounds, such as synthetic pesticides, synthetic detergents, food additives, pharmaceuticals, insecticides, paints, synthetic fibers, plastics, solvents and volatile organic compounds (VOCs) are also considered sources of pollution to water media (Sousa, Ribeiro, Barbosa, Pereira, & Silva, 2018).

An additional source of pollution due to organic compounds arises from the spill of oils, especially on the surfaces of oceans and seas. In case of oil spills due to accidents from tankers, or rigs, the result is a tremendous environmental impact to all inhabitants in the spills area. This is related to the fact that oil is lighter than water, thus it spreads over the surface, thus prevents air and sunrays permeation. Accordingly, this results in the reduction of DO. Moreover, oi spills deposit onto the feathers of birds and coastal plants and adversely affect the normal activities. In addition, a number of polycyclic aromatic hydrocarbons (PAH), which are part of oil, are known to be carcinogenic (Figure 1).

Figure 1: Damage caused by oil pollutants

1.2.2 Pathogens and Agricultural Run-offs

Sewage discharge or the wastewater from industries like slaughterhouses are major sources of pathogeni**c** microorganisms in water body. Viruses and bacteria can cause diseases, such as cholera, typhoid, dysentery, polio and infectious hepatitis in human. Nutrients like nitrogen and phosphorous coming from the agriculture run-off, sewage and wastewater from fertilizer industry may stimulate the growth of algae and other aquatic weeds in receiving waters and in long run may reduce DO, which ends up as a dead pool of water. People swimming in contaminated blue-green algae water can have skin and eye irritation, gastroenteritis and vomiting.

1.2.3 Inorganic Pollutants

Inorganic pollutants such as mineral acids, inorganic salts, trace elements, metals, and their complexes with organic compounds, cyanides, sulphates, etc. are non-biodegradable and persist in the environment. The accumulation of heavy metals has a negative effect on aquatic flora and fauna and may cause a health problem where contaminated plants or animals are used for food. Heavy metal ions, with density greater than 5 g/cm^3, and Arsenic have tremendous chemical and ecological effects on all inhabitants. Metallic elements are intrinsic components of the environments. Although, the natural background of metal fractions in the air, soil and plants are highly variable, there are anomalous areas of high levels caused by man-made activities (Table 1).

Table 1: Sources of eight man-made common heavy metals

Source	As	Cd	Cr	Cu	Pb	Hg	Ni	Zn
Mining & ore processing	+	+	-	+	-	+	-	+
Metallurgy	+	+	+	+	+	+	+	+
Chemical industry	+	+	+	+	+	+	-	+
Alloys industry	-	-	-	-	+	-	-	-
Paint industry	-	+	+	-	+	-	-	+
Glass industry	+	-	-	-	+	+	-	-
Pulp and paper industry	-	-	+	+	+	+	+	-
Leather tanning	+	-	+	-	-	+	-	+
Textile dying & printing	+	+	-	+	+	+	+	+
Chemical fertilizer industry	+	+	+	+	+	+	+	+
Chloro-alkali industry	+	+	+	-	+	+	-	+
Petroleum refining	+	+	+	+	+	+	-	+
Coal burning	+	+	+	+	+	+	+	-

Heavy metals largely distributed in the environment through industrial effluents and organic wastes cannot be combusted. Instead, they are usually carried to other places that far away from the sources by wind, depending upon whether they are in gaseous form or as particulates. Moreover, metallic pollutants are ultimately washed out of the air by rain into land or the surface waters. Heavy metals in the aquatic environment occur in soluble, colloidal or suspended states (Table 2). Most metals remain in the soluble form at low pH, especially in aerobic conditions. With increase in pH, first carbonates and then oxides and hydroxides of metals formed, which may settle down as insoluble precipitates. Silicates of metals can also form at certain times and precipitate. Many metals in waters can form organometallic compounds, coordination compounds and salts of organic acids (Agarwal, 2009).

Cadmium, a model heavy metal that has been investigated in the current study, does not exist in nature as native metal but mostly as sulfide ore namely greenokite, which is associated with the zinc sulphide as salphalerite, and is recovered from some copper ores during smelting and refining (Haileslassie & Gebremedhin, 2015). It is widely distributed in the earth's crust at an average concentration of about 0.1 mg/kg (Tchounwou, Yedjou, Patlolla, & Sutton, 2012) but rarely found in natural water. Cadmium is toxic if its concentration exceeds 0.01 mg/L both in drinking and irrigation water (Hem, Lind, & Roberson, 1989). Cadmium intoxication causes high blood pressure, kidney damage, destruction of testicular tissue as well as destruction of red blood cells (Figure 2) (Taha, El-Mahmoudi, & El-Haddad, 2004).

Table 2: Soluble and suspended forms of heavy metals encountered in natural water

State of metal	Chemical form of metal
Soluble	Simple free metal ions (Cu^{2+}, Fe^{3+}, Pb^{2+}). Complex inorganic ions ($CdCl^{+}$). Inorganic ion pairs [$Cu_2(OH)_2^{2+} \cdot Fe_2(OH)_2^{4+} \cdot Pb(CO_3)^{2-}$]. Unionized organometallic chelates. Salts of organic acids.
Colloidal or suspended	Hydroxides ($Fe(OH)_3$, $Cr(OH)_3$), oxides (MnO_2), silicates and carbonates of metals, sulfides (CdS, PbS, HgS, FeS). Sorbed metals on clays, silica or suspended organic matter.

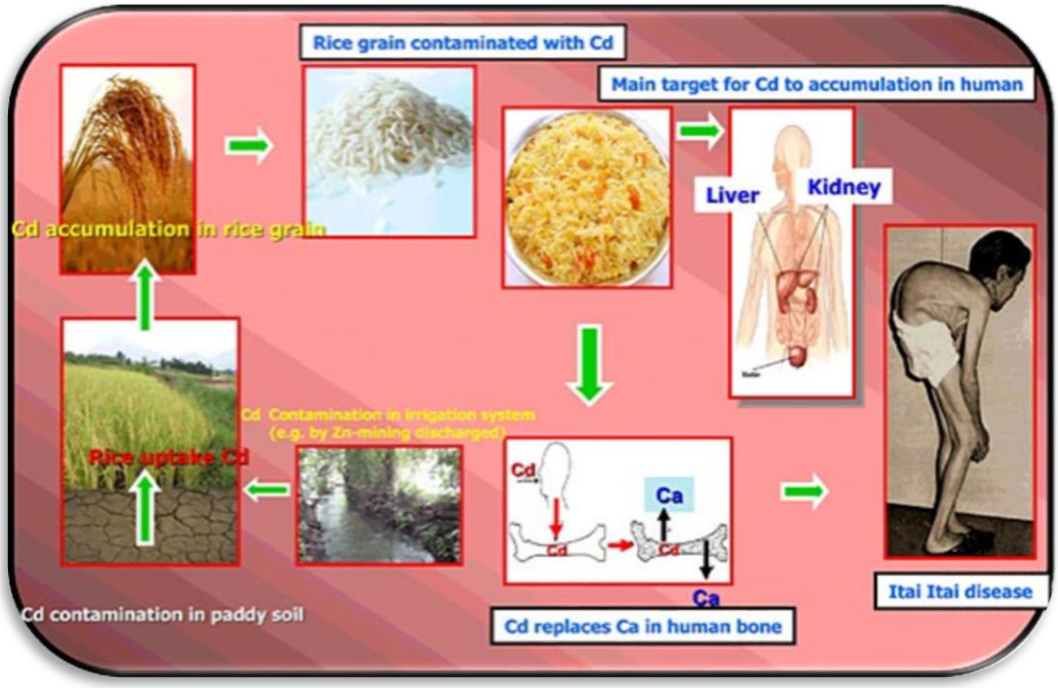

Figure 2: Impact of Cd^{2+} ions on human life

In industry, cadmium is used mainly for electroplating on other metals to prevent their corrosion. It is also used as an additive to paints, printing ink, plastics and electrical batteries. Wastes from these resources eventually make the element available to water that comes in contact with other buried wastes. Cadmium is also present as a pollutant in phosphate fertilizers. Cadmium containing products are rarely recycled, but frequently dumped together with household waste, thereby contaminating the environment, especially if the waste is incinerated (Haileslassie & Gebremedhin, 2015). Also, cadmium pollutant in water may arise from industrial discharges and mining wastes (Taha et al., 2004).

1.3 Water Purification Methods

Toxicity of heavy metals becomes a primary concern in the treatment of industrial wastewater. Different methods have been explored to remove heavy metal ions from waste water. These include chemical precipitation, ion-exchange, membrane filtration, electrochemical treatment technologies, and adsorption (Fu & Wang, 2011). A brief description of each of these methods is given in the following sections.

1.3.1 Chemical Precipitation

Chemical precipitation is widely used for heavy metal removal from inorganic effluents (Kurniawan, Chan, Lo, & Babel, 2006). In this approach, most metals are precipitated as hydroxides. Precipitation in the form of sulfides and carbonates was also used. In some cases, oxidation or reduction of ions to another valence state that allows its direct precipitation is required. Chemical precipitation has the advantage of low capital cost and simple operation. However, its major disadvantages are its

operating costs from the chemical expense and the cost of disposing of the precipitated sludge produced from the process (L. K. Wang, Vaccari, Li, & Shammas, 2005).

1.3.2 Membrane Filtration

Membrane filtration technologies have great promise for heavy metal removal because of their high efficiency, easy operation and space saving. According to the membrane type and the nature of filtration force there are different processes used to remove metals from the wastewater such as ultrafiltration, reverse osmosis, nanofiltration and electrodialysis (Fu & Wang, 2011).

1.3.3 Electrochemical Methods

In the electrochemical treatment of wastewaters, a particular focus was given to electrodeposition, electrocoagulation (EC), electroflotation (EF) and electrooxidation (Fu & Wang, 2011). Generally, electrochemical methods can be described as a deposition of metal ions on a cathode surface and their further recovery in the elemental form of the metal. The main disadvantage of the electrochemical treatment is relatively large capital and operation expenses. Accordingly, electrochemical technologies did not find a wide application worldwide. In addition, increasing standard of drinking water supply and restrictions in environmental regulations for the wastewater discharge brought electrochemical technologies to the new level allowing being compatible with other technologies in terms of cost, efficiency and being more compact (G. Chen, 2004).

1.3.4 Ion-exchange

Ion-exchange processes are widely used to remove heavy metals from wastewater due to a number of advantages, such as high treatment capacity, high removal efficiency and fast kinetics (Kang, Lee, Moon, & Kim, 2004). Synthetic or natural solid resins have specific ability to exchange its cations with the metals in the wastewater. Synthetic resins are commonly preferred in ion-exchange process as they have a high removal capacity for the heavy metals (Alyuz & Veli, 2009).

1.3.5 Adsorption

Adsorption is a promising and effective technique, due to considerably the low cost and abundance of materials used; called adsorbents. This method is flexible in design and operation and in many cases has high sorption capacity. Moreover, some adsorbents can be regenerated which allows a significant cost reduction. Natural adsorbents are available on a large scale. On the other hand, some industrial waste products such as fly ash, coal, and oxides, may have potential as inexpensive sorbents. Accordingly, they can be disposed without expensive regeneration after use (Babel, 2003; Bailey, Olin, Bricka, & Adrian, 1999).

In adsorption, the removal process highly depends on the specific surface area, internal porous structure and surface functional groups along the adsorbent materials (Gong et al., 2015). Therefore, adsorbents with high adsorption capacity, fast adsorption rate and good recyclability are usually made of solid particles at the nanometer scale with designed porous structure to maximize their surface area, hence obtain the highest sorption results (F. Liu, Yu, Ji, & Qian, 2015). Natural organic materials such as chitosan, and cellulose, and inorganic materials such as zeolites,

clays, and apatite have high potential as sorbents. This has attracted environmental researchers to fabricate a large scale of different materials that are based on the structure of these materials. In general, sorbent materials can be classified based on their chemical structure - organic and inorganic, as well as their combination. In the following sections, examples of commonly used sorbents that utilize these mechanisms will be detailed.

1.3.5.1 Organic Sorbents

Chitosan is a natural polysaccharide obtained from fishery wastes such as shrimp, lobster, and crab shells. This makes chitosan a low-cost sorbent material. Consequently, chitosan offers many promising benefits for wastewater treatment applications today (Babel, 2003). The chemical structure of chitosan is shown in Figure 3a. Chitosan has an excellent metal-binding capacity and relatively low cost. It chelates a large number of metal ions due to the free amino groups exposed during de-acetylation (Bailey et al., 1999). In fact, it was noted that crystallinity, affinity for water, percent de-acetylation and amino group content impact adsorption capacity of chitosan (Kurita, Sannan, & Iwakura, 1979). Polysaccharides with about 50% de-acetylation are considered the most effective for adsorption. However, their high solubility in water makes them difficult to be practically used. Accordingly, chitosan with 50 % de-acetylation were cross-linked to hinder them insoluble in water and make them more effective as sorbents (Kurita, Koyama, & Taniguchi, 1986).

Chitin, a polymer composed of N-acetyl-d-glucosamine residues, extracted from crab and shrimp shells, is the second most abundant resource (next to cellulose) in nature. The chemical structure of Chitin is shown in Figure 3b. Chitin can be degraded by chitinase (Ravi Kumar, 2000). Chitosan is the N-deacetylated derivative

of chitin. It is worth noting that both chitin and chitosan are recognized as excellent metal ligands, forming stable complexes with many metal ions (Chui, Mok, Ng, Luong, & Ma, 1996). The formation of a coordination complex between the metal and the chitin nitrogen or oxygen has been reported (Sağ & Aktay, 2000). Usually, the adsorption ability of chitosan is much higher than that of chitin. However, some of metal ions, such as Fe^{3+} and Pb^{2+}, are adsorbed much better on chitin than chitosan (Gyliene, Rekertas, & Salkauskas, 2002). Moreover, chitosan is soluble in dilute acidic solutions while chitin is resistant to the action of acids. Hence, metal ions cannot be removed by acids from chitosan, but it can be easily eluted with acidic solutions from chitin. However, the use of chitin as powder is very difficult for the separation after adsorption (Srinivasan & Viraraghavan, 2014). It is well-known that chitin is insoluble in many solvents, and is very brittle, leading to a limitation in its reactivity and processability for utilization.

Cellulose is another type of natural polysaccharides. Its chemical structure is shown in Figure 3c. Cellulose is a non-toxic, renewable, biodegradable and with readily modifiable properties (Estrella et al., 2015). Unfortunately, it has a low reactivity to heavy metals. Therefore, chemical modification of cellulose is essential to achieve higher sorption capacity (Kamel, Hassan, & El-Sakhawy, 2006). On the other hand, cellulose acetate (CA) is one of the first polymers that have been used as a membrane for the separation in aqueous solutions such as reverse osmosis and ultrafiltration techniques (Kutowy & Sourirajan, 1975). The chemical structure of CA is shown in Figure 3d. Cellulose acetate fibers have comparatively high modulus, adequate flexural and tensile strength (Aoki, Teramoto, & Nishio, 2007). Grafted with

functional groups such as –COOH, $–SO_3H$ and $–NH_2$ groups, CA can bind with heavy metal ions through surface complexation mechanisms (C. Liu & Bai, 2006).

Recently a novel solvent (aqueous 6 wt% NaOH/5 wt% thiourea) was used to dissolve cellulose and chitin to obtain a homogeneous solution that was eventually made into a blended membrane (L. Zhang, Ruan, & Gao, 2002, Zhou, Zhang, Zhou, & Guo, 2004). The adsorption mechanisms of heavy metals by cellulose/chitin membranes mainly involve complexation between heavy metal ions and chitin at low pH range as well as hydrolysis adsorption and surface micro-precipitation at high pH range. In addition, the network structure and hydrophilic skeleton of the cellulose/chitin membranes promoted adsorption (Zhou, Zhang, Zhou, & Guo, 2004).

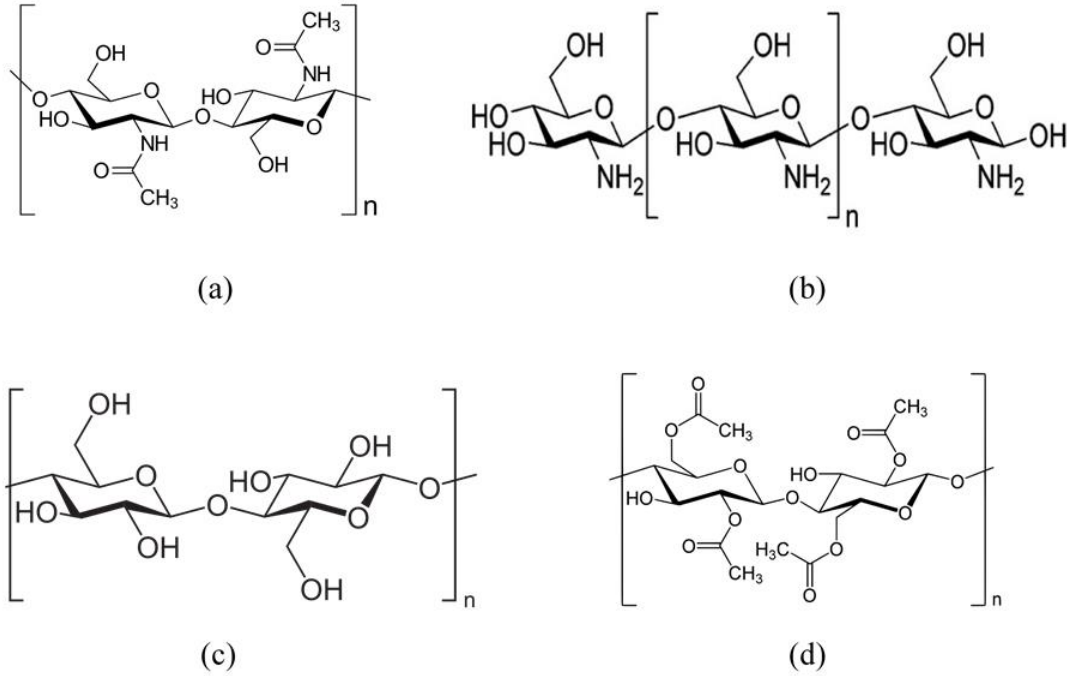

Figure 3: Chemical structure of (a) chitin (b) chitosan (c) cellulose and (d) cellulose acetate

Bacterial cellulose (BC) has potential to be used as a new adsorbent for effective separation of heavy metal ions (Lu, Li, Guan, & Wei, 2010; Rezaee et al., 2008; Shen et al., 2009). It has unique properties including high water holding capacity, fine fiber network with high specific surface, no secondary pollution and numerous hydroxyl groups in the chains as well as high tensile strength. However, BC is not suitable for heavy metal ions adsorption because of lower adsorption capacity and poorer selectivity. Therefore, the modification by new functional groups (S. Chen et al., 2009; Lu, Guan, & Wei, 2011; Wan et al., 2007), such as amino groups (Lu, Zhang, Guan, Xu, & Gao, 2014), that will improve the adsorption activity of BC has become one of hot topics. The absorption of metal ions on amino-BC is controlled by both film diffusion and particle diffusion, and could be further accelerated with the increase of reaction temperature (Lu et al., 2014).

The use of activated carbon and ion exchange resins is not suitable for developing countries due to their high capital and operational costs (Cao et al, 2010). This has encouraged researchers into discovering materials that are both efficient and cheap (Abdel-Halim, Abou-Okeil, & Hashem, 2007; Abdel-Halim & Al-Deyab, 2011; Hashem, Abdel-Halim, Maauof, Ramadan, & Abo-Okeil, 2007; Hashem, Abdel-Halim, & Sokker, 2007; Hashem, Sokker, Halim, & Gamal, 2005; Sokkar, Abdel-Halim, Aly, & Hashem, 2004). Modified cellulosic wastes are among them. Conversion of cellulosic wastes to valuable industrial product was achieved by one-step bleaching and grafting methacrylic acid onto cellulosic wastes using sodium chlorite/potassium permanganate redox system. This economical one-step treatment has converted low-value cellulosic fabric processing wastes to valuable industrial product.

The obtained polymethacrylic acid/cellulose graft copolymer (PMAAC) was used as an adsorbent for different divalent cations, such as Cu^{2+}, Co^{2+}, and Ni^{2+} (Abdel-Halim & Al-Deyab, 2012).

A more recent novel material has been synthesized for the adsorption of Cu^{2+}, Cd^{2+}, Hg^{2+}, Pb^{2+} and Zn^{2+} metal ions from aqueous solution. This novel chelating fibrous sorbent is a guanyl-modified cellulose (Gu-MC) (Kenawy, Hafez, Ismail, & Hashem, 2018).

1.3.5.2 Inorganic Sorbents

Zeolites are natural aluminosilicates with tetrahedral nanocrystals, linked with each other by shared oxygen atoms. Figure 4a shows a typical zeolite crystal structure. Natural zeolites have significant ion-exchange capability, which makes them favorable for wastewater treatment (Babel, 2003). Zeolites consist of a wide variety of species such as clinoptilolite and chabazite. (Mier, Callejas, Gehr, Cisneros, & Alvarez, 2001). Clinoptilolite was shown to have high selectivity heavy metal ions such as Pb^{2+}, Cd^{2+}, Zn^{2+}, and Cu^{2+}. It was found that clinoptilolite seems to be more selective for Pb^{2+}, but Cd^{2+} is also exchanged at satisfactory level. Effect of temperature also plays important role on the adsorption process: metals uptake is favored at higher temperature (Malliou, Loizidou, & Spyrellis, 1994) since a higher temperature activates the metal ions for enhancing adsorption at the coordination site of zeolites. Moreover, pretreatment of zeolites affects the cation exchange capacity (CEC) and selectivity for metal ions (Kesraoui-Ouki, Cheeseman, & Perry, 1993)(Ćurković, Cerjan-Stefanović, & Filipan, 1997; Inglezakis, Papadeas, Loizidou, & Grigoropoulou, 2001; Semmens & Martin, 1988).

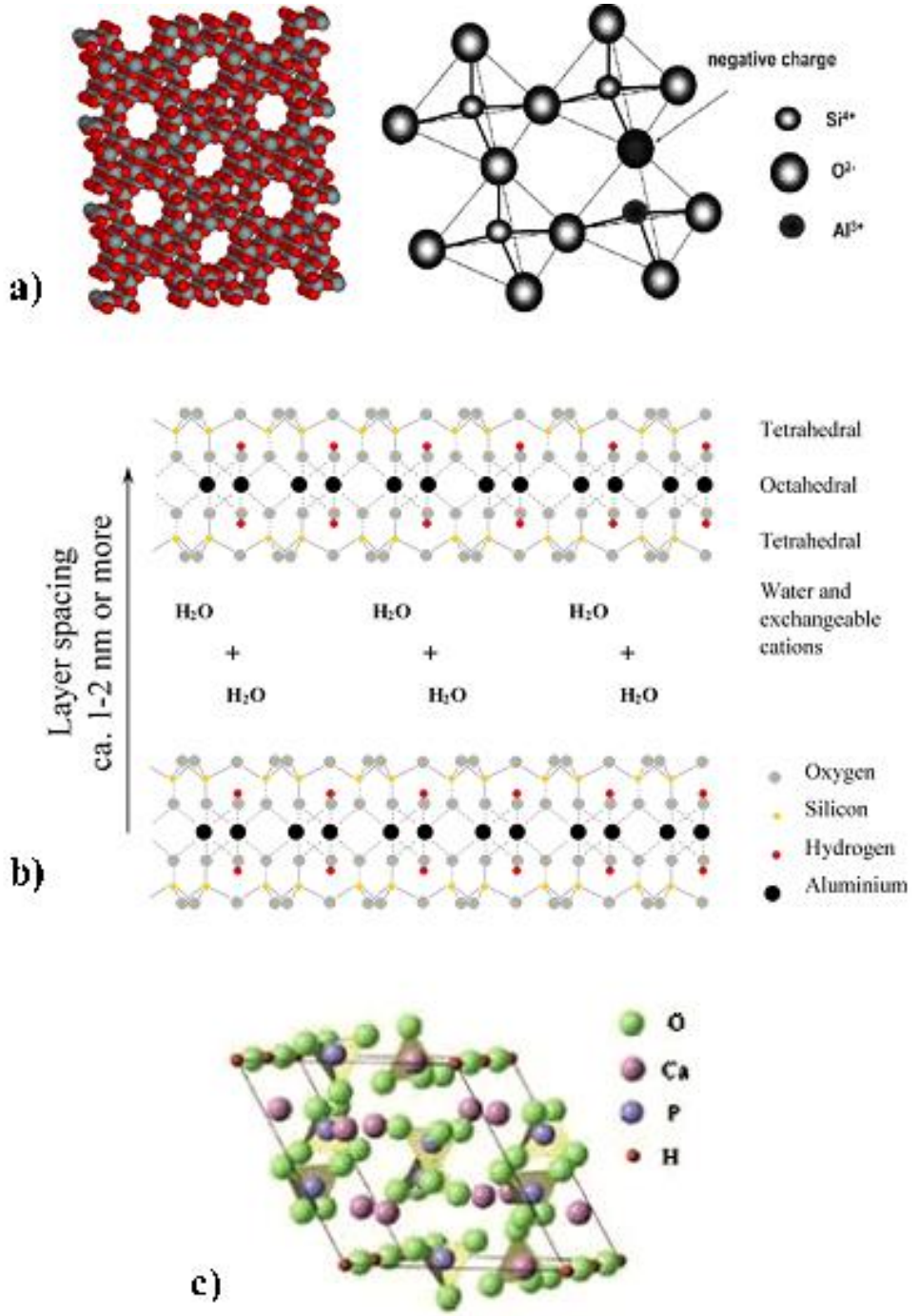

Figure 4: Typical crystal structures of (a) zeolite (b) montmorillonite clay (c) apatite minerals

For example, treatment of zeolites with NaOH solution can improve removal efficiency both the chabazite and clinoptilolite (Babel, 2003; Mier et al., 2001).

Similar to zeolite, clay materials have been also explored as sorbents for heavy metal ions. The adsorption properties of clay come from a net negative charge on the structure of fine-grain silicate minerals, which are neutralized by the adsorption of positively charged species, giving clay the ability to attract and hold heavy metals cations (Candena, Rizvi, & Peters, 1990). Three main groups of clays can be specified: kaolinite, micas (such as illite), and smectites (for example montmorillonite). Among those clays, montmorillonite has the smallest crystals, the largest surface area and the highest sorption capacity towards Pb^{2+} and Cd^{2+} ions (Bailey et al., 1999; Srivastava, Tyagi, Pant, & Pal, 1989). Figure 4b shows a typical crystal structure of montmorillonite clay material. The presence of cationic surfactant can reduce the uptake of both ions, while the anionic surfactants enhance the removal process. Thus, montmorillonite, which is naturally abundant, is becoming a good candidate as an adsorbent for the removal of heavy metals from wastewaters (Viraraghavan & Kapoor, 1994). However, and unlike zeolites, when clays used for industrial application, the swelling factor may cause a remarkable pressure dropping due to the structure and ion exchange mechanism. Nevertheless, availability and low cost of clays compensates their drawbacks compare with zeolites (Babel, 2003).

Hydroxyapatite (HAp) is an inorganic compound with nominal composition $Ca_{10}(PO_4)_6(OH)_2$; its crystal structure is shown in Figure 4c, has gained its prominence due to its analogical composition of human bone mineral. As such, HAp has been widely used as a bone substitute and ceramic implants. In addition, HAp can be extensively used as catalyst or catalyst support, biosensor and in wastewater treatment.

Moreover, HAp has also been recognized for its potential in trapping and retaining of toxic heavy metals in ground waters and soils. Various mechanisms have been explored in this regard. Among those, ion exchange between M^{2+} (representing a divalent heavy metal cation) and Ca^{2+} at the HAp lattice is thought to be the most acceptable mechanism. HAp is believed to have a hexagonal unit cell with a highly flexible composition. A detailed crystal structure of HAp is shown in Figure 5. HAp has a compact assemblage of PO_4^{3-} and Ca^{2+} ions distributed within the lattice, defining two types of zeolite-like channels. The first type of channel has a diameter of about 2.5 Å and contain Ca^{2+} ions (called Ca^{2+} (I)) surrounded by nine oxygen atoms. The second type of channels (3.5 Å in diameter) hosts the hydroxyl (OH^-) groups and pseudo-octahedral Ca^{2+} (called Ca^{2+} (II)) ions. The later type of calcium ions plays an important role in the acid-base and electrical properties of HAp. An additional advantage that explains the effective immobilizing efficiency of HAp to heavy metal ions is its moderate solubility (Hodson, Valsami-Jones, & Cotter-Howells, 2000).

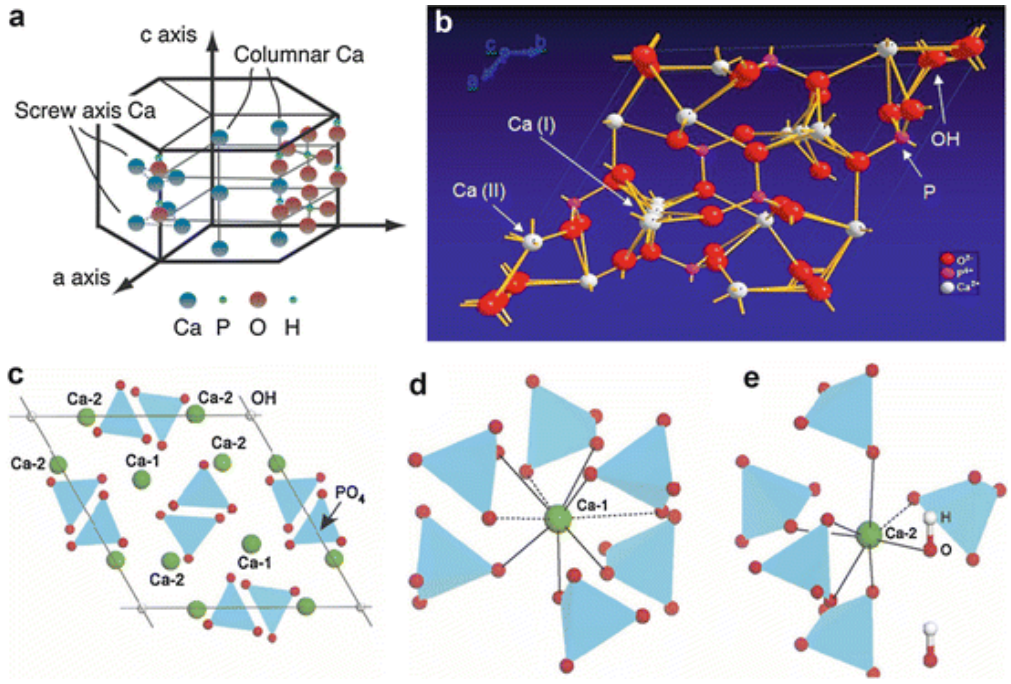

Figure 5: Hydroxyapatite crystal structure: (a) columnar Ca site (Ca(I)) and the screw axis Ca (Ca(II)) (b) calcium triangle and tunnel (c) hydroxyapatite lattice viewed along the c-axis (d) and (e) coordination and local atomic structures around Ca(I) and Ca(II) in perfect hydroxyapatite

Various research data show that divalent metal sorption capacities on HAp and the sorption mechanisms strongly depend on: type of divalent metal, HAp physical and chemical properties and other factors, such as metal concentration, solution pH, contact time, and the presence of other ionic species (Ma, 1996; Monteil-Rivera & Fedoroff, 2002). As an example, Cd^{2+} sorption capacity was found to be the highest in solutions with initial pH range from 5 to 7, which was related to the amphoteric nature of the HAp surface (Smičiklas, Milonjić, Pfendt, & Raičević, 2000). Additionally, surface complexation and diffusion into the structure of nano-hydroxyapatite (nHAp) are main mechanisms for Cd^{2+} sorption on nHAp. It showed higher immobilizing capacity of Cd^{2+} than normal HAp material due to its high surface area (Z. Zhang et al., 2010).

In addition to HAp, a list of other calcium phosphates were found to exist naturally and can be synthesized as well. Table 3 shows the different types of calcium phosphates over a variable range of Ca/P ratios. It should be noted that basic calcium phosphates have Ca/P ratios ≥ 1.5, while acidic types have lower Ca/P ratios. Apatitic crystal structure can be extended over the range of 1.5 to 1.67 where the overall crystal structure is maintained as apatite, with the decrease in the Ca/P molar ratio taking place in the form of deficiency in the Ca^{2+} proportion in the crystal lattice. The chemical composition of HAp can be modified from the stoichiometric form $Ca_{10}(PO_4)_6(OH)_2$ to the Ca-deficient form $Ca_{10-x}(HPO_4)_x(PO_4)_{6-x}(OH)_{2-x}$ by selecting appropriate Ca/P molar ratios during their preparation. Ca-deficient HAp has vacant Ca^{2+} sites within its crystal structure and can potentially exhibit a higher sorption ratio for heavy metals than stoichiometric hydroxyapatite. In a recent study, it was found that Sr^{2+} ions preferentially adsorbed into specific sites within the crystal lattice of a Ca-deficient hydroxyapatite sorbent material (Sekine et al., 2017).

Table 3: Types of calcium phosphate with their formulae and Ca/P molar ratios

Name	Formula	Ca/P ratio
Monocalcium Phosphate Monohydrate (MCPM)	$Ca(H_2PO_4)_2.H_2O$	0.5
Monocalcium Phosphate (MCP)	$Ca(H_2PO_4)_2$	0.5
Dicalcium Phosphate Dihydrate (DCPD)	$CaHPO_4.2H_2O$	1.0
Dicalcium Phosphate (Anhydrous) (DCPA)	$CaHPO_4$	1.0
Octacalcium Phosphate (OCP)	$Ca_8H_2(PO_4)_6.5H_2O$	1.33
Tricalcium Phosphate (TCP)	α,β-$Ca_3(PO_4)_2$	1.5
Amorphous Calcium Phosphate (ACP)	~ $Ca_9(PO_4)_6.3H_2O$	1.5
Hydroxyapatite (HAp)	$Ca_{10}(PO_4)_6(OH)_2$	1.67
Tetracalcium Phosphate (TetCP)	$Ca_4(PO_4)_2O$	2.00

1.3.5.3 Organic-Inorganic Composite Sorbents

Hybrid sorbent materials made of organic and inorganic constituents were also considered for the removal of soluble heavy metal ions in waste water. This combination provides collective properties of the constituents, in what is also known as composite structures. An example is shown in the combination of zeolite with a polymeric material, such as cellulose acetate. In this regard, zeolite particles were dispersed and embedded in the cellulose acetate polymeric matrix, because it could be easily molded into different forms, such as membranes, fibers and spheres. Moreover, the hydrophilic surfaces of the produced composite membranes were shown to improve the accessibility of aqueous solutions to the surface of these hybrid materials (Z. Chen et al., 2004; C. Liu & Bai, 2006; Zhou et al., 2004). The possible use of the zeolite/CA composite fiber as an easily separated, reusable adsorbent for the removal of Cu^{2+} and Ni^{2+} ions from aqueous solution was investigated. The sponge-like structure of the as-prepared fiber allowed rapid free passage and diffusion of heavy metal ions into the internal pores for contact with the adsorptive sites on the zeolite (Ji et al., 2012).

An additional example is shown in the deposition of HAp onto the surfaces of a CA membrane to make use of the combined advantages of both materials as sorbents for heavy metal ions. The removal of Pb^{2+} ions from aqueous solution suggests that porous HAp/CA composite membranes have the potential to immobilize Pb^{2+} ions in Pb^{2+}-contaminated wastes (Ciobanu, Carja, Ignat, Luca, & Harja, 2010).

1.4 Physical Nature of Sorbents

There are several types of adsorbents in regard to their physical state. Powders and fibers are among them. One of the main requirements of these sorbents is the size, where the most widely used adsorbents have micrometer and nanometer size in the form of particles or fibers. Therefore, nanomaterials are believed to have enhanced sorption performance compared with regular materials due to their higher surface area. A number of chemical methods have been used for the preparation of nanoparticles, such as wet (P. Wang et al., 2010), sol-gel (Yusoff, Salimi, & Anuar, 2015), hydrothermal (Nagata, Yamauchi, Tomita, & Kato, 2013), and microwave (Cai, Peng, Zi, Chen, & Qian, 2015) methods. The main advantages of chemical methods include the mass production and the ability to control the structure and size distribution of the prepared nanoparticles by optimizing the experimental conditions.

On the other hand, fibrous sorbents have been prepared by a number of methods (Huie, 2003; Luong-Van et al., 2006; Perez, 2000; Pike, 1999; Reneker, Chun, & Ertley, 2003; Tseng, Notargiacomo, & Chen, 2005). Among these methods, electrospinning is considered a robust technique that provides the capability to fabricate fibers, woven and non-woven, with controlled size and size distribution within the micrometer-nanometer scale. Electrospinning has been widely used in manufacture of polymer and ceramic nanofiber (Li & Xia, 2004; Sigmund et al., 2006). Electrospinning **(**Figure 6**)** is a process where static electrical charges applied on the molecules of a solution have such density that it overcomes the surface tension and liquid stretching into a fiber in an electric field (Warner & Buer, 2001). Through the control of the solution characteristics, such as concentration, viscosity and conductivity, as well as process parameters, such as the feeding rate, the spinning

distance and the applied voltage, a non-woven fibrous product can be fabricated with a homogeneous fiber size distribution. During the electrospinning process. a high voltage is applied to the solution, causing an ohmic current to distribute the charges throughout the molecules and solution ejects from the spinneret tip where cone, called Taylor's cone, forms and fibers deposit on the grounded collector (Teo, Inai, & Ramakrishna, 2011).

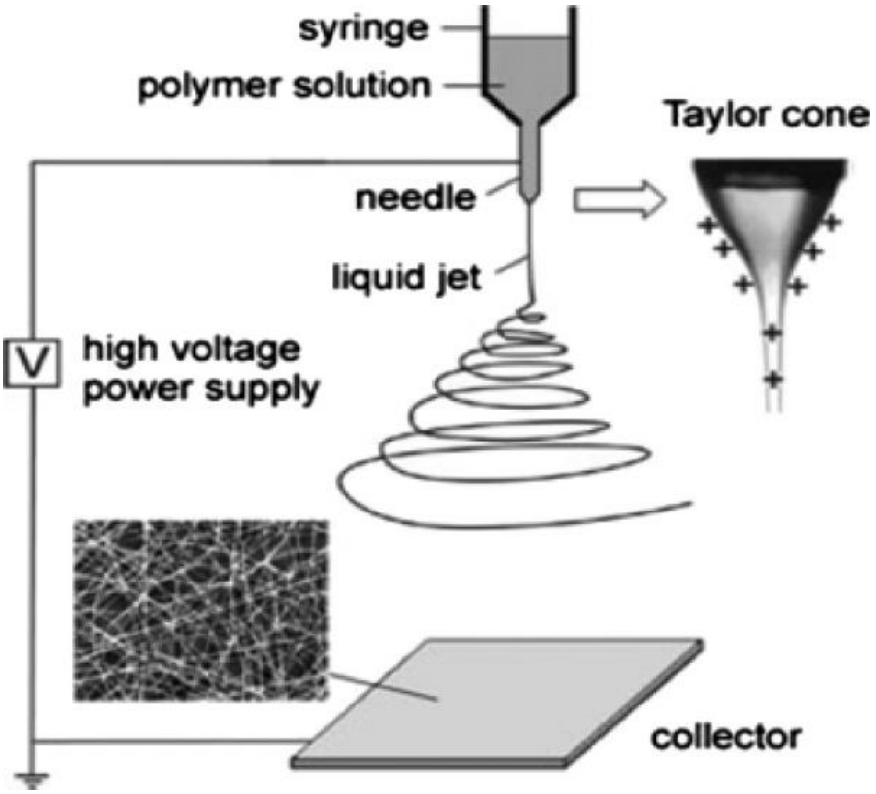

Figure 6: Schematic illustration of the electrospinning process

The charges are transported from the electrospinning tip to the collector through the deposition of the fiber (Deitzel, Kleinmeyer, Harris, & Beck Tan, 2001). After the deposition stabilizes, the current stops fluctuating and it can be used to monitor the electrospinning process (Samatham & Kim, 2006). The electrical charges used for electrospinning can be positive, negative or both (alternating current) (Kessick, Fenn, & Tepper, 2004; Sarkar, Deevi, & Tepper, 2007; Yeo, Gagnon, & Chang, 2005). Majority of electrospinning done using a positive potential. Although, according to some research, a negative potential produces nanofibers with a narrower diameter distribution because electrons can be dispersed more rapidly and uniformly than protons due to heavier proton's weight (Kalayci, Patra, Kim, Ugbolue, & Warner, 2005). It should be noted that a careful and thorough optimization of the electrospinning process is always required to avoid the formation of other impure fiber morphologies, such as those shown in Figure 7 A-D. On the other hand, typical woven and non-woven fibrous membrane e made by electrospinning are shown in Figure 7 E-F.

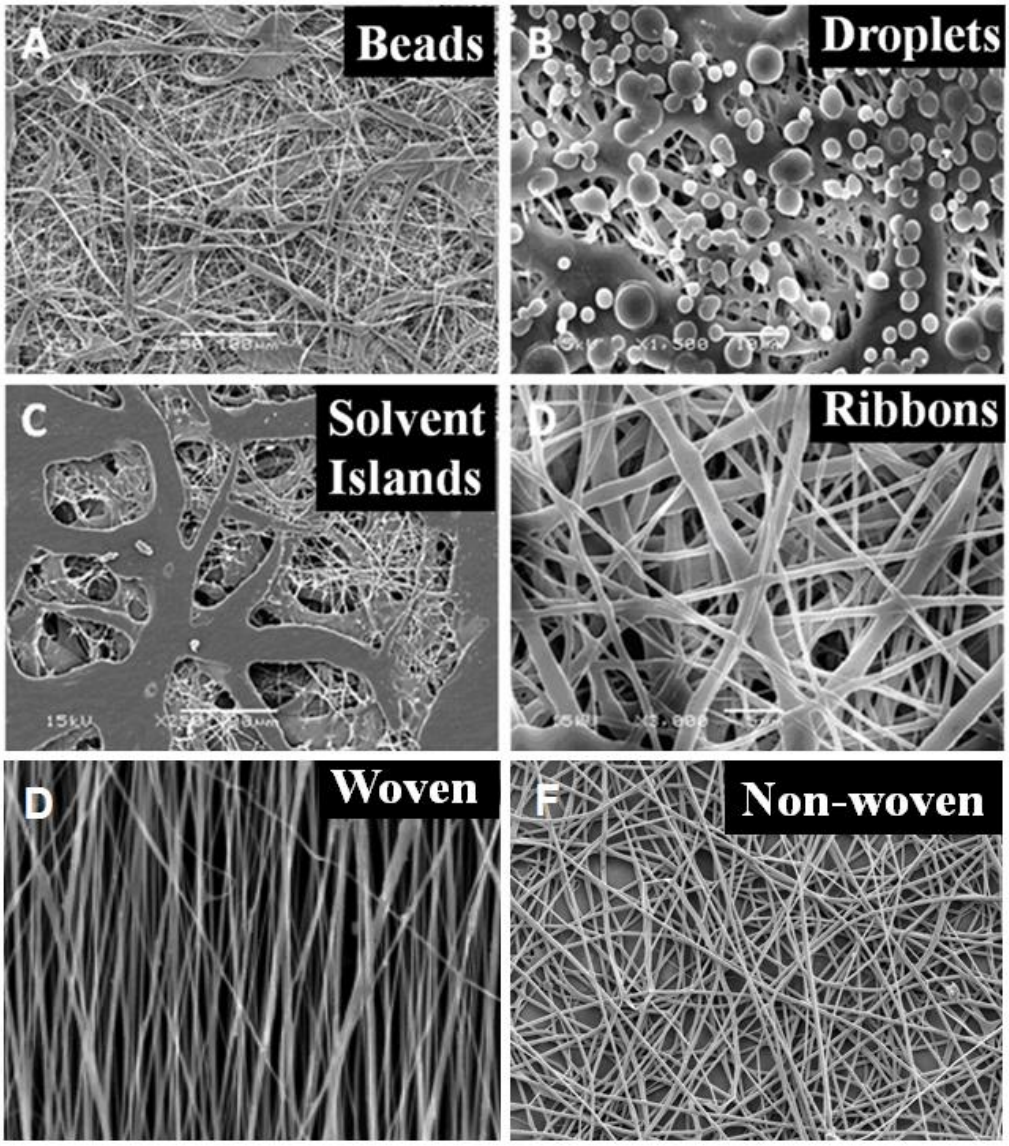

Figure 7: Electrospun typical nano-fibers (A) beaded (B) droplets (C) solvent islands (D) ribbons (E) pure woven (F) pure non-woven

In the current study, the removal of Cd^{2+} ions from simulated polluted aqueous medium using calcium phosphate nanoparticles, cellulose acetate nanofibers and their combinations was thoroughly investigated. The study is divided into two parts. In part 1, the structural composition and morphology of four types of calcium phosphate nanoparticles with variable Ca/P molar ratios, as well as their evaluation for the efficiency of removing Cd^{2+} ions, are outlined. In part 2, composite nanofibrous membranes made of cellulose acetate and selected types of calcium phosphate sorbent systems were also investigated for their structure, morphology and efficiency in collecting Cd^{2+} ions from simulated polluted aqueous media.

Thus, the aims of the current study are:

- To prepare and characterize stoichiometric and non-stoichiometric nano-hydroxyapatite sorbents.
- To fabricate and characterize membrane materials based on cellulose acetate nanofibers reinforced by hydroxyapatite particles
- To evaluate the prepared pure and composite sorbent materials for the removal of Cd^{2+} ions from simulated aqueous media.

Chapter 2: Materials and Methods

2.1 Materials

For the preparation of calcium deficient hydroxyapatite powders, ammonium dihydrogen phosphate, calcium chloride, ammonia solution from Sigma-Aldrich, USA were used.

Acetone and N, N – Dimethylacetamide (Sigma-Aldrich, USA) were used as a binary solvent to prepare cellulose acetate solution using cellulose acetate powder from Sigma-Aldrich, USA. Tricalcium phosphate powder and hydroxyapatite nano-powder, from Sigma-Aldrich, USA were used for the preparation of combined cellulose acetate-hydroxyapatite nanofibers.

Cadmium chloride (Sigma-Aldrich, USA) was used as a source of Cd^{2+} ions to prepare simulated polluted aqueous media. Sodium hydroxide and nitric acid from Sigma-Aldrich, USA were used in preparation of solutions for the adjustment of pH of simulated Cd^{2+} solutions.

Cadmium standard, diluted in nitric acid from AccuStandard, INC, USA was used for the ICP-OES to evaluate Cd^{2+} concentration in effluents after sorption experiments.

Potassium bromide from Sigma-Aldrich, USA was used to prepare pellets for the FTIR.

2.2 Methods

2.2.1 Preparation of HAp Powders

Stoichiometric HAp and Ca deficient HAp were prepared by wet precipitation method. Solution of 0.299 M $NH_4H_2PO_4$ (to prepare stoichiometric HAp) was added drop wise to 0.5 M solution of $CaCl_2$ while vigorously stirring. For the preparation of Ca deficient HAp with CA/P ratios 1.5, 1.55, 1.6 solutions of 0.333 M, 0.323 M and 0.313 M $NH_4H_2PO_4$ were used. Temperature of the solutions was maintained at 70°C. At the end of adding $NH_4H_2PO_4$, pH of the solution was adjusted to reach 10-11 and left stirring for 30 min. Obtained precipitates were left to sediment, then decanted, and washed with deionized water. All products were left to dry in the oven at 90°C for 24 hours. After drying all powders were grinded and divided for one part to undergo thermal treatment in the furnace at 800°C for 2 hours.

2.2.2 Preparation of CA-HAp Fibers

Cellulose acetate fibers doped by HAp powder were prepared by electrospinning method. Electrospinning solutions of 12 w/v% of cellulose acetate were prepared using dual solvent containing 1 part of dimethylacetamide and 2 parts of acetone while stirring for 24 h at the room temperature. 5 and 10 wt% to CA of HAp powders were added to the CA solution. In total, 13 solution were prepared: pure 12% CA solution; 12% CA and 5, 10% synthetic stoichiometric HAp; 12% CA and 5, 10 % commercial HAp; 12% CA and 5, 10% nano-HAp; 12% CA and 5, 10% synthetic stoichiometric heat-treated HAp; 12% CA and 5, 10% commercial heat-treated HAp; 12% CA and 5, 10% heat-treated nano-HAp. Heat treatment of all HAp powders was done as described in 2.2.1.

2.2.3 Characterization of Sorbents

Synthesized, as-received and heat-treated materials were characterized by X-ray diffraction (XRD), infrared spectroscopy (IR), thermogravimetric analysis (TGA), N_2-dasorption technique, and scanning electron microscopy (SEM).

XRD analysis was carried out using PW1840 diffractometer with a Cu K_α line at 1.5404 Å, an operating voltage of 40 kV and a 30 mA current generator. All powder samples were analyzed over a 2 theta (2θ) range 10-70°. IR analysis was performed using a Nexus 470 FTIR spectrometer, Thermo-Nicolet, USA with KBr pellet over a wave number range of 400-4000 cm^{-1}. TGA was performed using a TGA-50 Shimadzu, Thermogravimetric Analyzer. A sample 5±1 mg was placed in an aluminum pan, heated in air up to the 600°C at the heating rate of 10°C/min. BET surface area of the prepared sorbents was measured by TriStar II Plus surface area and porosity analyzer Micrometrix, USA using nitrogen gas adsorption at 77 K. SEM analysis was performed using a JEOL microscope at an operating voltage of 15 kV. Fibrous samples were pre-coated with gold for 30 sec and powder samples were pre-coaled for 1 min.

2.2.4 Sorption Experiments

2.2.4.1 Effect of Solution pH

A 0.001M of Cd^{2+} solution was prepared. A 0.1 g of calcium deficient HAp powders (as-prepared and heat treated) and 0.01 g of CA and CA-HAp composite sorbents were put in test tubes and then simulated Cd^{2+} solution of different pH values were added. Solutions of 0.1M of HNO_3 and KOH were used to adjust pH of Cd^{2+} solution to the values 3, 4, 5, 6, 7, 8. Experiment was performed using magnet shaker

at 160 rpm with stabilized temperature 25°C for 24 hours. After 24 hours all solutions were filtered for the following analysis by ICP-OES and precipitates were dried.

2.2.4.2 Effect of the Sorbent Weight

A 0.001M of Cd^{2+} solution was prepared as in pH experiment. The following weights – 0.05, 0.1, 0.15, 0.2, 0.25, 0.3, 0.35, 0.4 g of calcium deficient HAp powders (as-prepared and heat treated) and 0.002, 0.005, 0.01, 0.015, 0.02 g of CA and CA-HAp composite sorbents were put in test tubes and then simulated Cd^{2+} solution was added. The pH value determined was adjusted by solutions of 0.1M of HNO_3 and KOH to the value of 5.5. Experiment was performed using magnet shaker at 160 rpm with stabilized temperature 25°C for 24 hours. At the end of the experiment all solutions were filtered for the following analysis by ICP-OES and precipitates were dried.

2.2.4.3 Effect of Initial Metal Concentration

The following concentrations of Cd^{2+} solution (0.01M, 0.001M, 0.0001M) were prepared. A 0.1 g of calcium deficient HAp powders (as-prepared and heat treated) and 0.01 g of CA and CA-HAp composite sorbents were put in test tubes and then simulated Cd^{2+} solutions of different initial concentrations were added. The pH value was adjusted by solutions of 0.1M of HNO_3 and KOH to the value of 5.5. Experiment was performed using magnet shaker at 160 rpm with stabilized temperature 25°C for 24 hours. At the end of each time length all solutions were filtered for the following analysis by ICP-OES and precipitates were dried.

2.2.4.4 Effect of Sorption Time

A 0.001M of Cd^{2+} solution was prepared as in pH experiment. A 0.1 g of calcium deficient HAp powders (as-prepared and heat treated) and 0.01 g of CA and CA-HAp composite sorbents were put in test tubes and then simulated Cd^{2+} solution was added. The pH value determined by experiment I adjusted by solutions of 0.1M of HNO_3 and KOH to the value of 5.5. Experiment was performed using magnet shaker at 160 rpm with stabilized temperature 25°C for 4, 6, 8, 10, 12, 14, 16, 18, 20 hours. At the end of each time length all solutions were filtered for the following analysis by ICP-OES (using Agilent 720-ES optical emission spectrometer by Agilent Technologies, USA) and precipitates were dried.

Chapter 3: Results and Discussion

Starting materials used in the first part of this study was based on calcium phosphate powders with variable Ca/P molar ratios. These were prepared by a typical wet method procedure using Ca^{2+} and PO_4^{3-} sources at initial Ca/P ratios of 1.5, 1.55, 1.6 and 1.67 while maintaining the pH of the medium in the basic range (pH above 7.00) to ensure the formation of basic types of calcium phosphates as planned prior to their formation. The formed calcium phosphate powders were characterized for their composition using x-ray diffraction, infrared spectroscopy, and thermogravimetric analysis to confirm their phase purity and to assess their crystallinity. In addition, particles of both commercial materials were assessed for their size and morphology using scanning electron microscopy, while their surface characteristics, such as surface area was evaluated using N_2-adsoprtion technique. Moreover, the effect of heat treatment of the prepared calcium phosphates at 800°C on their composition, morphology and powder characteristics was also studied. The main objective of these powders is to use them as sorbents for Cd^{2+} ions in waste water media. Therefore, their structural composition, morphology and surface characteristics were assessed to be correlated with their reactivity towards Cd^{2+} ions in solution. In the following sections, details about these measurements will be discussed.

3.1 Structure and Evaluation of HAp Nanoparticulate Sorbents

3.1.1 Characterization of As-prepared and Thermally-treated Calcium Phosphates

3.1.1.1 X-Ray Diffraction (XRD)

Figure 8 shows the XRD patterns of the as-prepared calcium phosphate powders as a function of their Ca/P molar ratios. All patterns show highly crystalline powders. Patterns included peaks with variable intensities at 2θ values of 22.96, 25.97, 28.24, 29.02, 31.92, 32.29, 33.05, 34.20, 39.95, 46.83 and 49.57°. These peaks are all attributed to the presence of apatitic calcium phosphate when compared with its standard JCPDS cards 9-432 and 72-1243 (NIST standard PDF cards). No signs were found for the presence of other types of calcium phosphates. Apatite, especially hydroxyapatite [$Ca_{10}(PO_4)_6(OH)_2$; HAp], with a stoichiometric Ca/P molar ratio of 1.67 is usually prepared by wet method and the final product is given by the formula given above. In the presence of reactants, with lower Ca/P molar ratios with the least value at 1.5, the XRD patterns shown in Figure 8 that all powders maintained the same crystalline structure of the stoichiometric HAp despite their difference composition, which is based on the difference in their Ca/P initial ratio. No indication of other calcium phosphate phases was found in all patterns despite the fact that the lowest Ca/P powder; 1.5, may also exist as tricalcium phosphate [$Ca_3(PO_4)_2$; TCP] in either it's α- or β- crystalline structures (Arahira, Maruta, & Matsuya, 2017). These phases have their standard JCPDS cards 09-0348 and 86-1585 respectively (Hung, Shih, Hon, & Wang, 2012).

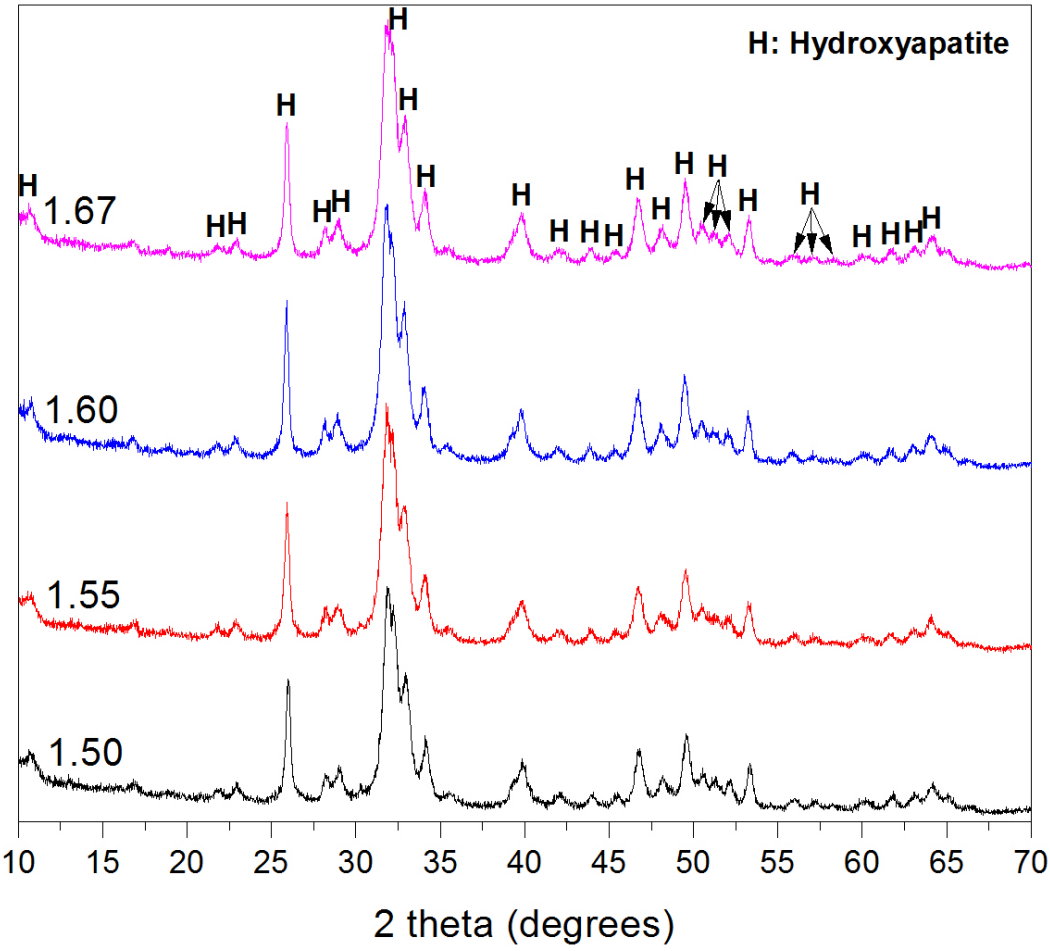

Figure 8: X-ray diffraction patterns of the as-prepared calcium phosphate powders

However, it is also known that a Ca-deficient HAp phase could exist with an apatitic crystal structure and a formula: $Ca_9(HPO_4)(PO_4)_5OH$ and a Ca/P molar ratio of 1.5 (Hung et al., 2012). The results in Figure 8, therefore, further confirm these suggestions of the formation of apatitic calcium phosphate phases with a variable degree of deficiency in the Ca^{2+} sites, depending on the initial Ca/P of their respective reactants.

All samples were thermally treated at 800°C to investigate their structural stability. Figure 9 shows the XRD patterns of these powders, where an overall improvement in the crystallinity of all powder samples was shown. This is evident in the increased sharpness of all peaks that were attributed to apatitic calcium phosphate in the last section. Improving crystallinity is a direct consequence of heat treatment of ceramic materials (Haberko et al., 2006). However, new peaks were shown at 2θ values of 13.6, 26.7, 27.9, 31.1, 34.6, 35.2, 37.4, 37.9, 41.2, 44.7, and 59.6°. These new peaks started to appear in the XRD pattern of Ca/P 1.6 and below with a gradual increase in intensity with lowering the Ca/P ratio. It should be also mentioned that one of these peaks appeared with a very low intensity at 2θ value of 31.1°. These peaks refer to the presence of a second phase; tricalcium phosphate (β-TCP) in the thermally treated powders (Hung et al., 2012). This type of calcium phosphate is not apatitic in nature and has the chemical formula $\beta\text{-}Ca_3(PO_4)_2$, in which no OH group nor water of crystallization are present. Interestingly, both β-TCP and the proposed chemical structure of Ca-def HAp, which is $Ca_9(HPO_4)(PO_4)_5OH$, have the same Ca/P ratio of 1.5 (Hung et al., 2012).

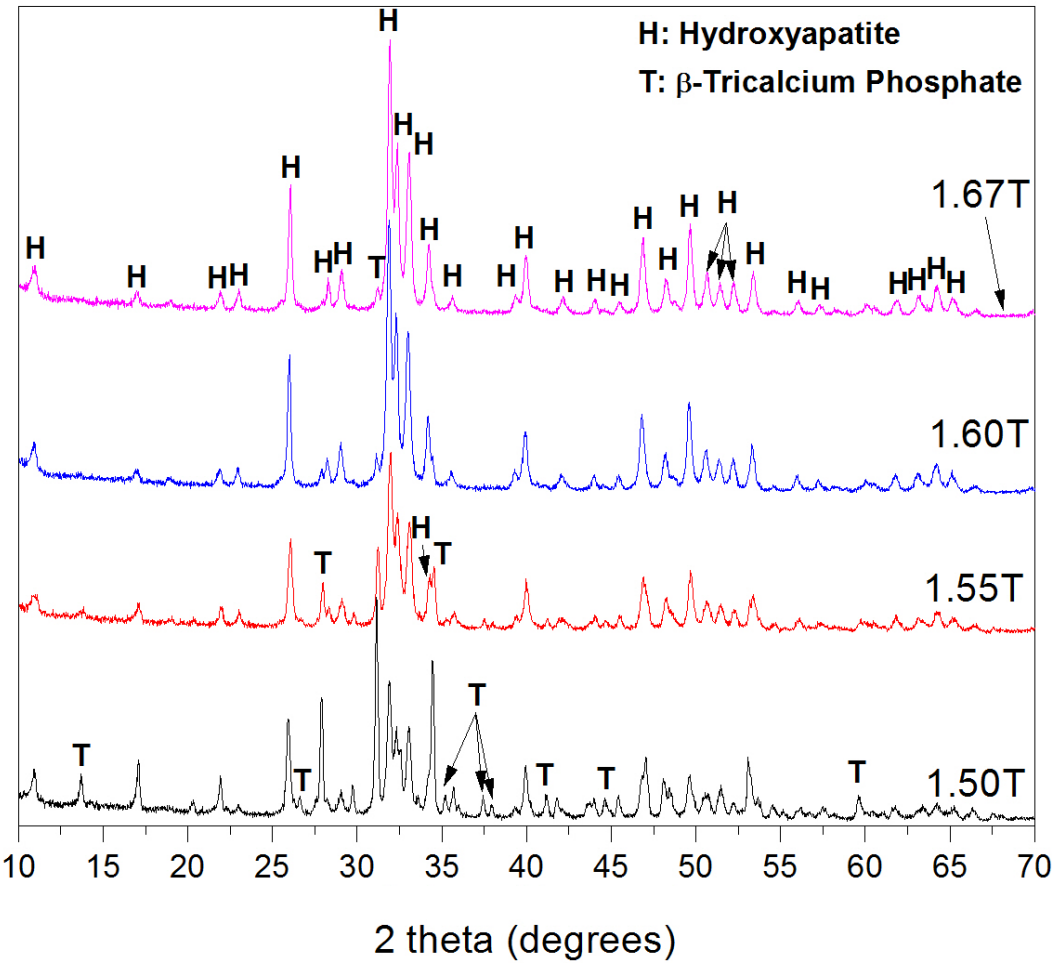

Figure 9: X-ray diffraction patterns of the calcium phosphate powders heat treated at 800°C

However, peaks related to apatitic crystal structure (H) have been also observed in the XRD patterns of Ca/P 1.5, 1.55 and 1.6 powder samples and mostly found in the patters of the stoichiometric HAp powder sample. These results indicate the decomposition of the apatitic structure of the calcium phosphate powders at Ca/P < 1.67 to Ca-def HAp and β-TCP, with an increased proportion of the latter phase with decreasing the Ca/P ratio to 1.5.

3.1.1.2 Infrared Spectroscopy (IR)

The structure of all as-prepared calcium phosphates was also studied by IR spectroscopy, as shown in Figure 10. A broad strong intensity band was observed at 2750-3650 cm^{-1} in the IR spectra of all calcium phosphate powders. This band is attributed to the stretching mode of vibration of O-H of physically and chemically bonded water. An additional band was shown at 1640 cm^{-1} and is attributed to the bending mode of physically and chemically attached water. The bending mode of vibration of the O-H group was also equally shown as a medium size shoulder at 640.5 cm^{-1}in the spectra of all powder samples. Moreover, a shoulder at 3572 cm^{-1} was also observed in the spectra of all powder samples and is related to the structural O-H band, which is part of the apatitic crystal structure. On the other hand, a sharp intensity broad band was shown in each of the spectra at 950-1150 cm^{-1} and is attributed to the stretching mode of vibration of the P-O of the orthophosphate (PO_4^{3-}) group, which is part of the chemical structure of HAp. On the other hand, the bending mode of vibration of this group appears as two un-resolved bands at 565.6 and 603.5 cm^{-1} in addition to a low intensity band at 472 cm^{-1}. The above-mentioned bands confirm the presence of apatitic calcium phosphate structure and provide additional evidence to the assumptions given above in the discussion of the XRD patterns of these samples in Figure 8. In addition to the above, two weak intensity bands were also shown at 1408 and 1460 cm^{-1} in addition to band at 872 cm^{-1} in the spectra of all samples. These bands are attributed to the possibility of presence of carbonates (CO_3^{2-}) in the HAp structure.

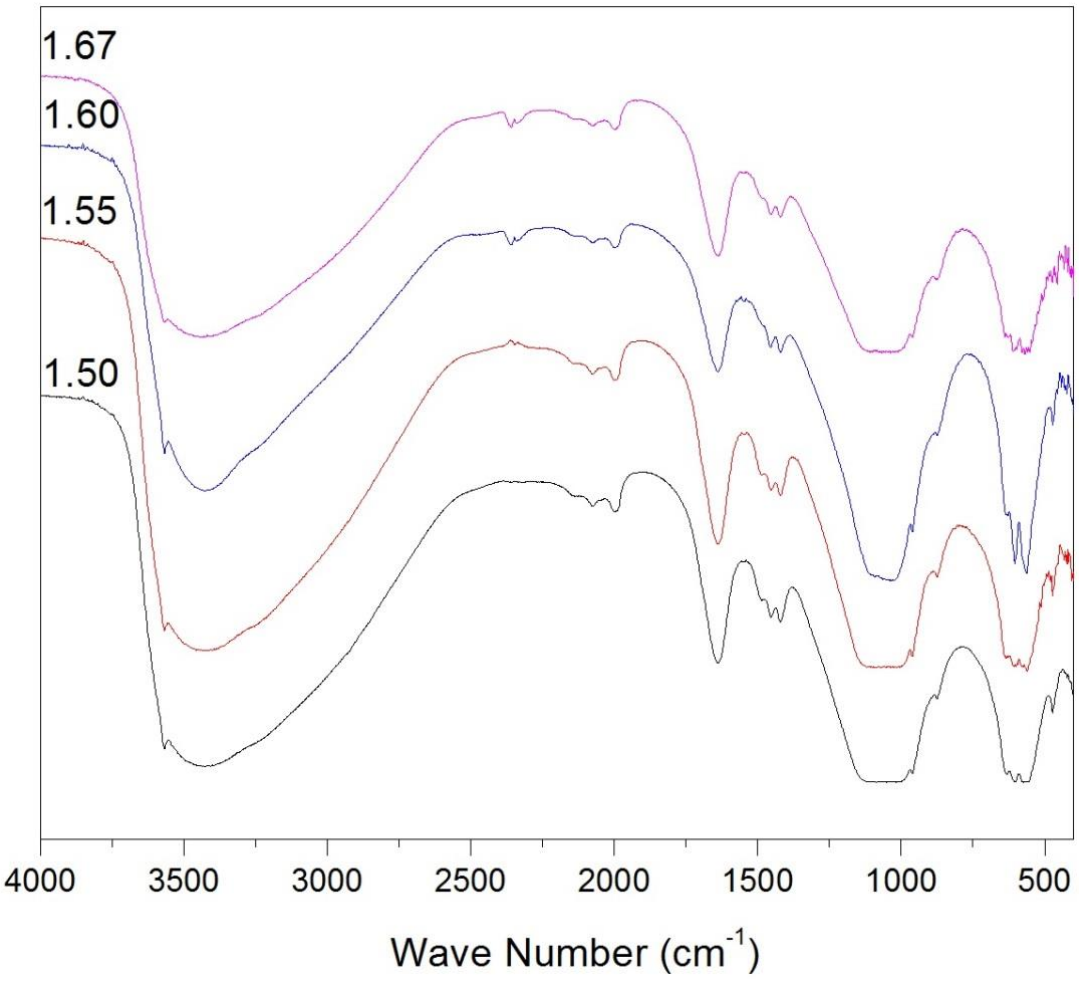

Figure 10: Infrared spectrum of the as-prepared calcium phosphate powders

However, the weak intensity of these bands indicate that these bands are related to the adsorption of CO_2 onto the surfaces of the powders during their handling and not to the presence of CO_3^{2-} groups within the crystal structure of any of the apatitic samples (Boanini, Gazzano, & Bigi, 2010; Elliott, 1994; Landi, Celotti, Logroscino, & Tampieri, 2003).

Upon thermal treatment of all powders (various Ca/P ratios) at 800^{o}C, their infrared spectra reflected the changes in their composition and crystallinity, as shown in Figure 11. Compared with the IR spectra in Figure 10, all thermally treated samples showed an overall decrease in the broadness of the bands accompanied by a relative increase in their resolution. A major difference was shown in the bands, characteristic to the stretching mode of O-H group within the range of 3200-3650 cm^{-1}. A remarkable decrease in the broadness and intensity of the physically attached water was shown in all samples, which was also accompanied with an increase in the sharpness of the chemically attached water at 3572 cm^{-1}, and a decrease in the intensity of bending O-H bands around 1640 cm^{-1}. These changes confirm the continued presence of the OH group within the crystal structure of the apatitic calcium phosphates after thermal treatment at 800°C. On the other hand, the bands characteristic to the P-O stretching mode of the PO_4^{3-} group were improved in sharpness and increase in intensity as a result of thermal treatment. These changes indicate an improvement in the crystallinity of the calcium phosphate powders by heat treatment at 800°C. The continued observation of the bands related to O-H group in the spectra of all thermally treated samples indicate that the apatitic calcium phosphate phase is dominating the powders of all samples, and that the β-TCP phase that was observed in the XRD patterns of the Ca/P < 1.67 samples, shown in Figure 9, is a minor phase.

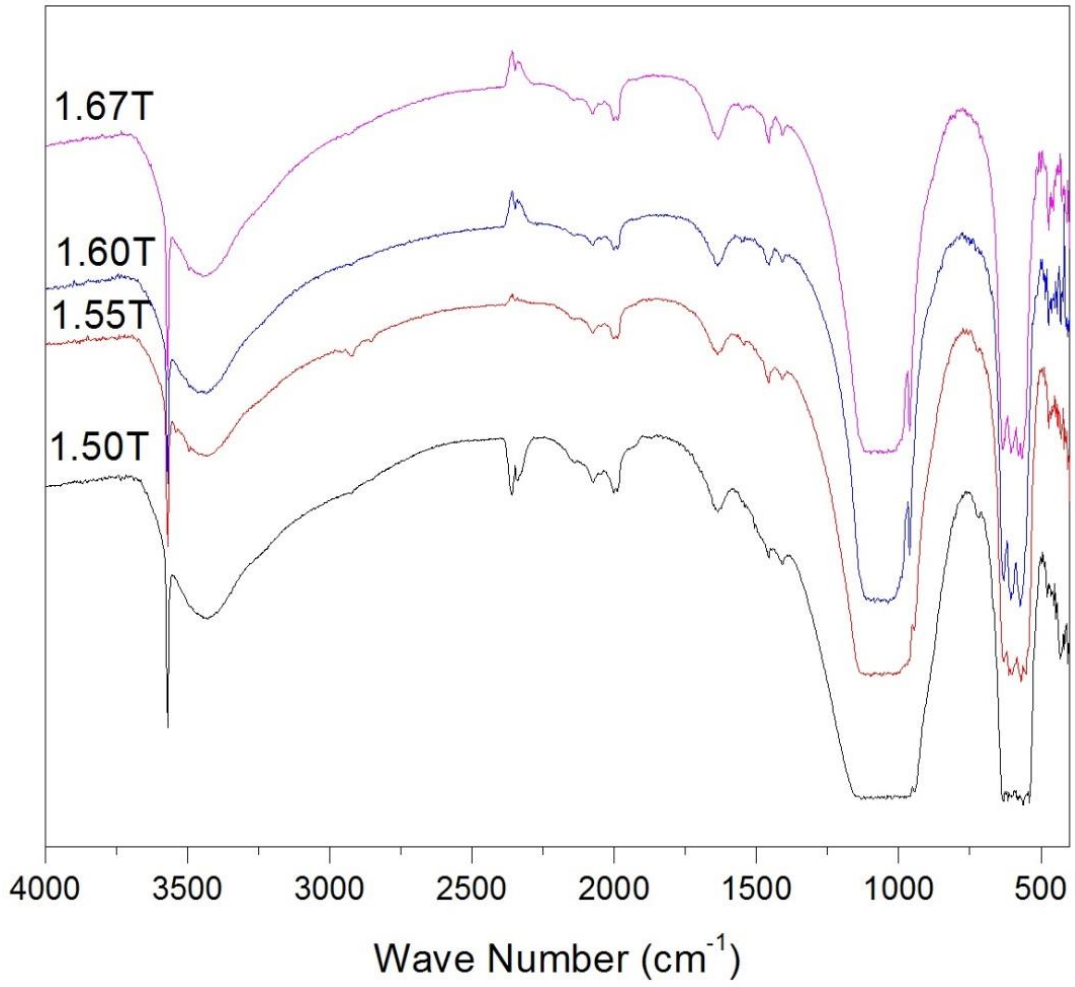

Figure 11: Infrared spectrum of the calcium phosphate powders heat treated at 800°C

3.1.1.3 Thermogravimetric Analysis (TGA)

The thermal history that describes the structural composition of the as-prepared calcium phosphates was studied by thermogravimetric (TGA) analysis, as shown in Figure 12. TGA provides information about the various functional groups and the physical- and chemically-bonded groups in the structure of the calcium phosphates, as heated to 600°C.

Two events were shown in the TGA thermogram of a powder sample of Ca/P ratio 1.67. These are referred to by (a) and (b) in the diagram in Figure 12. The first event (a) takes place below 100°C a gradually increase in weight loss until 125°C. This is attributed to the evaporation of the physically attached water, also known as water of hydration, and is usually related to the atmospheric moisture (Haberko et al., 2006). The second event (b) takes place at 250°C and extends until 350°C and is related to the chemically-attached water, also known as water of crystallization (Haberko et al., 2006). At temperatures above 350°C, a plateau was reached in the TGA thermogram of the stoichiometric HAp powder sample (Ca/P 1.67). These results indicate the structural stability of this particular powder sample until 600°C. This is confirmed by the literature, where stoichiometric HAp is structurally stable until 1250°C above which it converts to oxyapatite through the loss of a water molecule from its typical formula (Haberko et al., 2006). The highest weight loss of this sample was 7% after heating at 600°C. On the other hand, TGA thermograms of other as-prepared calcium phosphate powders showed variable extents of thermal events around (a) and (b) with lower weight loss within the range of 5-5.5%, which could be attributed to the presence of lower concentrations of water, both physically- and chemically-bonded, within the crystal structure of the calcium phosphate powders.

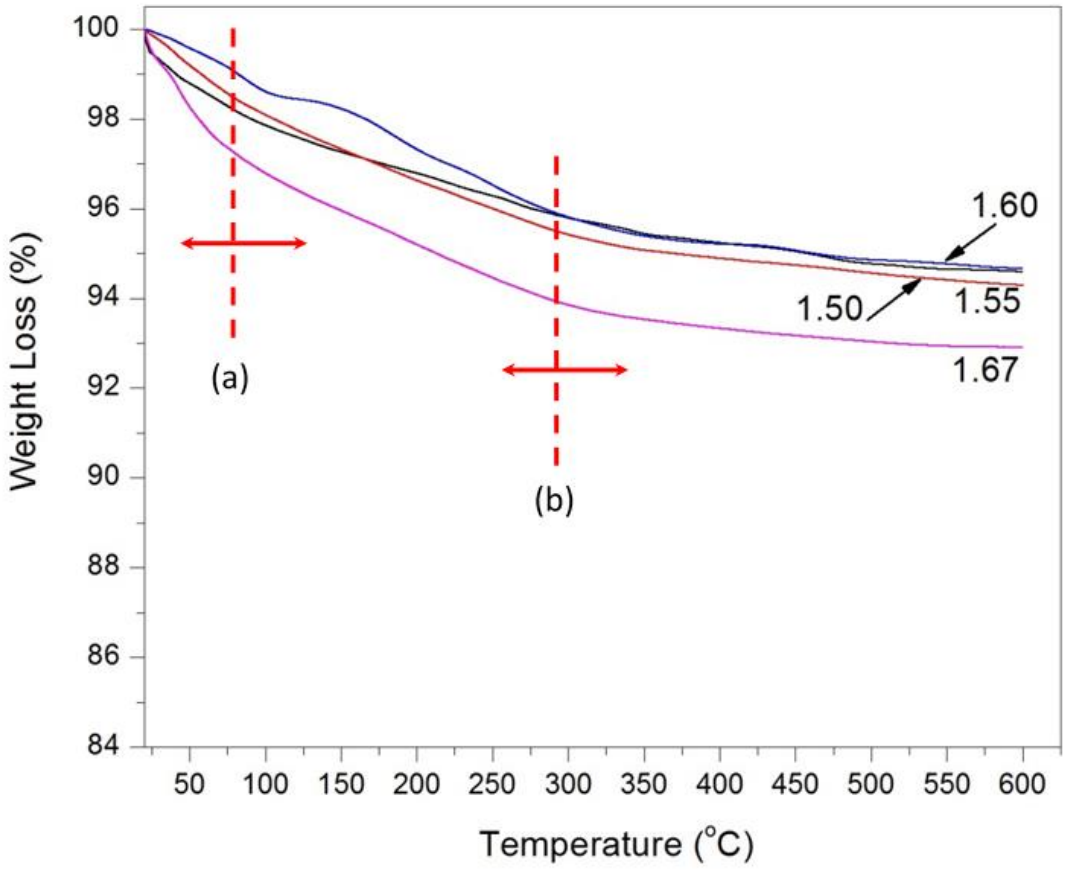

Figure 12: Thermogravimetric diagram of as-prepared calcium phosphate powders

Figure 13 shows the TGA thermograms of all thermally treated calcium phosphate powders as a function of their initial Ca/P ratio. Despite the resolution of the weight loss events into two; due to the evaporation of physically- and chemically-attached water in the as-prepared samples, the thermograms shown in Figure 13 shows a continuous weight loss. The highest weight loss of 10% was achieved in the thermogram of Ca/1.67 sample. The weight loss decreased gradually with the decrease in the Ca/P of the calcium phosphate powders, showing a weight loss of 5% achieved with the Ca/P 1.5 thermally treated sample. These findings indicate the higher susceptibility of the higher Ca/P (1.6 and 1.67) to be hydrated than the lower Ca/P (1.5 and 1.55) thermally treated powders towards the adsorption of atmospheric water.

Thermal treatment of the calcium phosphate powders at 800^{o}C was shown to result in changes in the phase composition of the powder samples, especially with those made of Ca/P molar ratios of 1.5 and 1.55, as shown in the XRD and IR results of the thermally treated powders. These changes were not reflected in their TGA thermograms shown in Figure 12 for the as-prepared and Figure 13 for the thermally treated powder samples. Knowing that TGA analysis takes place by subjecting the powder samples to slow heating (10°C/min) up to 600°C indicate that these phase changes took place between 600°C and 800°C.

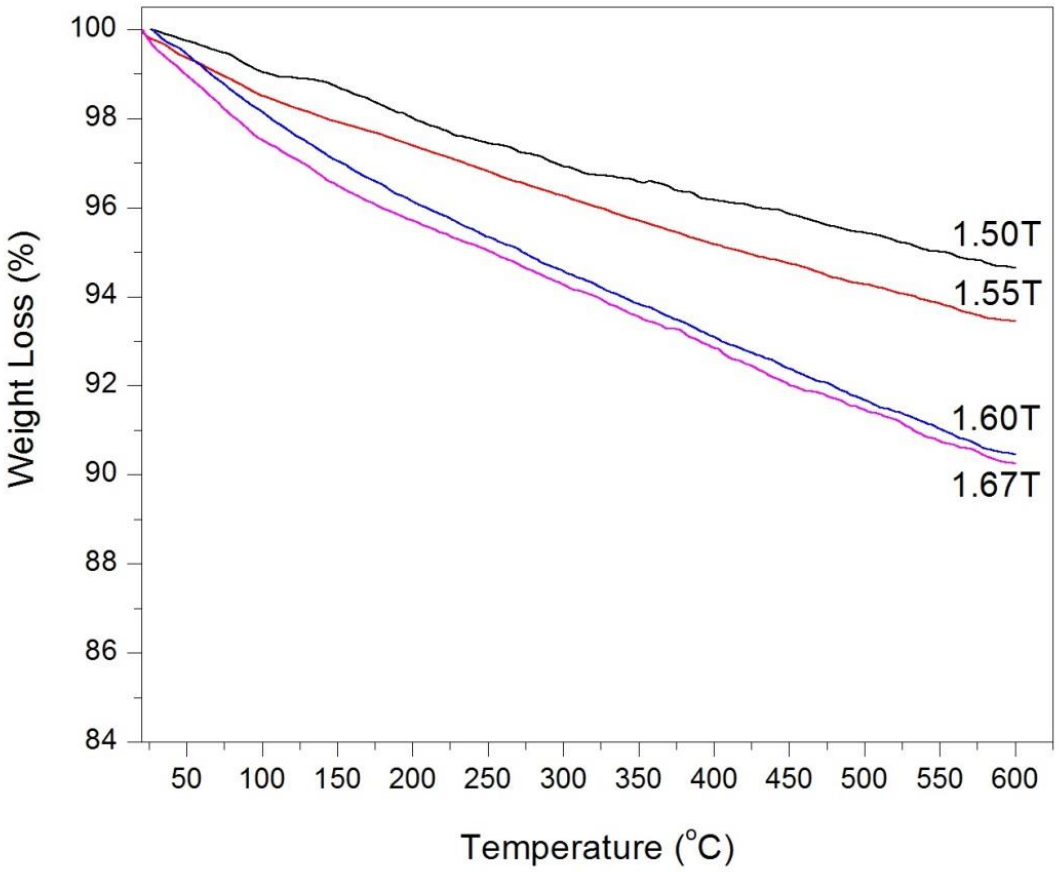

Figure 13: Thermogravimetric diagram of the calcium phosphate powders heat treated at 800°C

3.1.1.4 Scanning Electron Microscopy (SEM)

The solid dried powders of both as-prepared and thermally-treated calcium phosphate sorbents with various Ca/P molar ratios were subjected to SEM investigation to reveal their microstructural characteristics. Figure 14 shows the SEM micrographs of these powders. All samples showed a particulate nature with a sign of agglomeration, especially with the as-prepared powders. On the other hand, the thermally treated powders showed a lower extent of agglomeration, which could be attributed to the fact that as-prepared powders were ground before thermally treated to avoid their hardening with heat treatment. However, an increase in the agglomeration was observed to take place with increasing the Ca/P ratio of the originally prepared powders. Moreover, particulates of all powders showed an overall homogeneous particle size distribution with an irregular morphology that was not affected by thermal treatment. It should be noted that the homogeneous particle sized distribution of the powders shown in Figure 14 indicates the suitability of the sorbent powders to be used as a packing material in a cartridge for water purification, as a proposed application of these loose powders. This suggestion stems from the fact of its homogeneous size distribution that will facilitate their packing within the sorbent cartridge and provide a homogeneous pore size distribution.

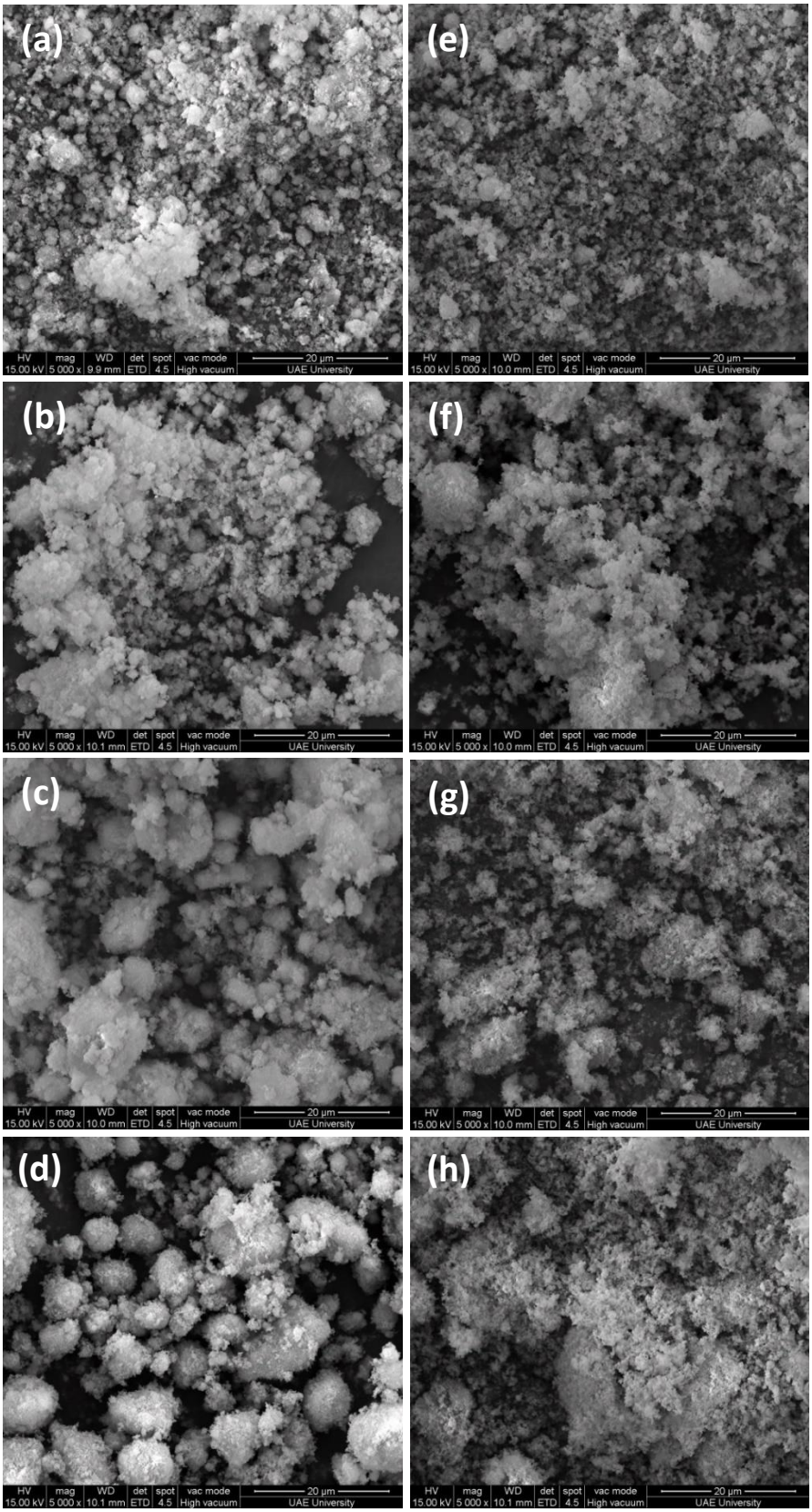

Figure 14: Scanning electron micrographs of the (a) 1.5 (b) 1.55 (c) 1.6 (d) 1.67 as-prepared and (e) 1.5T (f) 1.55T (g) 1.6T (h) 1.67T heat treated calcium phosphate powders

3.1.1.5 Surface Area (BET) Measurements

Based on the particulate nature of the prepared and thermally treated calcium phosphate sorbents, they were subjected to N_2 adsorption measurements, as a tool to investigate their BET surface area. Figure 15 shows the variation in the BET surface area of the tested powders with the initial Ca/P molar ratio and the thermal treatment. Due to the agglomeration that was observed in the as-prepared powders (Figure 14), the Ca/P 1.5 sample showed the lowest surface area with a value of 17.5 m^2/g, while other as-prepared powders showed similar average surface area of 60 m^2/g. On the other hand, all samples showed a dramatic decrease in their surface area after thermal treatment. Even though these powders were ground before thermal treatment to de-agglomerate them, the decrease in the surface area could be related to the coarsening of the grains making the powders by heat treatment, which is a common feature of heat treatment of ceramic fine particulates.

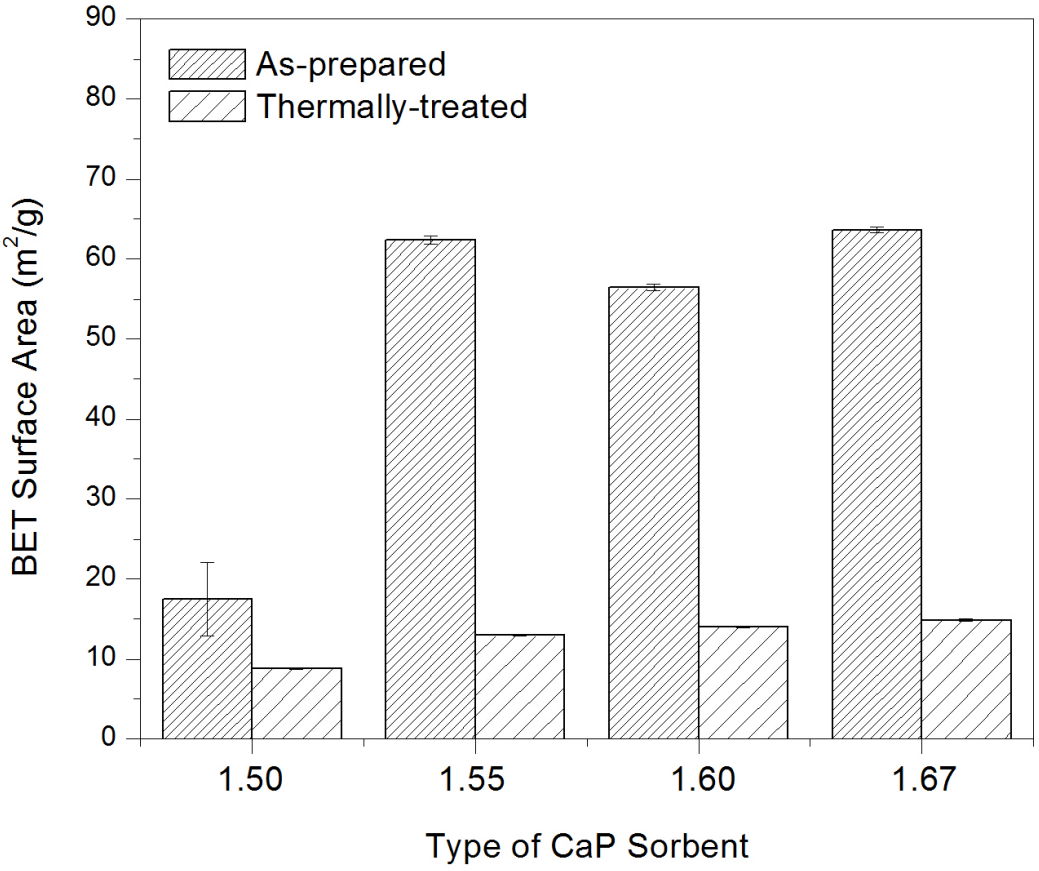

Figure 15: BET surface area distribution of as-prepared and heat treated calcium phosphate powders

3.1.2 Sorption of Cd^{2+} Ions

Calcium phosphate powders with various Ca/P molar ratios in both forms; as-prepared and after thermal treatment at 800ºC, were evaluated for their efficiency in the adsorption and removal of Cd^{2+} ions from simulated polluted aqueous media. Those were prepared by adding a pre-determined proportion of soluble Cd^{2+} ions to de-ionized water. Each of the calcium phosphate powders were finely ground and added to the Cd^{2+}-polluted media, while the effect of changing the media pH, the sorbent (calcium phosphate powder) weight, the sorbate (Cd^{2+}) concentration and the contact time, on the sorption capacity of the various types of sorbents were evaluated. The following sections will outline the results obtained in this regard.

3.1.2.1 Effect of pH

The importance of this parameter stems from the fact that industrial waste water in which various types of soluble ions, such as Cd^{2+} ions, are acidic or basic in nature depending on the types and concentrations of the pollutants in it. Therefore, solutions containing a fixed concentration of Cd^{2+} ions 1 mmol, was adjusted at various pH values 3-8, using 0.1M KOH and HNO_3 solutions, to evaluate this parameter. Figures 16-17 show the variation of the remaining Cd^{2+} ions in solution with changing the pH of the media in which a fixed amount of the each of the calcium phosphate sorbent; 0.1 g, was added, while the experiment was carried out for 24 hours as a fixed contact time. All sorbents showed a high sorption capacity for Cd^{2+} ions, with increasing the Ca/P molar ratio of the sorbents; both as-prepared and heat treated. Comparing the results shown in Figures 16 and 17 indicate the higher efficiency of Cd^{2+} removal of the as-prepared calcium phosphates as compared with the heat-treated respective samples.

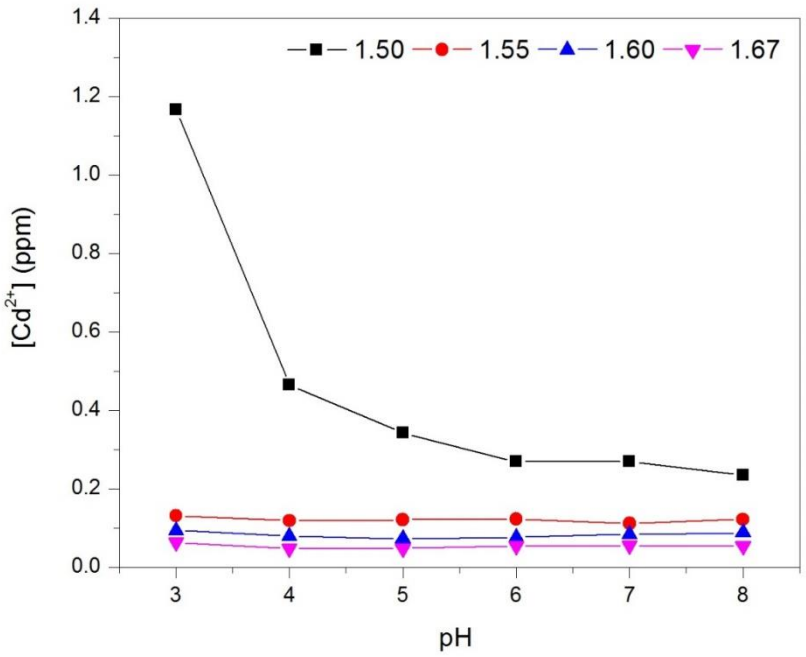

Figure 16: Effect of changing solution pH on the sorption of Cd^{2+} ions using as-prepared calcium phosphate sorbents

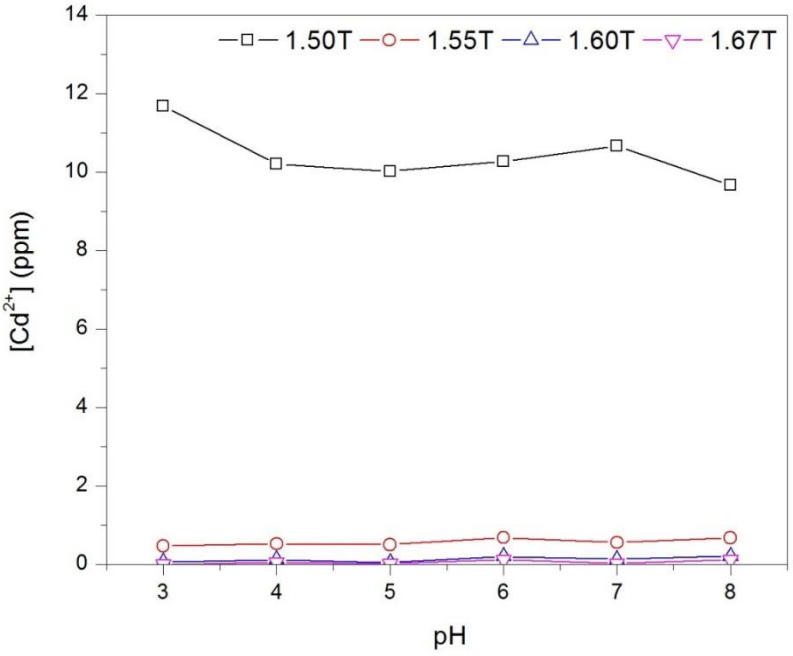

Figure 17: Effect of changing solution pH on the sorption of Cd^{2+} ions using heat-treated calcium phosphate sorbents

With the exception of the Ca/P 1.5 as-prepared and heat-treated powder, the as-prepared calcium phosphates were 5 times higher in efficiency than the heat-treated samples. Considering the exchange mechanism that is expected to take place where Cd^{2+} ions exchange with Ca^{2+} ions from the calcium phosphate sorbents, the decreased efficiency of exchange of the heat-treated powders could be related to the decrease reactivity of the powders by heating. This is a common criterion in ceramic materials, where heating largely participates in the decreased reactivity of the powders. The lowest performance was observed with both as-prepared and heat treated Ca/P 1.5 calcium phosphate could be related to the presence of non-apatitic calcium phosphate in the composition of these powders, as was shown in Figures 8 and 9. Moreover, the relative increase in the efficiency of the Ca/P 1.5 powder with increasing the pH of the medium could be related to the increased stability of the apatitic Ca-deficient HAp phase in these powders with pH. This is also related to the basic nature of the apatitic phases, which are chemically more stable in basic media (Boudia, Zuddas, Fernane, Fiallo, & Sharrock, 2018). Based on these results, a pH 5.5 was selected as an optimum value to be considered for the next set of experiments. Highly acidic media were not considered due to the possibility of dissolution of the calcium phosphate sorbents in the media, and their consequent disposal instead of being used as sorbent (Boudia et al., 2018). On the other hand, highly basic pH media were not selected to avoid the possibility of precipitation of the Cd^{2+} ions in the form of $Cd(OH)_2$ and the subsequent removal from the solution by precipitation unlike the proposed function of the calcium phosphate powders as sorbents of the soluble Cd^{2+} ions.

3.1.2.2 Effect of Sorbent Weight

In these experiments, the sorbent weight was varied at a constant sorbate concentration of 1 mmol and a pH 5.5 for 24 hours. Figures 18-19 show the variation of the Cd^{2+} concentration with changing the sorbent weight of the as-prepared and heat-treated calcium phosphate sorbent particulates. Due to the difference in the chemical reactivity between the as-prepared and heat-treated calcium phosphate powders, the former sorbents showed a higher efficiency of sorption of Cd^{2+} ions than the latter ones. The as-prepared samples showed a range of Cd^{2+} ions between 0 and 3.5 ppm (Figure 18), while the heat-treated samples showed a higher range of Cd^{2+} ions between 0 and 50 ppm (Figure 19). All samples showed a decrease in the remaining Cd^{2+} concentrations with increasing the sorbent weight used, which is in a direct agreement with the proposed mechanism of exchange between the Cd^{2+} pollutant ions and the sorbent Ca^{2+} ions, where more Cd^{2+} ions were removed by providing higher concentration of the exchange sites; sorbent particulates. The overall performance of removing Cd^{2+} ions was shown to increase with increasing the Ca/P molar ratio of the sorbents used. This could be related to the higher chemical stability of the higher Ca/P calcium phosphate sorbents, where at pH 5.5, the possibility of partial dissolution of the low Ca/P sorbents may be considered.

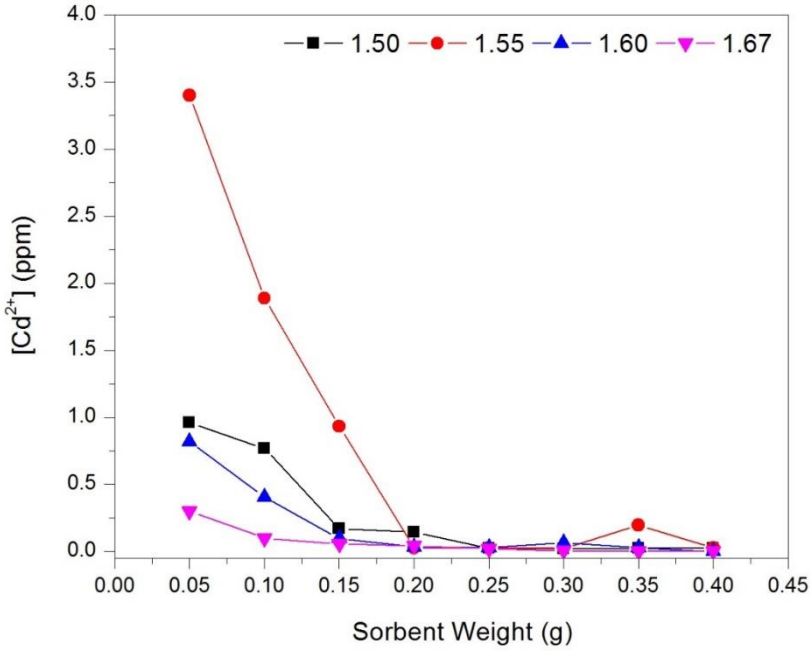

Figure 18: Effect of changing sorbent weight on the sorption of Cd^{2+} ions using as-prepared calcium phosphate sorbents

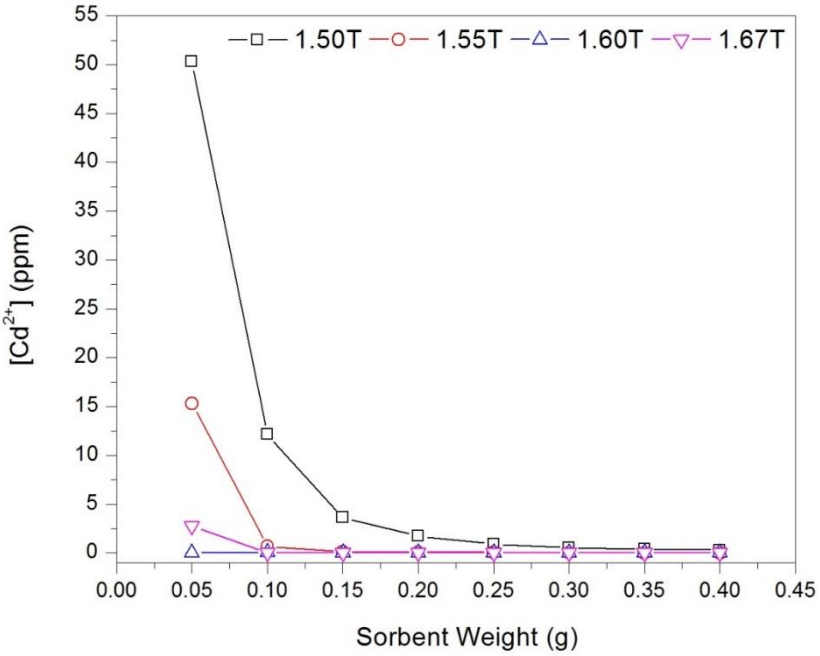

Figure 19: Effect of changing sorbent weight on the sorption of Cd^{2+} ions using heat-treated calcium phosphate sorbents

3.1.2.3 Effect of Sorbate (Cd^{2+}) Concentration

At a constant pH of 5.5, a constant contact time of 24 hours and a fixed sorbent weight of 0.1 g, the effect of varying the initial concentration of Cd^{2+} ion on the efficiency of the as-prepared and heat-treated calcium phosphate sorbents was studied. Figures 20-21 show the variation of the remaining Cd^{2+} ions in solution with changing the initial sorbate concentration as a function of the type of calcium phosphate sorbent. All sorbents showed a similar trend where the lowest concentrations of Cd^{2+} ions were observed when the starting Cd^{2+} concentrations were 0.1 mmol and 1 mmol. Increasing the initial sorbate concentration to 10 mmol while maintaining the sorbent weight constant showed a dramatic increase in the remaining Cd^{2+} ions concentrations, which indicates the incapability of the available amount of sorbent for the added sorbate ions. Interestingly, the affinity of the heat-treated sorbents was higher than the as-prepared sorbents towards the absorption of Cd^{2+} ions from the media with 10 mmol concentration of the Cd^{2+} ions. This could be related to the removal of the water of hydration and crystallization by heat treatment, which is believed to facilitate the access of the Cd^{2+} ions to the Ca^{2+} (I) sites within the crystal lattice of the apatitic sorbent. It was also observed that higher Ca/P sorbents, both as-prepared and heat treated were more efficient than the lower Ca/P ones with respect to the removal of Cd^{2+} ions. These findings suggest the difficulty of the Cd^{2+} ions to fill in the vacancies in the crystal lattice of the Ca-deficient apatitic sorbents (Ca/P: 1.5 and 1.55). On the other hand, the direct exchange of the apatitic Ca^{2+} ions by Cd^{2+} ions was more feasible. Moreover, these results suggest that deficiency in the crystal structure of apatite sorbent leads to a partial decrease in the lattice volume, which is therefore considered an explanation of the lower efficiency of the low Ca/P sorbents.

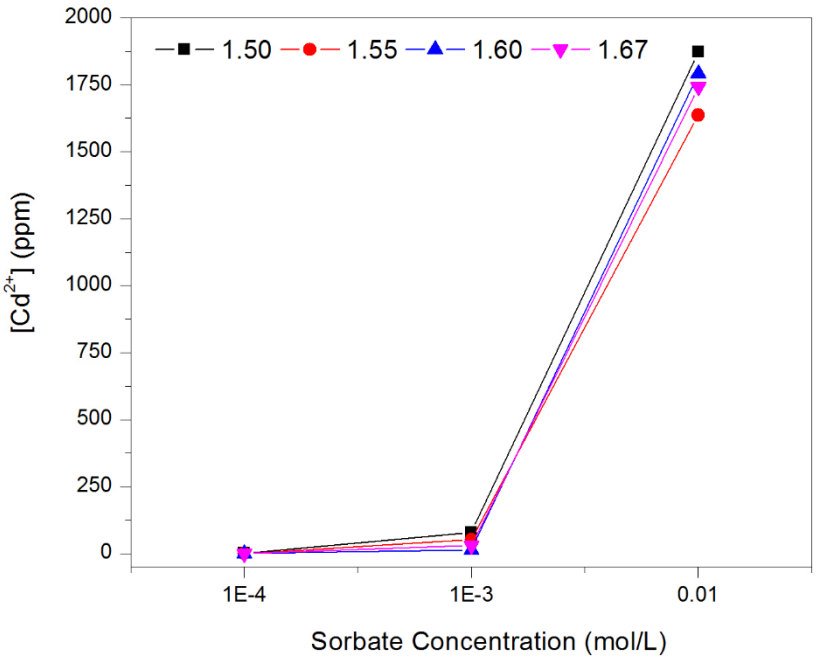

Figure 20: Effect of varying initial concentration of Cd^{2+} ions on the efficiency of the as-prepared calcium phosphate sorbents

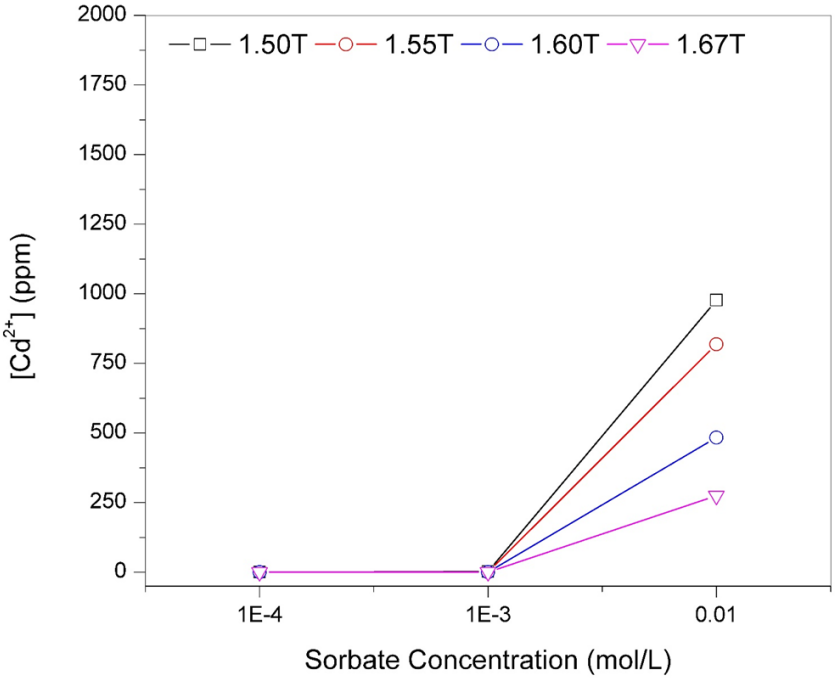

Figure 21: Effect of varying initial concentration of Cd^{2+} ions on the efficiency of the heat-treated calcium phosphate sorbents

3.1.2.4 Effect of Sorption Time

Based on the above experiments, the effect of varying the time of contact between each of the sorbents and Cd^{2+} ions on the efficiency of removal of these ions was evaluated. Figures 22-23 show the results obtained in this regard. All sorbents showed a dramatic decrease in the concentrations of Cd^{2+} ions in solution in less than 4 hours of contact. All as-prepared sorbents showed the same trend **(**insert in Figure 22**)**, while the thermally treated Ca/P 1.5 sorbent was less efficient **(**insert in Figure 23**)**. These results are in accordance of the above-mentioned assumptions, where the thermally treated low Ca/P sorbent was found to contain non apatitic crystal structure in a mixture with Ca-deficient apatite. This phase was declared to be β-TCP, which is not known in the literature to be used as a sorbent for the removal of heavy metal ions.

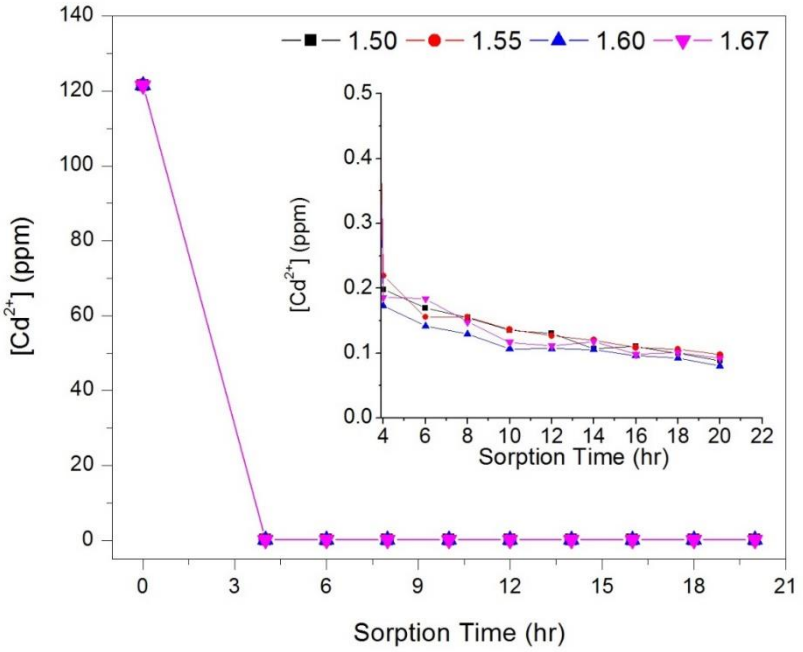

Figure 22: Effect of varying contact time on the efficiency of the removal of Cd^{2+} ions using as-prepared calcium phosphate sorbents

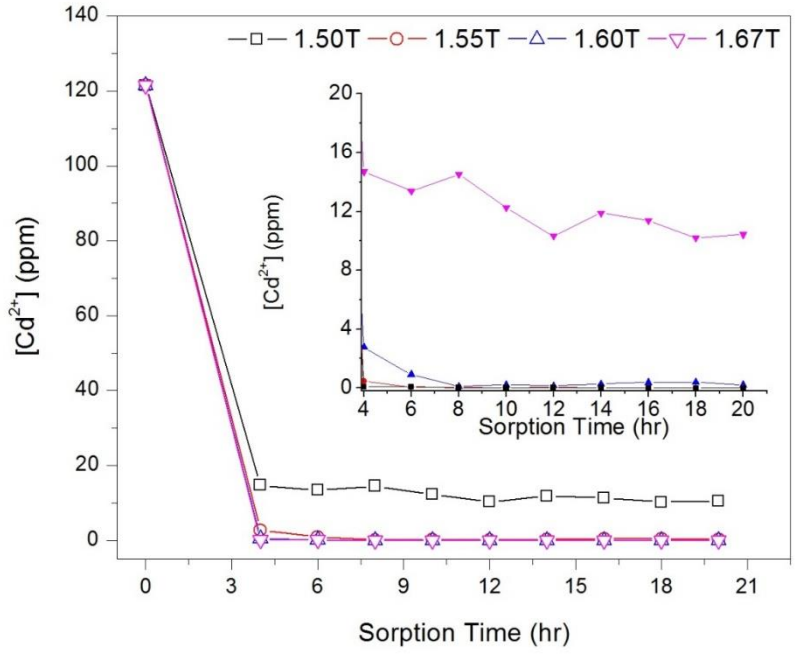

Figure 23: Effect of varying contact time on the efficiency of the removal of Cd^{2+} ions using heat-treated calcium phosphate sorbents

3.2 Structure and Evaluation of CA-HAp Composite Fibrous Sorbents

3.2.1 Characterization of Stoichiometric HAp Sorbents

Three types of stoichiometric calcium phosphates were selected for this study. They differ in origin but share the same stoichiometric Ca/P molar ratio of 1.67. These were commercial HAp, both micro particles and nanoparticles, and synthetic HAp that was prepared in our laboratories using a wet chemical synthesis route in a manner similar to that discussed in the first part of the Thesis. Selection of stoichiometric HAp to be combined with cellulose acetate nanofibers for making fibrous composite membrane was based on the fact that HAp is the most chemically stable structure among the various types of calcium phosphates with variable Ca/P molar ratios; discussed in the first part of the current study. Prior mixing with CA and making the composites, HAp powder samples, both as-received and thermally treated, were characterized for their composition and morphology as will be discussed in the following sections.

3.2.1.1 X-ray Diffraction (XRD)

Figure 24 shows XRD patterns of the as-received HAp (1.67) powder samples. Compared with a JCPDS card # 9-432 for standard HAp (Ca/P molar ratio 1.67), sHAp and cHAp powders showed a complete matching with the standard peaks of HAp. Peaks with variable intensities at 2θ values of 22.96, 25.97, 28.24, 29.02, 31.92, 32.29, 33.05, 34.20, 39.95, 46.83 and 49.57° were similar to those found in the JCPDS card of pure HAp. The broadness of the peaks in both types of HAp powders indicated their ill-crystallinity.

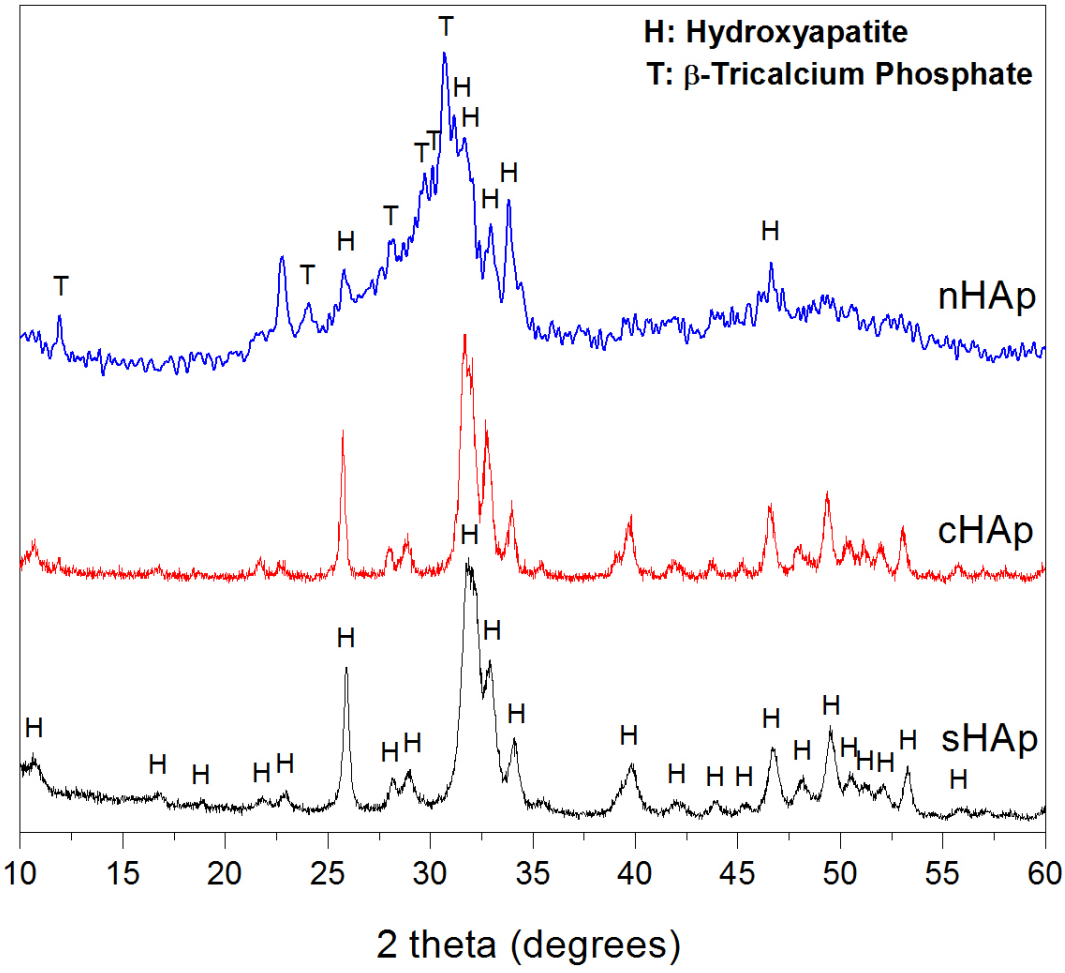

Figure 24: X-ray diffraction patterns of the as-received HAp (1.67) powder samples

No signs of other types of calcium phosphates were observed in these samples. The XRD pattern of nHAp, on the other hand, showed a higher degree of peak broadening than that observed in the patterns of sHAp and cHAp. This is attributed to the size difference between nHAp; nanometer scale particulates, and that in the sHAp and cHAp; micrometer scale particulates. In addition, an additional phase was also observed in the XRD pattern of nHAp with its peaks at 23.4, 22.8, 22.4, 20.8, 16.8, 11.9°. These are related to the presence of β-TCP as a second phase with HAp. Due to the high broadness of the peaks of this sample, it was difficult to assess the relative proportions of HAp and β-TCP in this powder sample. It should be mentioned that nHAp is a commercially available HAp nano powder, as claimed by the supplier; Sigma-Aldrich, USA.

Upon heat treatment of the stoichiometric HAp powders from different origins at 800^{o}C, an overall improvement in the crystallinity of the powders was observed, as shown in Figure 25. This was observed as a pronounced decrease in the broadness of the peaks together with an increase in their sharpness. No other phases were detected in the XRD pattern of the thermally treated sHAp and cHAp powders. On the other hand, the presence of β-TCP as a second phase in the XRD pattern of nHAp was confirmed after thermal treatment. This was shown in the improvement of the sharpness of these peaks at the same 2θ values that were found in their XRD pattern before thermal treatment. No other phases were observed in the XRD pattern of thermally treated nHAp.

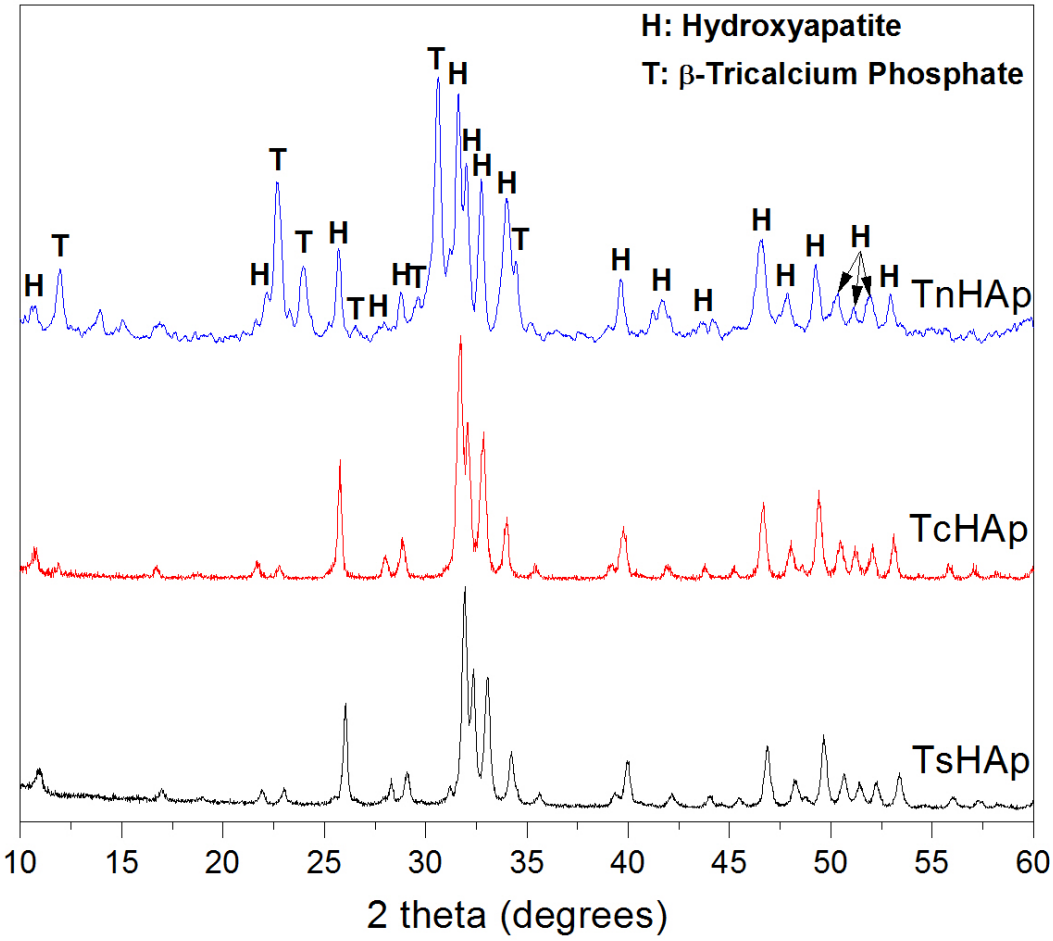

Figure 25: X-ray diffraction patterns of the heat-treated HAp (1.67) powder samples

3.2.1.2 Infrared Spectroscopy (IR)

Infrared spectroscopy was also used to study the composition of the as-received and thermally treated stoichiometric HAp powder samples. Figure 26 shows the IR spectra of the as-received HAp (1.67) powders. Each powder showed a typical IR spectrum of hydroxyapatite with the bands, characteristic to OH^- and PO_4^{3-} groups at their designated wave numbers that were previously mentioned in the first part of this work. Please refer to 3.1.2 for more details. The broadness of the OH^- band at 2750-3650 cm^{-1} is attributed to the presence of physically and chemical bound water in the structure of all HAp powder samples. However, the relatively lower intensity band within this range, as well as the lower intensity band at 1640 cm^{-1}, which is characteristic to the OH^- bending mode of vibration, in the IR spectrum of nHAp, confirm the presence of a β-TCP with HAp as was discussed in the XRD patterns of this powder. It should be mentioned that no significant variation in the intensities or location of the bands, characteristic to the PO_4^{3-} were observed between the various types of stoichiometric HAp.

Figure 27, on the other hand, show the IR spectra of thermally treated HAp (1.67) powder samples. A pronounced decrease in the broadness of the OH^--related band within the range of 2750-3650 cm^{-1} was observed, which is a normal behavior considering the thermal treatment and the evaporation of the physically attached water leaving behind the most stable water of crystallization. The latter type of water was observed through its OH^- band at 3572 cm^{-1}, especially in the spectra of the sHAp and cHAp powder samples.

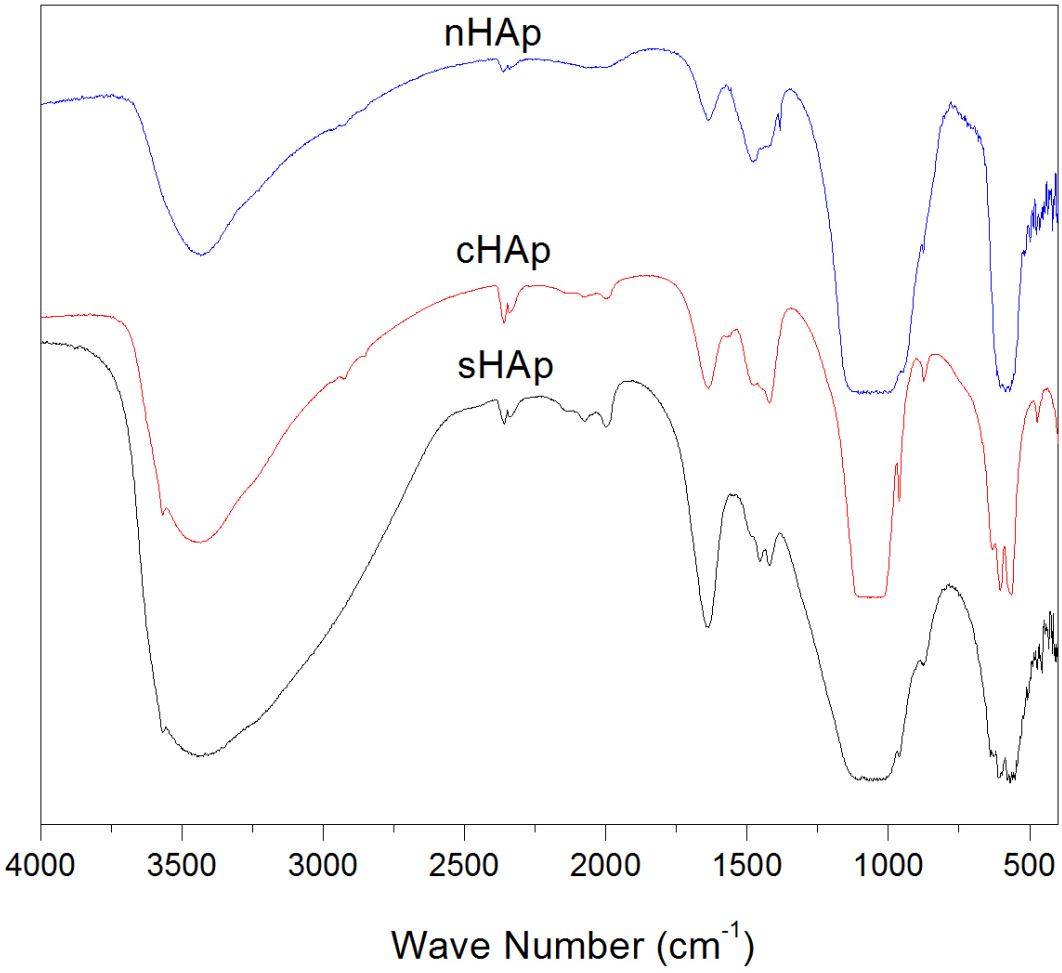

Figure 26: Infrared spectra of the as-received stoichiometric HAp powders

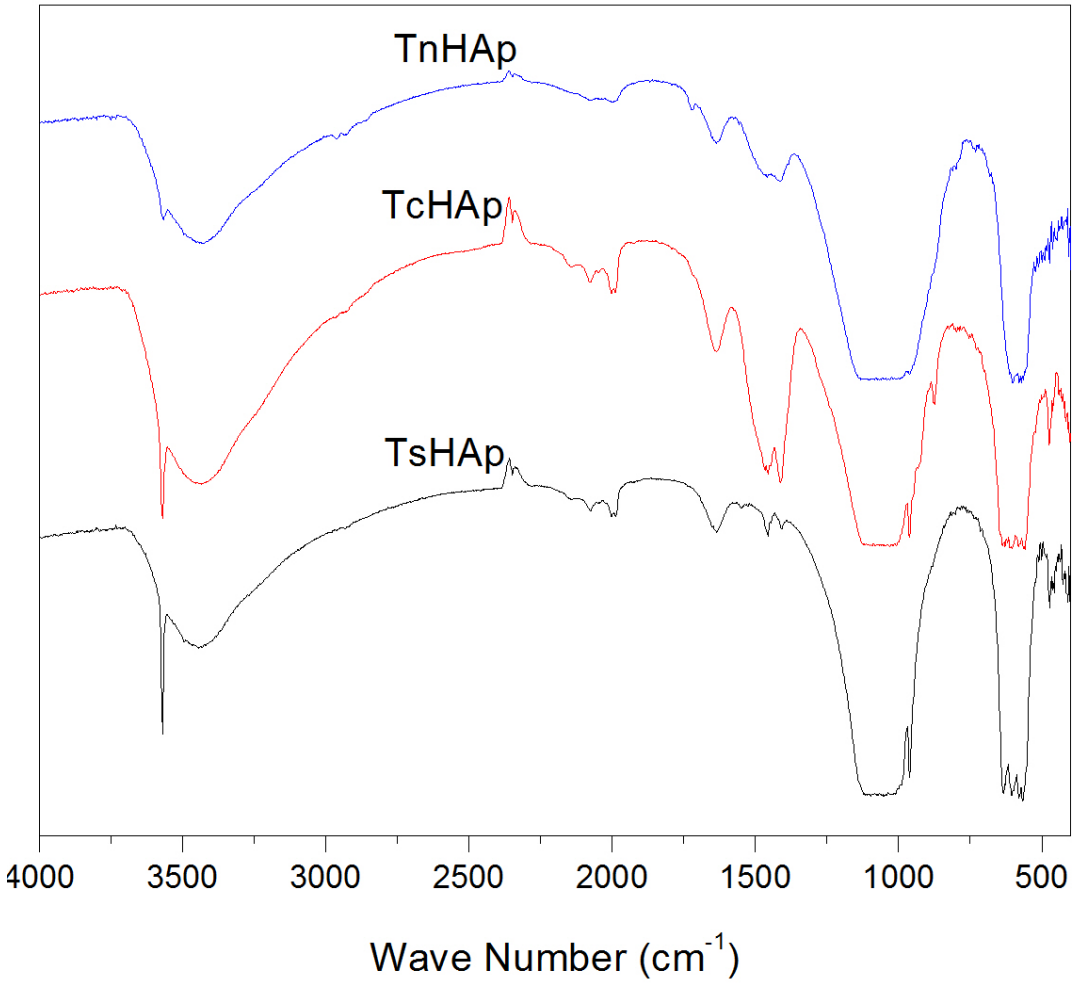

Figure 27: Infrared spectra of the heat-treated stoichiometric HAp powders

However, this band was slightly observed in the spectrum of the nHAp powder sample and is also attributed to the lower proportion of OH^- in the composition of nHAP as it was found to be a mixture of HAp and β-TCP. In addition, the IR spectrum of the thermally treated cHAp showed an increased intensity of a band around 1480-1520 cm^{-1}, which could be related to the presence of carbonates in the structure of the cHAp. Considering the high temperature of the thermal treatment, 800°C, the continued presence of this band unlike the spectra of sHAp and nHAp suggests the possibility of having carbonates within the structure of cHAp.

3.2.1.3 Thermogravimetric Analysis (TGA)

Figures 28-29 shows the TGA thermograms of the all types of stoichiometric HAp before and after thermal treatment, respectively. Both neat cHAp and sHAp showed two main events of weight loss at 100°C and 275°C, as average temperatures, which are related to the evaporation of the physically and chemically attached water, respectively. These events showed an overall weight loss of 6 and 7% for the cHAp and sHAp powder samples, respectively. On the other hand, the TGA thermogram of pure nHAp showed an overall weight loss of 1% via a single event commencing at 100°C, which could be related to the evaporation of the weakly attached water of hydration. Moreover, the lower weight loss of the neat nHAp powder could be also related to the presence of other non-hydrated phases with HAp, as discussed in the XRD and IR results of this powder.

On the other hand, thermal treatment of these powders resulted in the removal of the weakly attached water of hydration, leaving behind the persistent water of crystallization that can be removed at temperatures higher than 800°C. It was found that nHAp and cHAp thermally treated powders show overall weight loss values of 0.5 and 1.5%, respectively, while the thermally treated sHAp was found to have higher weight loss approaching 3% by the end of the heating cycle at 600°C. Referring to the XRD and IR results of sHAp before and after thermal treatment, it was found that only pure HAp was the only phase with an increased crystallinity with heat treatment. No phase changes were observed by thermal treatment of this synthetic HAp powder. These findings provide an evidence of the structural stability of the stoichiometric HAp powder samples.

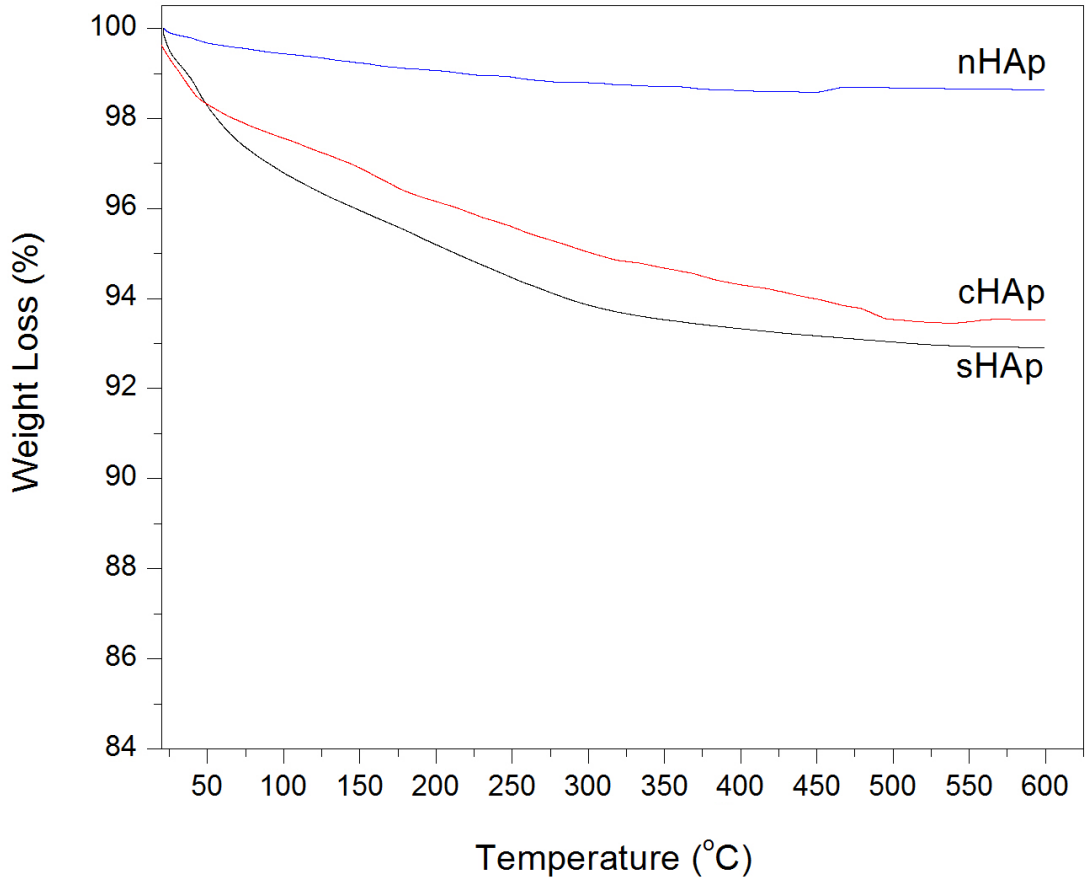

Figure 28: Thermogravimetric diagram of the as-received stoichiometric HAp powders

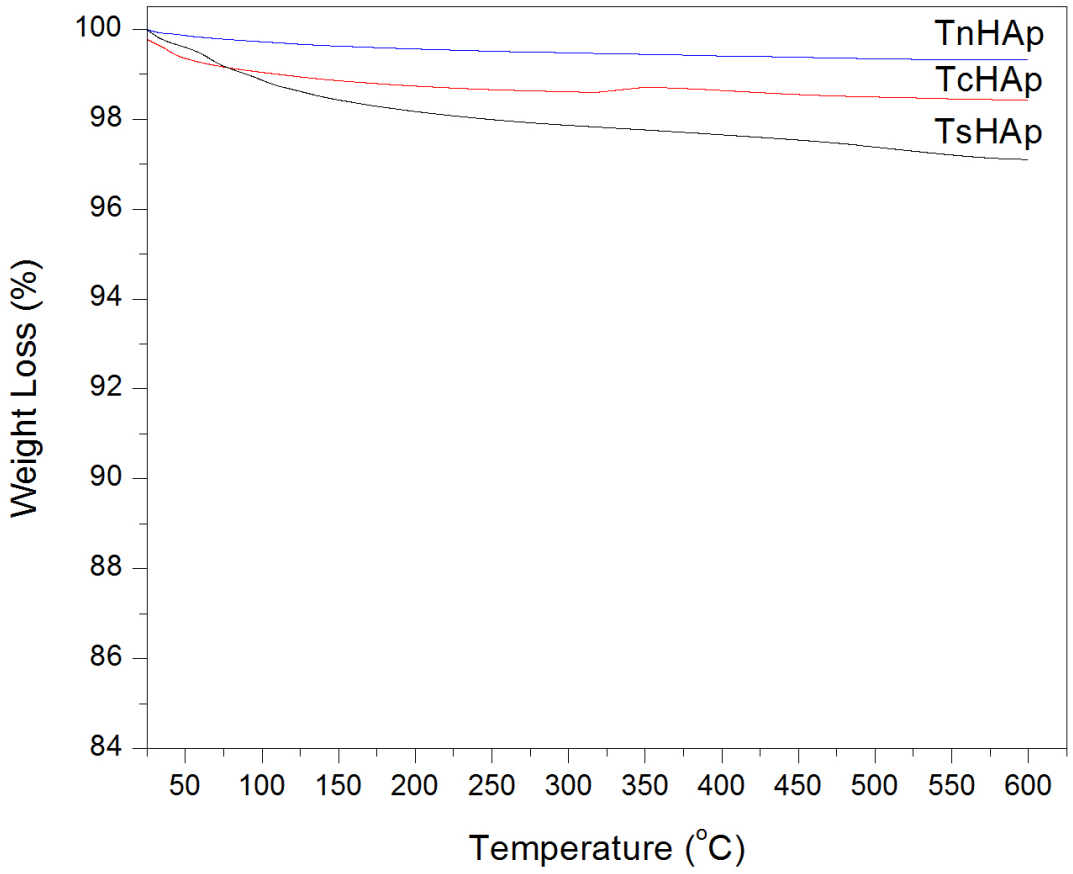

Figure 29: Thermogravimetric diagram of the heat-treated stoichiometric HAp powders

3.2.1.4 Scanning Electron Microscopy (SEM)

Apatitic powders of various origins were investigated for their morphology by SEM before being mixed with CA and forming their corresponding composite fibrous membranes. Figure 30 shows SEM micrographs of the as-received/prepared and the thermally treated sorbent powders. All powders showed particles with an irregular morphology with a higher extent of agglomeration observed in the powders of nHAp before and after thermal treatment (Figure 30 c, f). This is a common feature of powders that are made of nanoparticulates where they tend to aggregate forming clusters that are made of a large number of nanoparticles. It was also observed that cHAp powder was larger in size than the as-prepared and the nHAp powders, with a pronounced coarsening with thermal treatment (Figure 30 b, e).

3.2.1.5 Surface Area (BET) Measurements

Figure 31 shows the variation in the BET surface area of the as-received/prepared and thermally treated apatitic powders. Both synthetic and commercial HAp powders showed an average surface area of 63 m^2/g. Despite the difference in particles size between sHAp and cHAp and that of nHAp, the later was anticipated to have a higher surface area due to its nm size. However, nHAp particulates showed an average surface area of 21 m^2/g which is therefore attributed to its high extent of agglomeration, which was shown in its micrograph in Figure 30. Upon thermal treatment, all powders showed a tremendous decrease in their BET surface area to the range of 14-28 m^2/g. This could be related to the grain coarsening effect caused by thermal treatment, as a common feature in ceramic materials.

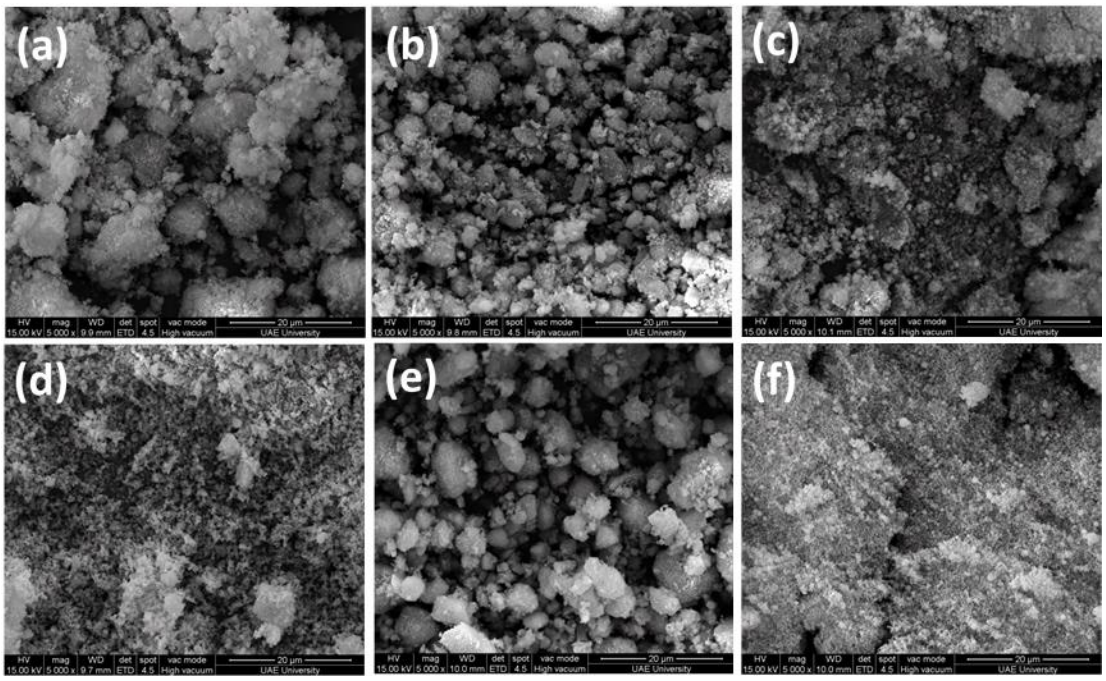

Figure 30: SEM micrographs of the as-received/prepared (a) sHAp (b) cHAp (c) nHAp and the thermally treated (d) sHApT (e) cHApT (f) nHApT sorbent powders

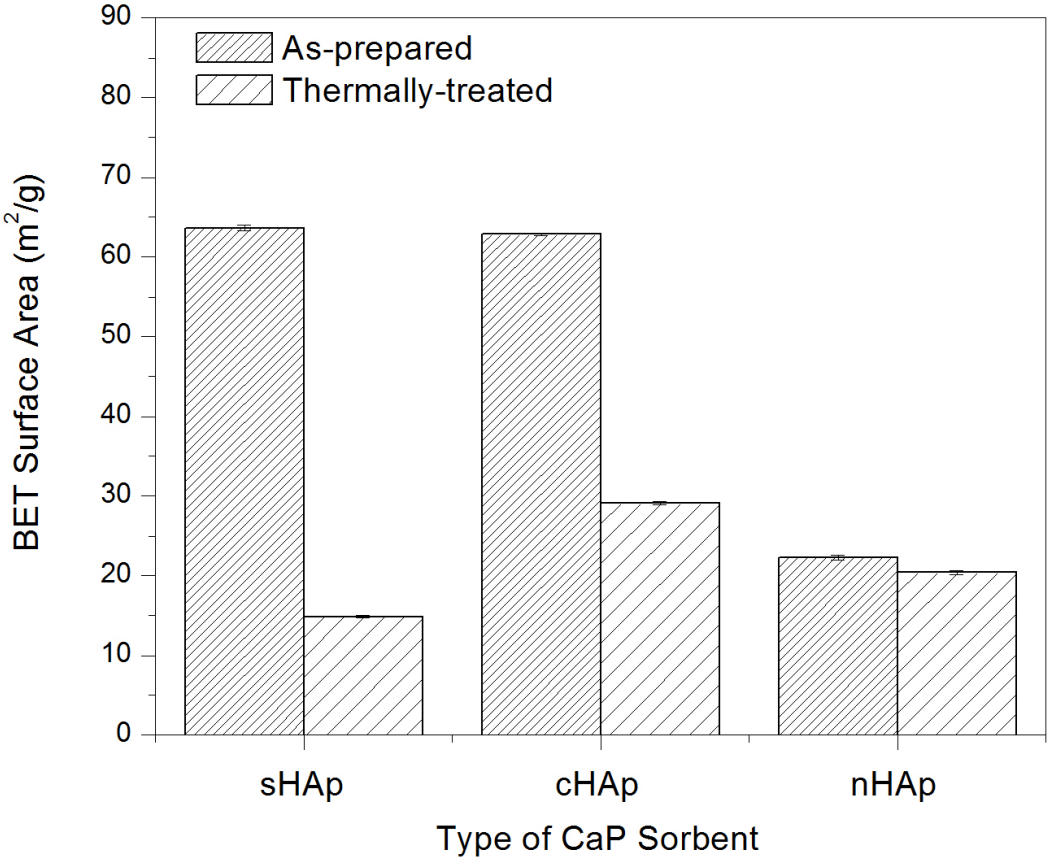

Figure 31: BET surface area distribution of the as-received and heat-treated stoichiometric HAp powders

This was also shown before in the variation of the BET surface area of thermally treated calcium phosphate sorbents with variable Ca/P molar ratio. The decrease in surface area may initially result in the decrease in their affinity towards the adsorption of soluble Cd^{2+} ions, as will be outlined in the following sections.

3.2.2 Characterization of HAp-Cellulose Acetate Sorbents

HAp powders of different origins (synthetic, commercial micro- and commercial nano-) were blended with cellulose acetate (CA) solutions in proportions of 5 and 10% by weight. HAp powders were dispersed in the CA solutions making suspensions with homogeneous distribution of the powders in it. The main objective was to ensure a homogeneous distribution of the HAp powders within the CA fibers prepared by electrospinning. Both as-received and thermally treated HAp powders were used in these experiments. Characterization of the prepared fibrous membranes was carried out for their morphology and composition before being evaluated for their ability to remove Cd^{2+} ions from polluted aqueous media. The following sections will discuss the findings of these characterizations.

3.2.2.1 Scanning Electron Microscopy (SEM)

Figure 32 shows SEM micrograph of a pure CA sample prepared by electrospinning a solution containing 12 wt% of CA in a mixed solvent of DMAc and acetone, as mentioned in detail in the Experimental section of the Thesis. Due to the applied voltage upon the liquid CA drop fed from the needle of the syringe that contains the solution, the drop acquired a negative charge that overcame the surface tension forced of the spherical drop and extended into the fibers shown in Figure 32.

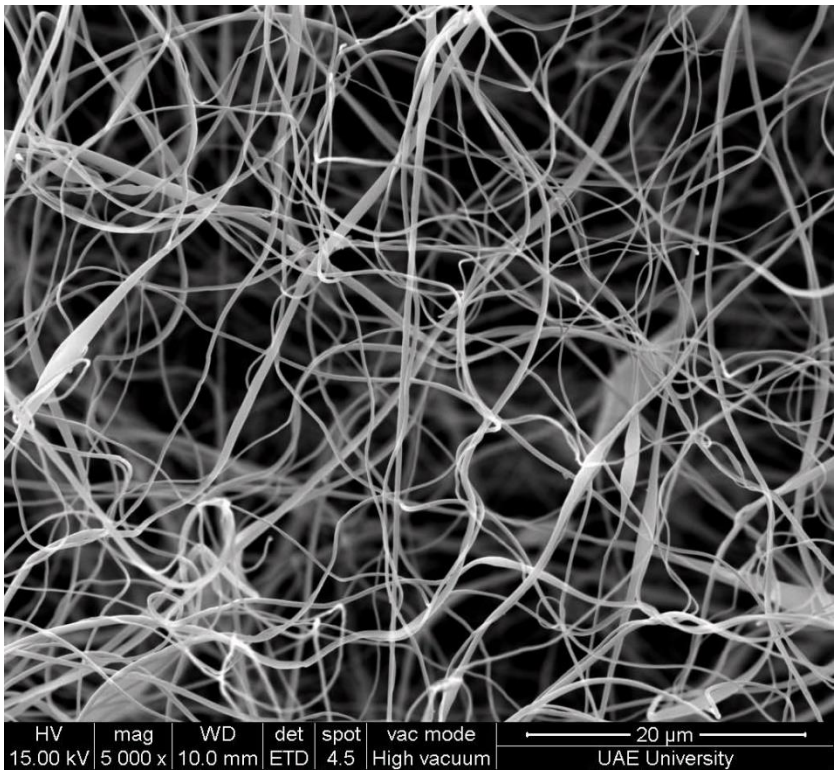

Figure 32: SEM micrograph of the as-prepared pure CA fibrous membrane

Normally, electrospinning is used for the preparation of fibrous membranes with fibers in the nanometer and micrometer scale dimensions. The CA fibers shown in Figure 32 have an average diameter of 0.5-2 μm with a homogeneous fiber size distribution. In addition, the randomness of the fibers, which is a common feature of fibers produced by electrospinning, provided an interconnected porosity that allows for the diffusion of liquids and nutrients in environmental and biomedical applications, respectively (Atila, Keskin, & Tezcaner, 2015; Tian et al., 2011). No deformation of the pure CA fibers was observed similar to those mentioned in Figure 3d, which is attributed to the optimized conditions of electrospinning that were previously obtained in our laboratory (Greish, Meetani, Al Matroushi, & Shamsi, 2010) to avoid these non-fibrous morphologies.

In the presence of 5 and 10 wt% of each of the as-received/prepared and thermally treated HAp powders, micrographs of the electrospun CA containing these powders were obtained, as shown in Figures 33-34. The presence of solid particulates of each of the HAp powders did not affect the morphology of the obtained fibers. Instead, membranes with a homogeneous fiber size and pore size distributions were obtained. This could be related to the low proportions of the added HAp particulates. However, instances of beading were observed in the SEM micrographs of CA fibrous membranes containing as-received and heat treated cHAp particulates, and those membranes containing 10 wt% of the sHAp particulates. This observation could be related to the higher particle size of the cHAp and sHAp particulates as compared with that of nHAp particulates.

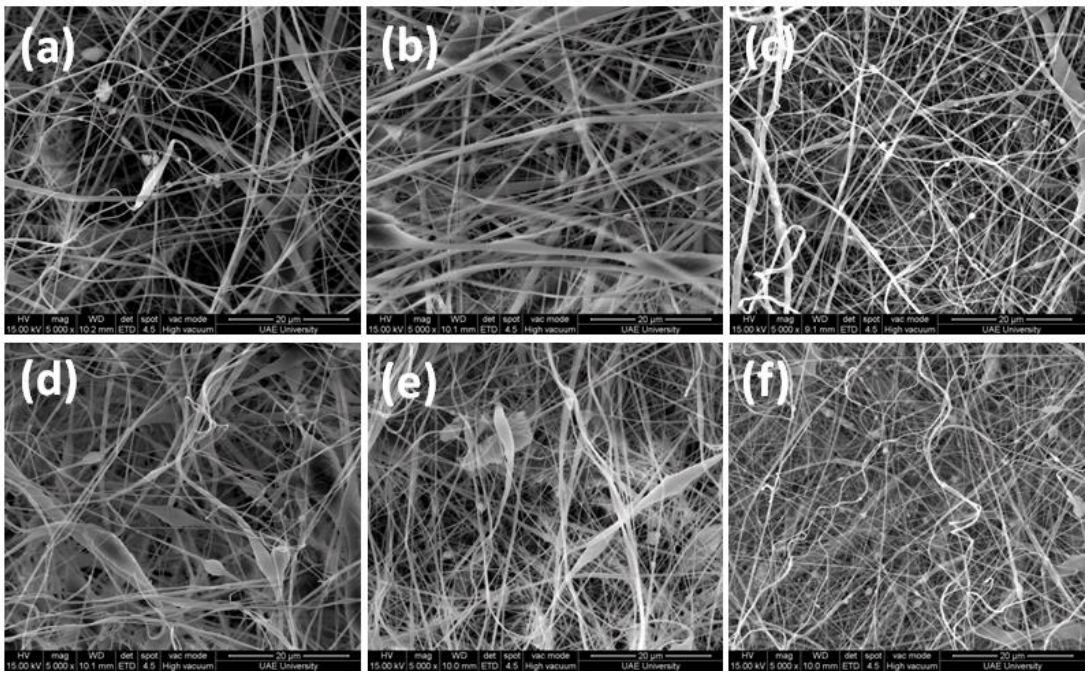

Figure 33: SEM micrographs of the as-prepared CA-all pure HAps fibrous membranes were (a) CA5s (b) CA5c (c) CA5n (d) CA10s (e) CA10c (f) CA10n

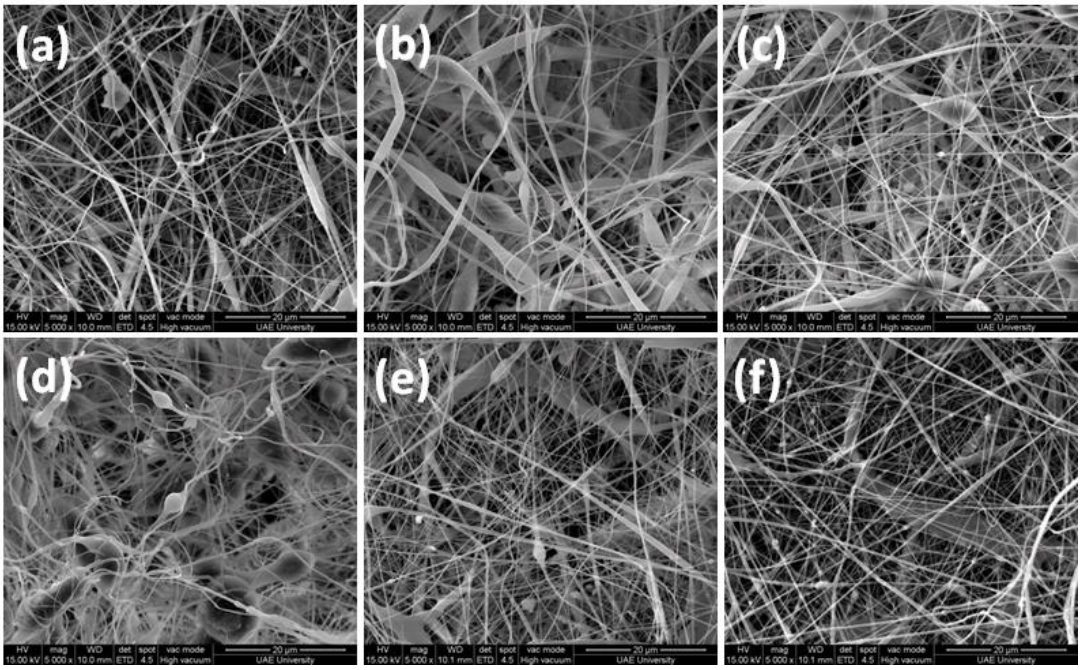

Figure 34: SEM micrographs of the as-prepared CA-all heat-treated HAps fibrous membranes were (a) CA5sT (b) CA5cT (c) CA5nT (d) CA10sT (e) CA10cT (f) CA10nT

3.2.2.2 Infrared Spectroscopy (IR)

Fibrous membranes made of CA and containing 5 and 10 wt% of each of the as-received/prepared and thermally treated HAp particulates were investigated by IR spectroscopy for their structural composition. Figures 35-36 show IR spectra of these composite fibrous membranes. An infrared spectrum of pure CA fibrous sample was also shown for comparison. The chemical formula of CA was previously shown in Figure 3d. The following functional groups of CA were identified in its IR spectrum (Sánchez-Márquez et al., 2015):

a) A broad medium intensity band with a peak at 3487 cm^{-1}, which is attributed to the stretching mode of -OH group, and a weak intensity band at 903 cm^{-1}, which can be assigned to the out-of-plane bending of the -OH group.
b) A sharp and intense band at 1756 cm^{-1}, which is attributed to the ester carbonyl (C=O) group.
c) Two medium intensity bands at 1227 and 1048 cm^{-1}, which are attributed to the C-O-C that exist in the ester group as well as the connection between the pyranose rings, respectively.
d) Weak intensity bands at 2958 cm^{-1} for the stretching vibration, and at 1436 cm^{-1} and 1368 cm^{-1} for the bending modes of vibration of the C-H of CH_3 group.

On the other hand, HAp main functional groups ($-OH^-$, $-PO_4^{3-}$) usually appear as bands within the same range of the corresponding $-OH^-$ and C-O bands of CA.

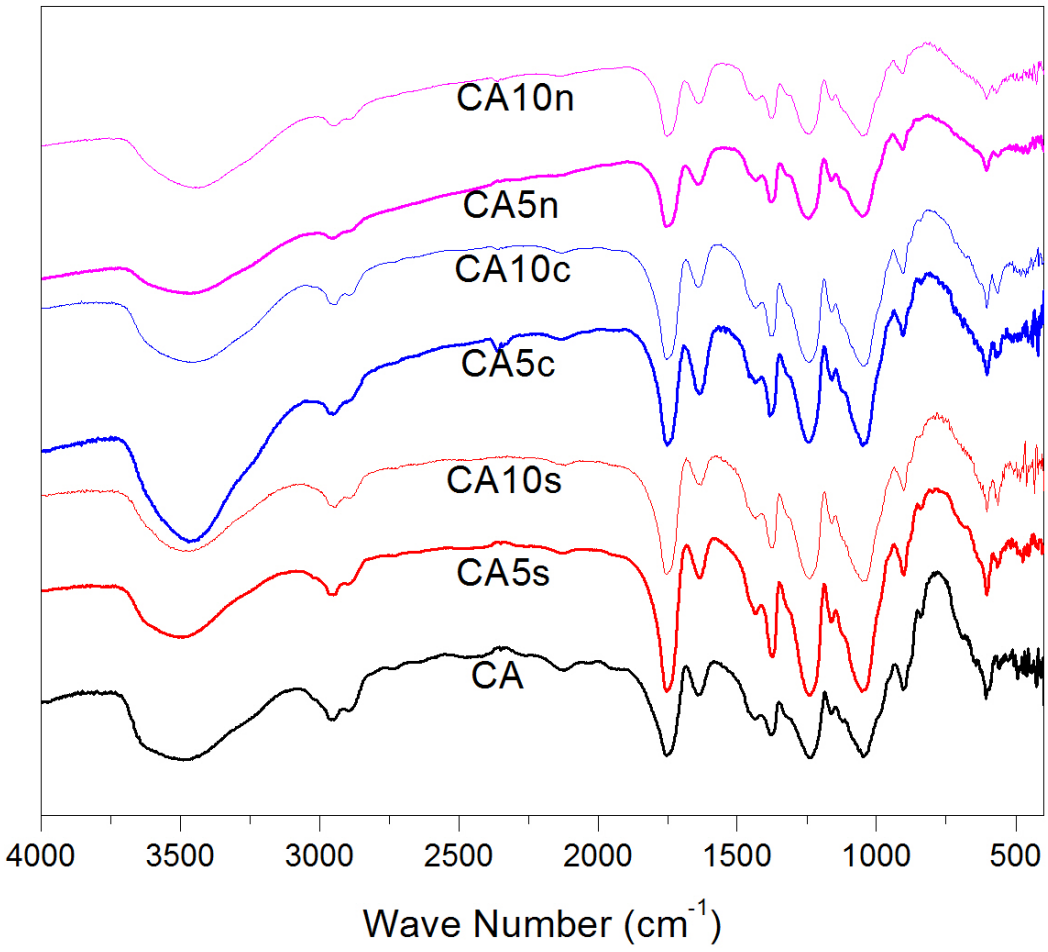

Figure 35: Infrared spectra of the pure CA and CA, containing as-received-prepared/received Haps, fibrous membranes

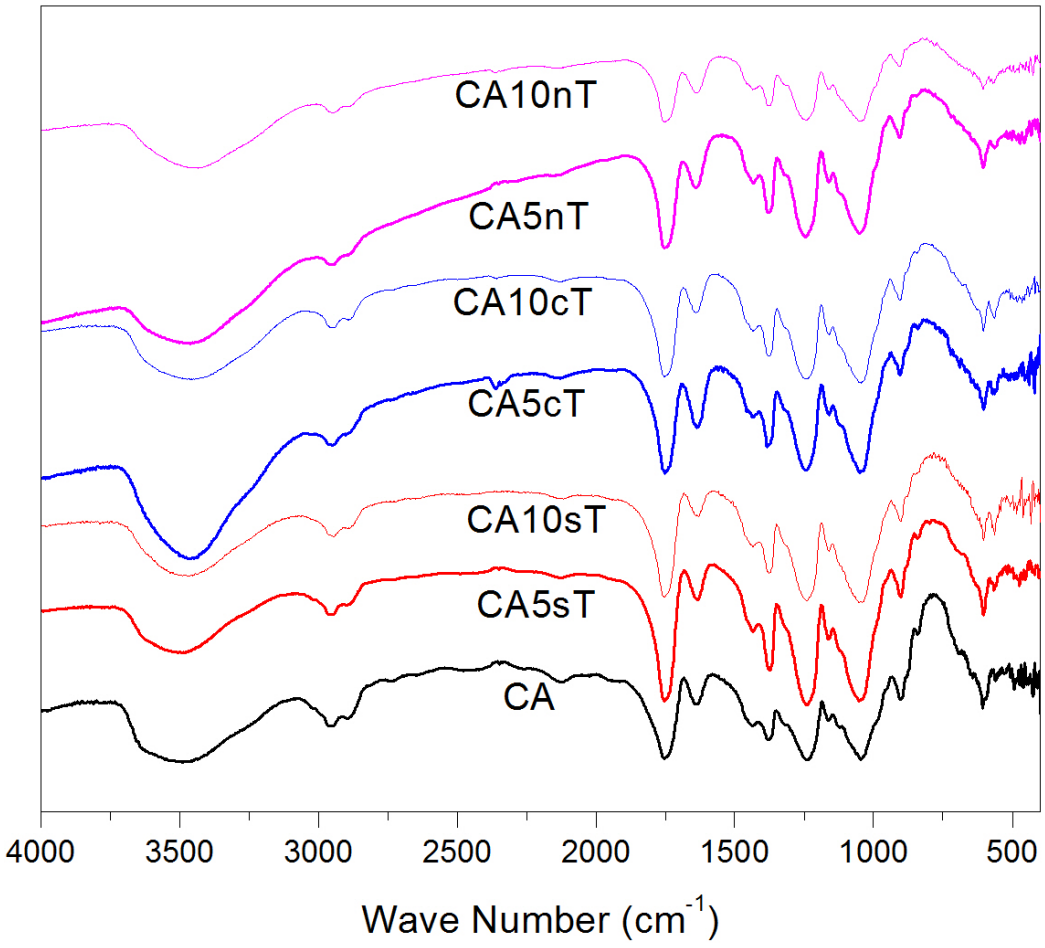

Figure 36: Infrared spectra of the pure CA and CA, containing heat-treated Haps, fibrous membranes

Due to the broadness of the CA bands and the presence of CA as a major phase (90-95% by weight), it was not obvious to directly detect the HAp main bands due to the pronounced overlap. However, a single band denoting the bending mode of vibration of P-O of the apatitic functional group (PO_4^{3-}) was shown at 564 cm^{-1} in all spectra of CA-HAp composite fibers. This specific band does not overlap with any of the CA bands and was therefore evident to find in the spectra of the CA-HAp composite fibers. The presence of this band was confirmed in the spectra of CA containing all types of HAp, both as received/prepared and thermal treated. The effect of increased crystallinity of the HAp powders as a result of thermal treatment, that was previously sown in the spectra of the thermally treated Ca-deficient apatitic powders, was not easily recognized in the spectra of the CA-stoichiometric HAp samples. This is also attributed to the dominating effect of the higher proportion CA in all samples in addition to the overlap between its bands and those of stoichiometric HAp.

3.2.2.3 Thermogravimetric Analysis (TGA)

All fibrous samples containing CA and 5 and 10 wt% of each of the as-received/prepared and thermally treated stoichiometric powders were investigated for their thermal history by TGA analysis. Figures 37-38 show the obtained TGA thermograms of all samples with that of pure CA fibrous sample as a control. Due to the organic nature of CA, mostly hydrophobic, it starts losing weight at temperatures above 300°C. Two thermal events were observed. The first started at 325°C until 415°C and accounts for the degradation of the CA polymeric chain. This gave rise to an average weight loss of 90%. This step was followed by combustion of the degraded species at 415°C until a complete combustion is reached at 495°C where the entire material was decomposed.

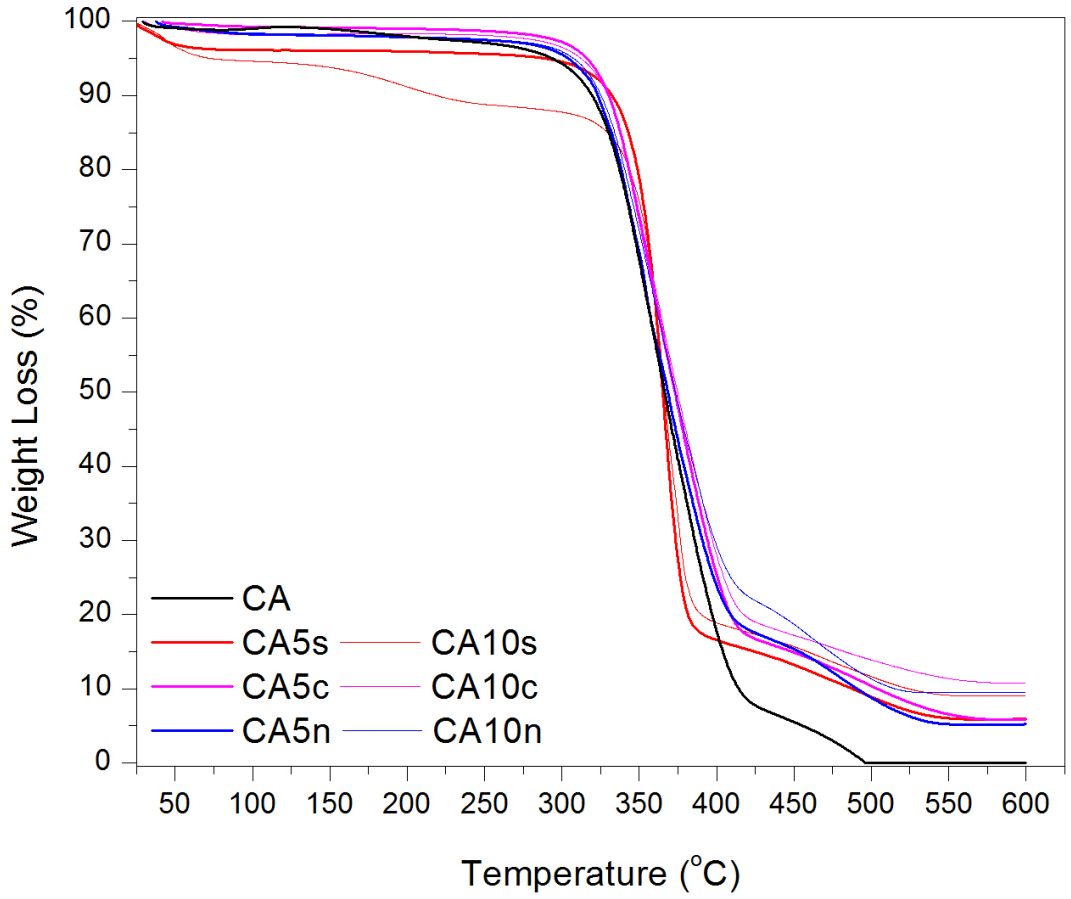

Figure 37: Thermogravimetric diagram of the pure CA and CA, containing as-received/prepared Haps, fibrous membranes

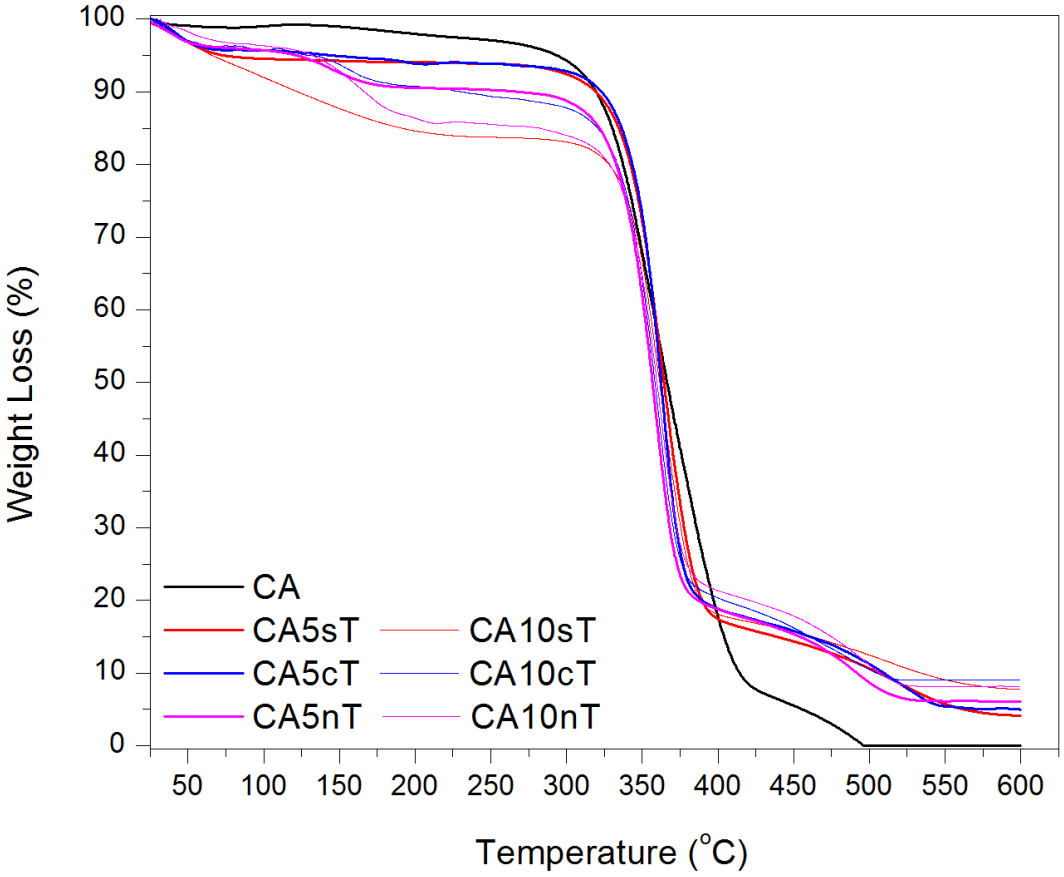

Figure 38: Thermogravimetric diagram of the pure CA and CA, containing heat-treated Haps, fibrous membranes

In the presence of inorganic stoichiometric HAp species, a similar weight loss pattern was followed with the exception of the sample containing synthetic HAp in which an earlier weight loss at 100°C was observed, as shown in Figure 37. This is related to the presence of physically attached water in the prepared sample, unlike the other commercial product that appear to be completely dry in the as-received form prior mixing with CA and making the composite fibrous membrane thereof. Additionally, the sample containing 10 wt% of sHAp showed another weight loss event at 240°C until 300°C, which is attributed to the removal of the chemically attached water (water of crystallization). Unlike the complete decomposition of the pure CA fibrous sample by reaching the end of the thermal treatment cycle at 600°C, all composite fibrous samples containing CA and stoichiometric HAp particulates showed a maximum overall weight loss of 95%, with the remaining material being the undecomposed HAp dispersed powder.

On the other hand, Figure 38 shows a similar weight loss pattern of all samples, with CA completely decomposed by the end of thermal treatment and other samples containing the inorganic HAp particulates ending their loss at a maximum of 95%. In addition, all composite fibrous samples containing HAp particulates showed an initial weight loss around 100°C, due to the removal of the weakly adsorbed water of hydration. A second weight loss event was also observed at 225-300°C due to the removal of the chemically attached water of crystallization. These results are in agreement with the fact that ceramic particulates that are deprived from their water of hydration by thermal treatment are more susceptible to adsorb moisture than the as prepared-received powders, which explains the initial weight loss around 100°C.

3.2.3 Sorption of Cd^{2+} Ions

Cellulose membranes containing various types of stoichiometric HAp particulates, both as received/prepared and heat treated, were evaluated for their efficiency in adsorbing and removing Cd^{2+} ions from simulated polluted aqueous media. These membranes were fabricated using an electrospinning technique, in which the solid apatitic particulates were homogeneously dispersed within the fibrous CA membrane, where the latter made the matrix of the composite fibrous membranes. It should be noted that CA was used in this regard as a non-expensive source of polymer that widely exist in nature, either in its form or in its original form as cellulose. Moreover, the fibrous nature of the membranes as prepared by electrospinning was designed to make a scaffold in which the main sorbent material; stoichiometric HAp, was contained. It should be also noted that CA was previously investigated for its sole capability to act as a sorbent for the removal of different types of heavy metal cations (Tian et al., 2011). However, its chemical structure that is shown in Figure 3d does not provide an acceptable explanation of its proposed success due to the presence of –OH groups only along its structural backbone. This functional group has a tendency towards the adsorption of positive cations in aqueous media, while the dominating ester groups have a weaker tendency to adsorb the positive ionic pollutants. Therefore, a combination of an ion exchange material such as HAp within the matrix of a fibrous CA membrane was believed to provide a reasonable alternative to pure CA fibrous membrane. Moreover, the fibrous geometry of the produced membranes makes it feasible to be used as filtering membranes for the purification of drinking water from heavy metal ions.

CA-HAp fibrous membranes were, therefore, evaluated for their affinity towards Cd^{2+} ions in solutions. The effect of varying the solution conditions, such as pH, sorbent weight, sorbate initial concentration and sorption contact time, on the efficiency of the combined membranes to remove Cd^{2+} ions was thoroughly investigated. The following sections describes the obtained results, where pure CA membranes were used for comparison, while the previous sorption results obtained in the first part of the thesis were also considered.

3.2.3.1 Effect of pH

Figures 39-40 show the variation of the concentrations of the remaining Cd^{2+} ions with the pH of the medium as a function of the type of sorbent material. It should be mentioned that the proportions of the stoichiometric HAp particulates within the fibrous CA membranes were 5 and 10% by weight. According to the results shown in both figures, it is evident that a slight difference was shown in the efficiency of the sorbents containing sHAp particulates than that of pure CA towards the removal of Cd^{2+} ions. This could be related to the low concentration of the sHAp particulates in the membranes, while the matrix was made of the less efficient CA fibrous material. However, it can be also seen that membranes containing 10% of all sHAp sorbent particulates were slightly more efficient than those containing 5 wt% and pure CA, as shown in Figure 39. Despite the fact that nHAp particulates were in the nanometer scale, which were believed to have a higher surface area, hence higher sorption capacity, their performance did not reflect these facts. This could be related to the agglomeration of the nanoparticles of nHAp, as was shown in their micrographs in Figure 30.

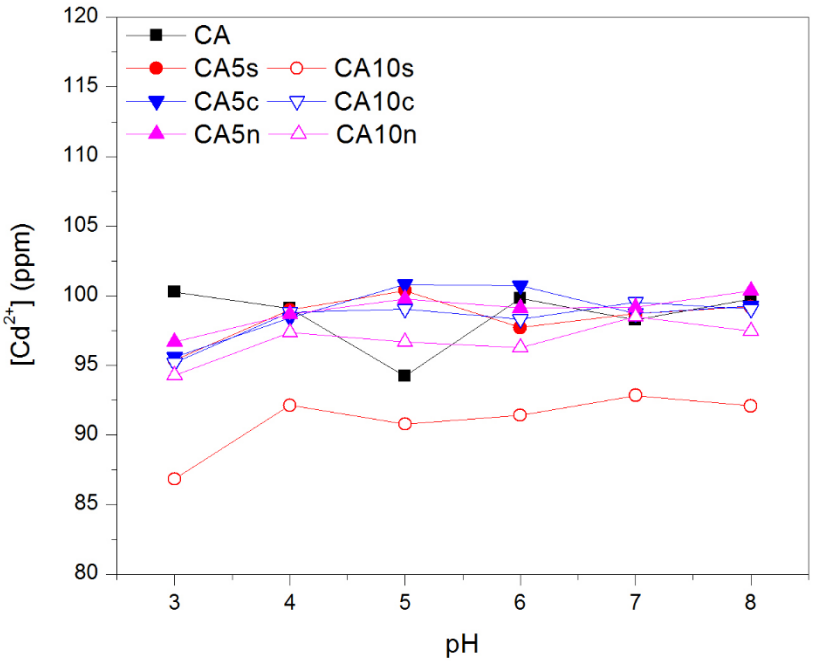

Figure 39: Effect of changing solution pH on the sorption of Cd^{2+} ions using CA-pure HAp composite membranes

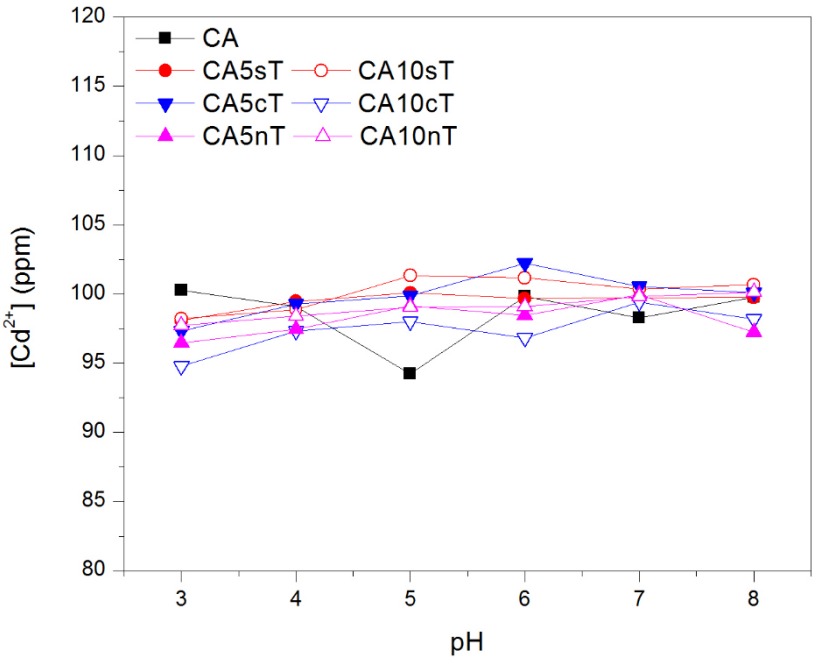

Figure 40: Effect of changing solution pH on the sorption of Cd^{2+} ions using CA-heat treated HAp composite membranes

Moreover, these agglomerated clusters of nHAp were electrospun within the CA fibers, as shown in their micrographs in Figures 33-34, which is believed to slightly hinder their sorption effect as being contained within the CA fibers. It is important to note, however, that electrospinning as a fiber-making technique, does not provide a method to control the location of solid particulates when electrospun in a matrix of a polymer. In fact, there is always a possibility to have the solid particulates distributed within the fibers and entrapped between the fibers within the obtained membranes. Based on these results, a pH 5.5 was selected to be maintained throughout the following experiments to avoid the degradation of CA at higher pH values, or the solubility of the apatitic filler particulates at lower pH values.

3.2.3.2 Effect of Sorbent Weight

The effect of varying the weight of the CA-HAp fibrous sorbent on their efficiency in the removal of Cd^{2+} ions was investigated, as shown in Figures 41-42. These experiments were carried out at a constant sorbate (Cd^{2+}) concentration of 1 mmol and contact time of 24 hours in a pH 5.5 adjusted media. A pure CA fibrous sorbent showed a minimal adsorption of Cd^{2+} ions from the medium, indicating its low affinity towards the adsorption of Cd^{2+} ions. Upon the addition of stoichiometric HAp particulates within the electrospun CA membranes, a noticeable increase in the affinity of the fibrous sorbents was observed. This improvement was noticed with the increase in the proportion of the apatitic sorbent particulates in the fibers, which is related to its anticipated higher affinity to adsorb Cd^{2+} ions, as shown in Figure 42. A continued decrease in the concentration of Cd^{2+} ions was observed with increasing the initial weight of the composite fibrous sorbent, both as-received/prepared and heat treated. However, this trend was more pronounced with the presence of the as-received/prepared apatitic particulates. This is related to the decreased chemical reactivity of the heat-treated apatite particulates of all types. The variation in the affinity of the composite fibrous sorbents containing heat treated apatitic particulates of various origins was not significant. A complete removal of the Cd^{2+} ions from the tested media samples was not possible using these composite fibrous sorbents, which can be related to the low proportion of the more effective apatitic sorbent particulates in the composite fibrous sorbents. Based on these results, a constant sorbent weight of 0.01 gram was selected for the following set of experiments.

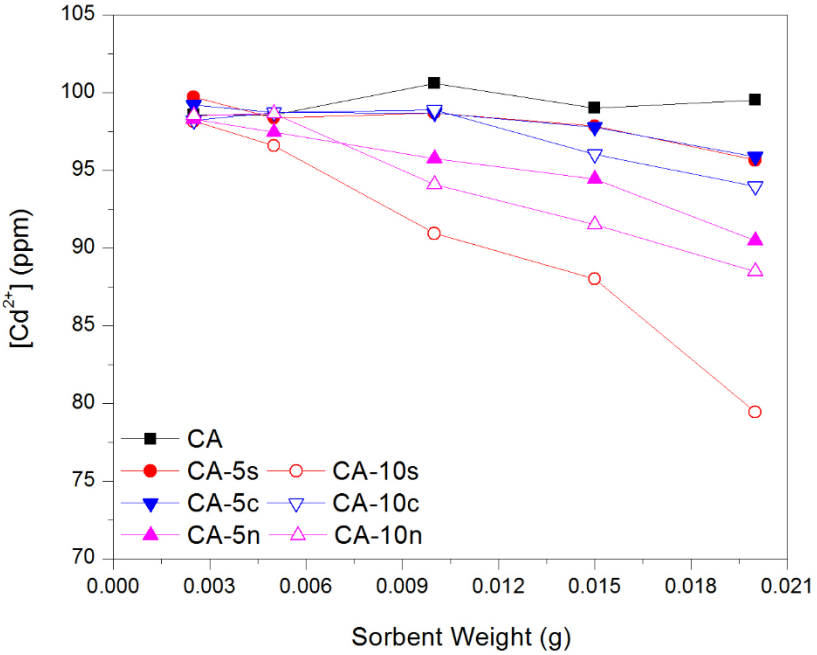

Figure 41: Effect of changing sorbent weight on the sorption of Cd^{2+} ions using CA-pure HAp composite membranes

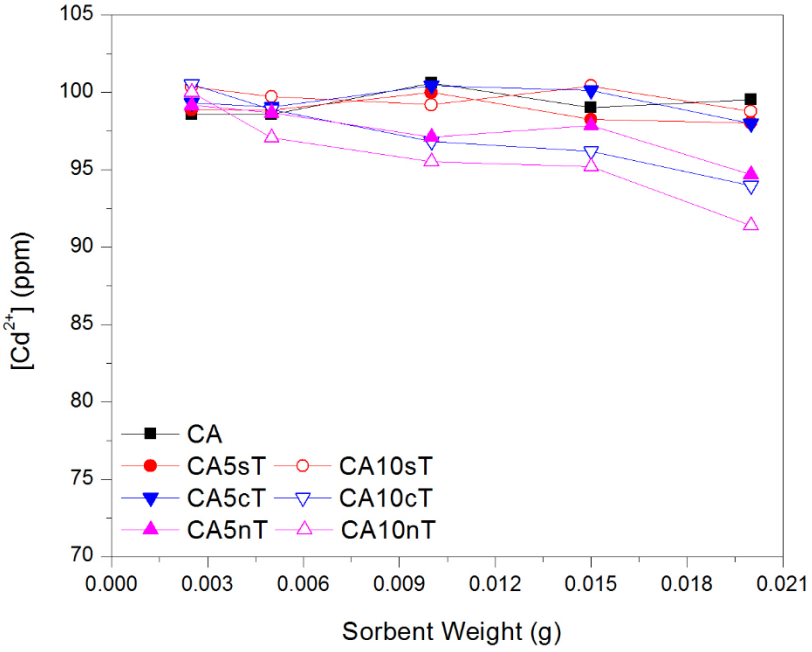

Figure 42: Effect of changing sorbent weight on the sorption of Cd^{2+} ions using CA-heat treated HAp composite membranes

3.2.3.3 Effect of Sorbate (Cd^{2+}) Concentration

Figures 43-44 show the variation in the concentration of Cd^{2+} ions initially added to the simulated polluted aqueous media on the efficiency of the tested composite fibrous sorbent to remove these ionic pollutants, as a function of the type of sorbent. A fixed sorbent weight, pH, and contact time were maintained throughout these experiments. An increase in the remaining concentrations of Cd^{2+} ions was observed with increasing the concentration of the initially added Cd^{2+} ions regardless of the type of sorbent used. The variation in the affinity of the tested sorbents with their different types was insignificant, where all sorbents showed a similar trend. This could be related to the limited affinity of the tested sorbents due to the low concentration of the active apatitic sorbent material originally added to the composite fibrous sorbents. Therefore, no significant variation was shown for replacing the as-received/prepared apatitic particulates with the heat-treated ones. Accordingly, a constant concentration of the initial sorbate solutions of 1 mmol was maintained for the following experiments, while keeping the sorbent weight and pH also constant.

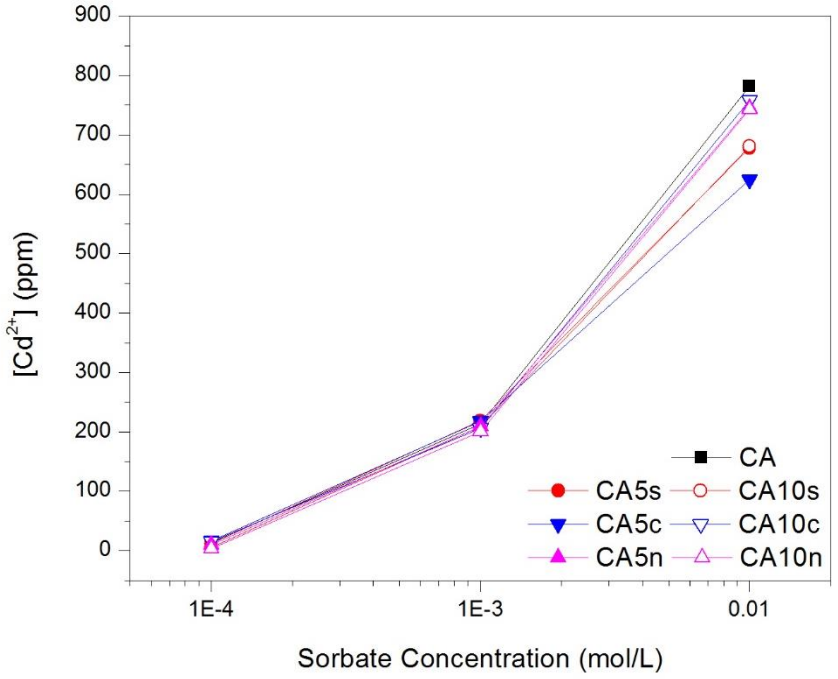

Figure 43: Effect of varying initial concentration of Cd^{2+} ions on the efficiency of the CA-pure HAp composite membranes

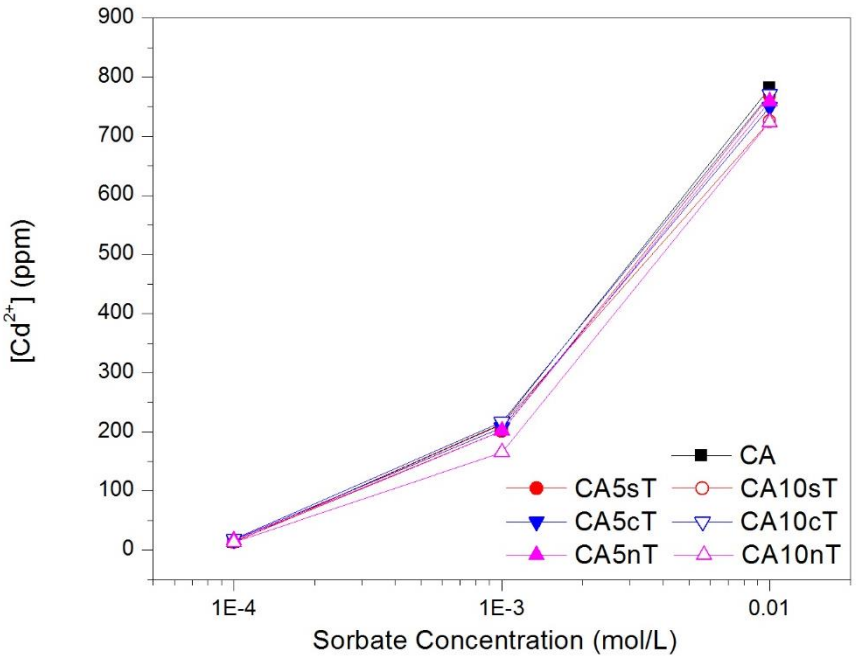

Figure 44: Effect of varying initial concentration of Cd^{2+} ions on the efficiency of the CA-heat treated HAp composite membranes

3.2.3.4 Effect of Sorption Time

The fourth parameter to be evaluated in this study was the effect of varying the contact time between the composite fibrous sorbent and the simulated polluted solution, while keeping the pH, sorbent weight, and sorbate concentration constant as a function of the type of composite fibrous sorbent. Figures 45-46 show these findings, where a pure CA fibrous membrane was also evaluated as a control. All samples showed a sudden decrease in the concentration of the remaining Cd^{2+} ions in solution within the first 90 minutes of exposure of the sorbents to the Cd^{2+}-containing media. This was related to the partial removal of Cd^{2+} ions from the media, where an estimation of 9% of Cd^{2+} ions was removed. This was followed by a plateau where the concentrations of the remaining Cd^{2+} ions were maintained, indicating the end of sorption of the Cd^{2+} ions and the saturation of the used sorbents. This trend was more evident in Figure 46, where CA fibrous sorbents containing heat-treated apatitic particulates were use. On the other hand, the sudden decrease in the concentrations of the remaining Cd^{2+} ions were followed by a second stage of slow adsorption of the Cd^{2+} ions when CA fibrous sorbents containing as-received/prepared apatitic particulates were used, as shown in Figure 45. This trend could be explained in terms of the relatively higher reactivity of the as-received/prepared apatitic particulates as compared with the heat-treated ones. Moreover, the slow sorption within this stage could be related to the diffusion of the Cd^{2+} ions within the fibrous membrane and the possibility of having the apatitic particulates entrapped within the 3D arrangement of the CA fibers.

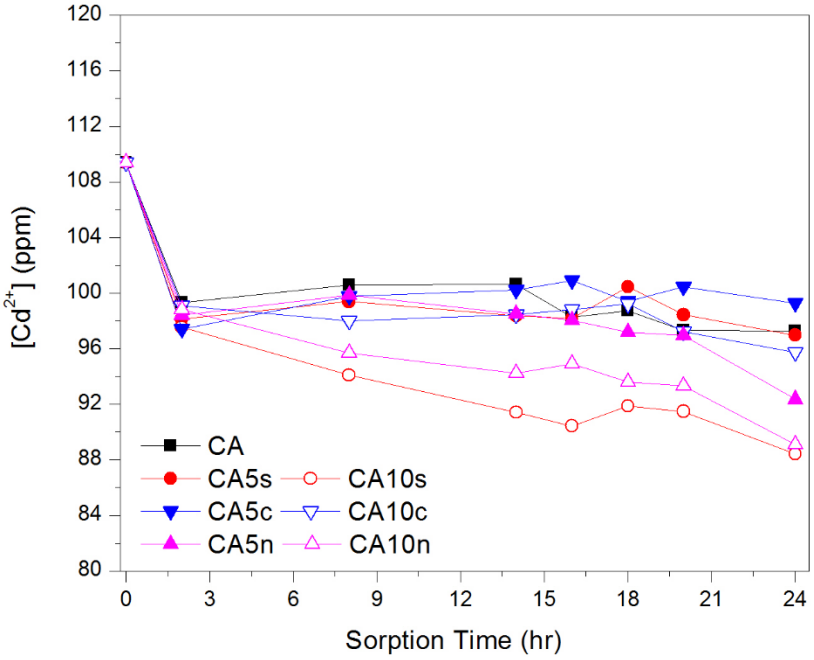

Figure 45: Effect of varying contact time on the efficiency of the removal of Cd^{2+} ions using CA-pure HAp composite membranes

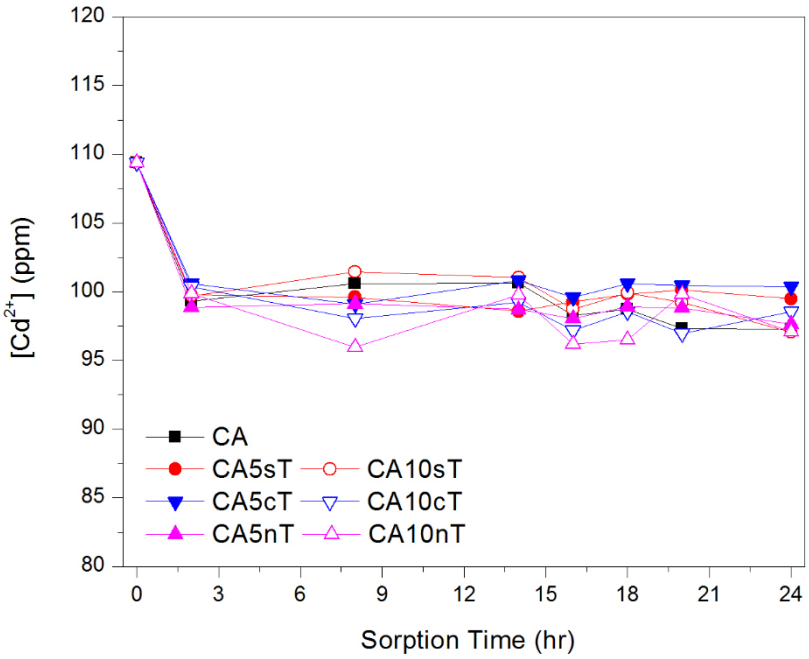

Figure 46: Effect of varying contact time on the efficiency of the removal of Cd^{2+} ions using CA-heat treated HAp composite membranes

Based on these results, it is evident that the sorption of Cd^{2+} ions is greatly dependent on the type and proportion of the apatitic sorbent particulates to a large extent. While the role of CA fibers was mainly to accommodate and contain the apatitic solid particulates so that a composite fibrous membrane could be used for the purification of aqueous media from the soluble Cd^{2+} ions. However, the low efficiency of the composite fibrous sorbent, which was related to the low proportion of the apatitic particulates in the membranes, should be enhanced while optimizing the electrospinning conditions to have a well-designed fibrous membrane.

Chapter 4: Conclusion

The current study investigated the use of two types of solid sorbents - particulates and particulate/fibrous assembly - for the removal of Cd^{2+} ions from simulated waste water media. The solid particulate sorbent material was based on calcium phosphate, which is known as an efficient ion-exchange material for soluble ions in aqueous media. The effect of varying the initial Ca/P molar ratio of the calcium phosphate solid particulate sorbent materials on their structure, morphology and affinity towards the sorption of Cd^{2+} ions were thoroughly evaluated. On the other hand, fibrous sorbent material that is based on CA was fabricated by an electrospinning technique. Both pure CA and CA-containing stoichiometric HAp particulates were made by the same technique and were also evaluated for their structure, morphology and affinity towards the sorption of Cd^{2+} ions from simulated polluted aqueous media. Moreover, the effect of thermal treatment of all calcium phosphate sorbents before being evaluated in their pure form and after being incorporated within the CA fibers, on the affinity of their corresponding sorbent materials towards Cd^{2+} ions was also investigated.

Results showed the high potential of the calcium phosphate sorbent materials towards the removal of Cd^{2+} ions through an ion-exchange mechanism. The presence of vacancies in the Ca-deficient apatite sorbent (Ca/P < 1.67) was found not to enhance their affinity towards Cd^{2+} ions, which could be related to the shrinkage of the crystal structure as a result of deficiency, where the produced vacancy size is not suitable to be accommodated by Cd^{2+} ions from solution. On the other hand, the presence of a lower proportion of the stoichiometric HAp in its various forms: synthetic, micrometer commercial and nanometer commercial, slightly participated in the sorption of Cd^{2+}

ions, when these solid particulates were included within a CA fibrous membrane. In addition to their low proportion, this was also attributed to the lower affinity of the CA fibrous incubator. Moreover, it was found that initial thermal treatment of the pure calcium phosphates and those, added to CA to make their composite sorbent membranes, slightly lowered the affinity of the produced sorbents towards Cd^{2+} ions.

These findings indicate the suitability of calcium phosphate sorbent materials, especially after thermal treatment to be made into the form of porous membrane so that it can be used as one of the steps of water treatment, for the removal of heavy metal ions such as Cd^{2+}. On the other hand, the effect of increasing the proportion of stoichiometric HAp particulates within the fibrous membranes of CA could be also re-visited without compromising the fibrous nature of the produced composite membranes. This is highly expected to result in the emerge of a highly porous 3D composite fibrous membrane that can be used for the removal of heavy metal ions, as well as solid sub-micrometer size particulates that was previously proven in our laboratory.

As a future prospect work, an evaluation of the kinetics of the sorption process using both types of sorbents will be conducted along with an investigation of the effect of conflicting ions on the sorption of Cd^{2+} and the possibility of recycling the sorbents.

References

Abdel-Halim, E. S., Abou-Okeil, A., & Hashem, A. (2007). Adsorption of Cr(VI) oxyanions onto modified wood pulp. *Polymer-Plastics Technology and Engineering*, *45*(1), 71–76.

Abdel-Halim, E. S., & Al-Deyab, S. S. (2011). Utilization of hydroxypropyl cellulose for green and efficient synthesis of silver nanoparticles. *Carbohydrate Polymers*, *86*(4), 1615–1622. https://doi.org/10.1016/j.carbpol.2011.06.072

Abdel-Halim, E. S., & Al-Deyab, S. S. (2012). Chemically modified cellulosic adsorbent for divalent cations removal from aqueous solutions. *Carbohydrate Polymers*, *87*(2), 1863–1868. https://doi.org/10.1016/j.carbpol.2011.10.028

Agarwal, S. K. (2009). *Heavy Metal Pollution*. New Delhi: A.P.H. Pub. Corp.

Alyuz, B., & Veli, S. (2009). Kinetics and equilibrium studies for the removal of nickel and zinc from aqueous solutions by ion exchange resins. *Journal of Hazardous Materials*, *167*(1–3), 482–488. https://doi.org/DOI 10.1016/j.jhazmat.2009.01.006

Aoki, D., Teramoto, Y., & Nishio, Y. (2007). SH-Containing Cellulose Acetate Derivatives: Preparation and Characterization as a Shape Memory-Recovery Material. *Biomacromolecules*, *8*(12), 3749–3757. https://doi.org/10.1021/bm7006828

Arahira, T., Maruta, M., & Matsuya, S. (2017). Characterization and in vitro evaluation of biphasic α-tricalcium phosphate/β-tricalcium phosphate cement. *Materials Science and Engineering: C*, *74*, 478–484. https://doi.org/10.1016/J.MSEC.2016.12.049

Atila, D., Keskin, D., & Tezcaner, A. (2015). Cellulose acetate based 3-dimensional electrospun scaffolds for skin tissue engineering applications. *Carbohydrate Polymers*, *133*, 251–261. https://doi.org/10.1016/j.carbpol.2015.06.109

Azizullah, A., Khattak, M. N. K., Richter, P., & Häder, D.-P. (2011). Water pollution in Pakistan and its impact on public health — A review. *Environment International*, *37*(2), 479–497. https://doi.org/10.1016/j.envint.2010.10.007

Babel, S. (2003). Low-cost adsorbents for heavy metals uptake from contaminated water: a review. *Journal of Hazardous Materials*, *97*(1–3), 219–243. https://doi.org/10.1016/S0304-3894(02)00263-7

Bailey, S. E., Olin, T. J., Bricka, R. M., & Adrian, D. D. (1999). A review of potentially low-cost sorbents for heavy metals. *Water Research*, *33*(11),

2469–2479. https://doi.org/10.1016/S0043-1354(98)00475-8

Boanini, E., Gazzano, M., & Bigi, A. (2010). Ionic substitutions in calcium phosphates synthesized at low temperature. *Acta Biomaterialia*, *6*(6), 1882–1894. https://doi.org/10.1016/j.actbio.2009.12.041

Boudia, S., Zuddas, P., Fernane, F., Fiallo, M., & Sharrock, P. (2018). Mineralogical transformation during hydroxyapatite dissolution in simple aqueous solutions. *Chemical Geology*, *477*, 85–91. https://doi.org/10.1016/J.CHEMGEO.2017.12.007

Cai, Z.-Y., Peng, F., Zi, Y.-P., Chen, F., & Qian, Q.-R. (2015). Microwave-Assisted Hydrothermal Rapid Synthesis of Calcium Phosphates: Structural Control and Application in Protein Adsorption. *Nanomaterials*, *5*(3), 1284–1296. https://doi.org/10.3390/nano5031284

Candena, F., Rizvi, R., & Peters, R. W. (1990). Feasibility studies for the removal of heavy metal from solution using Tailored bentonite. In *Twenty-second Mid-Atlantic Industrial Waste Conference* (p. 77).

Cao, J., Tan, Y., Che, Y., & Xin, H. (2010). Novel complex gel beads composed of hydrolyzed polyacrylamide and chitosan: An effective adsorbent for the removal of heavy metal from aqueous solution. *Bioresource Technology*, *101*(7), 2558–2561. https://doi.org/10.1016/j.biortech.2009.10.069

Chen, G. (2004). Electrochemical technologies in wastewater treatment. *Separation and Purification Technology*, *38*(1), 11–41. https://doi.org/10.1016/j.seppur.2003.10.006

Chen, S., Zou, Y., Yan, Z., Shen, W., Shi, S., Zhang, X., & Wang, H. (2009). Carboxymethylated-bacterial cellulose for copper and lead ion removal. *Journal of Hazardous Materials*, *161*(2–3), 1355–1359. https://doi.org/10.1016/j.jhazmat.2008.04.098

Chen, Z., Deng, M., Chen, Y., He, G., Wu, M., & Wang, J. (2004). Preparation and performance of cellulose acetate/polyethyleneimine blend microfiltration membranes and their applications. *Journal of Membrane Science*, *235*(1–2), 73–86. https://doi.org/10.1016/j.memsci.2004.01.024

Chui, V., Mok, K., Ng, C., Luong, B., & Ma, K. (1996). Removal and recovery of copper (II), chromium (III), and nickel (II) from solutions using crude shrimp chitin paked in small columns. *Environment International*, *22*(4), 463–468.

Ciobanu, G., Carja, G., Ignat, D., Luca, C., & Harja, M. (2010). Lead Ions Removal with Cellulose Acetate/Hydroxyapatite Composite Membranes. *Petroleum - Gas University of Ploiesti Bulletin, Technical Serie*, *62*(3A), 47.

Ćurković, L., Cerjan-Stefanović, Š., & Filipan, T. (1997). Metal ion exchange by natural and modified zeolites. *Water Research*, *31*(6), 1379–1382. https://doi.org/10.1016/S0043-1354(96)00411-3

Deitzel, J. ., Kleinmeyer, J., Harris, D., & Beck Tan, N. (2001). The effect of processing variables on the morphology of electrospun nanofibers and textiles. *Polymer*, *42*(1), 261–272. https://doi.org/10.1016/S0032-3861(00)00250-0

Elliott, J. C. (1994). *Structure and chemistry of the apatites and other calcium orthophosphates*. Amsterdam [The Netherlands] : New York: Elsevier.

Estrella, M. B. de, Flores, S. T. de, Bonini, N. A., Gonzo, E., Pérez, N. P., & Arias, A. N. (2015). Rapid Synthesis of Nanometric Cellulose Hydroxyapatite. *Procedia Materials Science*, *8*, 608–616. https://doi.org/10.1016/j.mspro.2015.04.115

Fu, F., & Wang, Q. (2011). Removal of heavy metal ions from wastewaters: A review. *Journal of Environmental Management*, *92*(3), 407–418. https://doi.org/10.1016/j.jenvman.2010.11.011

Gong, J., Liu, J., Jiang, Z., Wen, X., Mijowska, E., Tang, T., & Chen, X. (2015). A facile approach to prepare porous cup-stacked carbon nanotube with high performance in adsorption of methylene blue. *Journal of Colloid and Interface Science*, *445*, 195–204. https://doi.org/10.1016/j.jcis.2014.12.078

Greish, Y. E., Meetani, M. A., Al Matroushi, E. A., & Al Shamsi, B. (2010). Effects of thermal and chemical treatments on the structural stability of cellulose acetate nanofibers. *Carbohydrate Polymers*, *82*(3), 569–577. https://doi.org/10.1016/j.carbpol.2010.05.012

Gyliene, O., Rekertas, R., & Salkauskas, M. (2002). Removal of free and complexed heavy-metal ions by sorbents produced from fly (Musca domestica) larva shells. *Water Research*, *36*(16), 4128–4136. https://doi.org/10.1016/S0043-1354(02)00105-7

Haberko, K., Bućko, M. M., Brzezińska-Miecznik, J., Haberko, M., Mozgawa, W., Panz, T., Zarębski, J. (2006). Natural hydroxyapatite—its behaviour during heat treatment. *Journal of the European Ceramic Society*, *26*(4–5), 537–542. https://doi.org/10.1016/J.JEURCERAMSOC.2005.07.033

Haileslassie, T., & Gebremedhin, K. (2015). Hazards Of Heavy Metal Contamination In Ground Water. *International Journal of Technology Enhancements and Emerging Engineering Research*, *3*(02), 1–6.

Hashem, A., Abdel-Halim, E. S., Maauof, H. A., Ramadan, M. A., & Abo-Okeil, A. (2007). Treatment of sawdust with polyamine for wastewater treatment.

Energy Education Science and Technology, *19*, 45–58.

Hashem, A., Abdel-Halim, E. S., & Sokker, H. H. (2007). Bi-functional Starch Composites Prepared by γ-irradiation for Removal of Anionic and Cationic Dyes from Aqueous Solutions. *Polymer-Plastics Technology and Engineering*, *46*(1), 71–77. https://doi.org/10.1080/03602550600950364

Hashem, A., Sokker, H. H., Halim, E. S. A., & Gamal, A. (2005). γ-Induced Graft Copolymerization onto Cellulosic Fabric Waste for Cationic Dye Removal. *Adsorption Science & Technology*, *23*(6), 455–466. https://doi.org/10.1260/026361705774859901

Hem, J. D., Lind, C. J., & Roberson, C. E. (1989). Coprecipitation and redox reactions of manganese oxides with copper and nickel. *Geochimica et Cosmochimica Acta*, *53*(11), 2811–2822. https://doi.org/10.1016/0016-7037(89)90159-2

Hinrichsen, D. Tacio, H. (2002). "The coming freshwater crisis is already here. Finding the Source". The Linkages between Population and Water, Woodrow Wilson International Center for Scholars, Washington, DC, ESCP Publication, Spring. Retrieved October 29, 2018, from http://www.sciepub.com/reference/169629

Hodson, M. E., Valsami-Jones, É., & Cotter-Howells, J. D. (2000). Bonemeal Additions as a Remediation Treatment for Metal Contaminated Soil. *Environmental Science & Technology*, *34*(16), 3501–3507. https://doi.org/10.1021/es990972a

Huie, J. C. (2003). Guided molecular self-assembly: a review of recent efforts. *Smart Materials and Structures*, *12*(2), 264–271. https://doi.org/10.1088/0964-1726/12/2/315

Hung, I.-M., Shih, W.-J., Hon, M.-H., & Wang, M.-C. (2012). The properties of sintered calcium phosphate with [Ca]/[P] = 1.50. *International Journal of Molecular Sciences*, *13*(10), 13569–13586. https://doi.org/10.3390/ijms131013569

Inglezakis, V. J., Papadeas, C. D., Loizidou, M. D., & Grigoropoulou, H. P. (2001). Effects of pretreatment on physical and ion exchange properties of natural clinoptilolite. *Environmental Technology*, *22*(1), 75–82. https://doi.org/10.1080/09593332208618308

Ji, F., Li, C., Tang, B., Xu, J., Lu, G., & Liu, P. (2012). Preparation of cellulose acetate/zeolite composite fiber and its adsorption behavior for heavy metal ions in aqueous solution. *Chemical Engineering Journal*, *209*, 325–333. https://doi.org/10.1016/j.cej.2012.08.014

Kalayci, V. E., Patra, P. K., Kim, Y. K., Ugbolue, S. C., & Warner, S. B. (2005). Charge consequences in electrospun polyacrylonitrile (PAN) nanofibers. *Polymer*, *46*(18), 7191–7200. https://doi.org/10.1016/J.POLYMER.2005.06.041

Kamel, S., Hassan, E. M., & El-Sakhawy, M. (2006). Preparation and application of acrylonitrile-grafted cyanoethyl cellulose for the removal of copper (II) ions. *Journal of Applied Polymer Science*, *100*(1), 329–334. https://doi.org/10.1002/app.23317

Kang, S.-Y., Lee, J.-U., Moon, S.-H., & Kim, K.-W. (2004). Competitive adsorption characteristics of Co2+, Ni2+, and Cr3+ by IRN-77 cation exchange resin in synthesized wastewater. *Chemosphere*, *56*(2), 141–147. https://doi.org/10.1016/j.chemosphere.2004.02.004

Kenawy, I. M., Hafez, M. A. H., Ismail, M. A., & Hashem, M. A. (2018). Adsorption of Cu(II), Cd(II), Hg(II), Pb(II) and Zn(II) from aqueous single metal solutions by guanyl-modified cellulose. *International Journal of Biological Macromolecules*, *107*, 1538–1549. https://doi.org/10.1016/J.IJBIOMAC.2017.10.017

Kesraoui-Ouki, S., Cheeseman, C., & Perry, R. (1993). Effects of conditioning and treatment of chabazite and clinoptilolite prior to lead and cadmium removal. *Environmental Science & Technology*, *27*(6), 1108–1116. https://doi.org/10.1021/es00043a009

Kessick, R., Fenn, J., & Tepper, G. (2004). The use of AC potentials in electrospraying and electrospinning processes. *Polymer*, *45*(9), 2981–2984. https://doi.org/10.1016/J.POLYMER.2004.02.056

Kurita, K., Koyama, Y., & Taniguchi, A. (1986). Studies on chitin. IX. Crosslinking of water-soluble chitin and evaluation of the products as adsorbents for cupric ion. *Journal of Applied Polymer Science*, *31*(5), 1169–1176. https://doi.org/10.1002/app.1986.070310502

Kurita, K., Sannan, T., & Iwakura, Y. (1979). Studies on chitin. VI. Binding of metal cations. *Journal of Applied Polymer Science*, *23*(2), 511–515. https://doi.org/10.1002/app.1979.070230221

Kurniawan, T. A., Chan, G. Y. S., Lo, W.-H., & Babel, S. (2006). Physico–chemical treatment techniques for wastewater laden with heavy metals. *Chemical Engineering Journal*, *118*(1), 83–98. https://doi.org/10.1016/j.cej.2006.01.015

Kutowy, O., & Sourirajan, S. (1975). Cellulose acetate ultrafiltration membranes. *Journal of Applied Polymer Science*, *19*(5), 1449–1460.

https://doi.org/10.1002/app.1975.070190525

Landi, E., Celotti, G., Logroscino, G., & Tampieri, A. (2003). Carbonated hydroxyapatite as bone substitute. *Journal of the European Ceramic Society*, *23*(15), 2931–2937. https://doi.org/10.1016/S0955-2219(03)00304-2

Li, D., & Xia, Y. (2004). Electrospinning of nanofibers: Reinventing the wheel? *Advanced Materials*. https://doi.org/10.1002/adma.200400719

Liu, C., & Bai, R. (2006). Adsorptive removal of copper ions with highly porous chitosan/cellulose acetate blend hollow fiber membranes. *Journal of Membrane Science*, *284*(1–2), 313–322. https://doi.org/10.1016/j.memsci.2006.07.045

Liu, F., Yu, J., Ji, X., & Qian, M. (2015). Nanosheet-structured boron nitride spheres with a versatile adsorption capacity for water cleaning. *ACS Applied Materials & Interfaces*, *7*(3), 1824–1832. https://doi.org/10.1021/am507491z

Lu, M., Guan, X., & Wei, D. (2011). Removing Cd 2+ by Composite Adsorbent Nano-Fe3O4 / Bacterial Cellulose. *Chemical Research in Chinese Universities*, *27*(50174014), 1031–1034.

Lu, M., Li, Y., Guan, X., & Wei, D. (2010). Preparation of bacterial cellulose and its adsorption (in Chinese). *Journal of Northeastern University: Natural Science*, *31*(8), 1196–1199.

Lu, M., Zhang, Y., Guan, X., Xu, X., & Gao, T. (2014). Thermodynamics and kinetics of adsorption for heavy metal ions from aqueous solutions onto surface amino-bacterial cellulose. *Transactions of Nonferrous Metals Society of China*, *24*(6), 1912–1917. https://doi.org/10.1016/S1003-6326(14)63271-4

Luong-Van, E., Grøndahl, L., Chua, K. N., Leong, K. W., Nurcombe, V., & Cool, S. M. (2006). Controlled release of heparin from poly(ε-caprolactone) electrospun fibers. *Biomaterials*, *27*(9), 2042–2050. https://doi.org/10.1016/J.BIOMATERIALS.2005.10.028

Ma, L. Q. Q. (1996). Factors influencing the effectiveness and stability of aqueous Pb immobilization by hydroxyapatite. *Journal of Environmental Quality*, *25*, 1420–1429.

Malliou, E., Loizidou, M., & Spyrellis, N. (1994). Uptake of lead and cadmium by clinoptilolite. *Science of the Total Environment, The*, *149*(3), 139–144. https://doi.org/10.1016/0048-9697(94)90174-0

Mier, M. V., Callejas, L. R., Gehr, R., Cisneros, B. E. J., & Alvarez, P. J. . (2001). Heavy metal removal with mexican clinoptilolite: *Water Research*, *35*(2), 373–378. https://doi.org/10.1016/S0043-1354(00)00270-0

Monteil-Rivera, F., & Fedoroff, M. (2002). Sorption of inorganic species on apatites from aqueous solutions. In *Encyclopedia of Surface and Colloid Science* (pp. 1–26). https://doi.org/10.1081/E-ESCS-120010190

Nagata, F., Yamauchi, Y., Tomita, M., & Kato, K. (2013). Hydrothermal synthesis of hydroxyapatite nanoparticles and their protein adsorption behavior. *Journal of the Ceramic Society of Japan*, *121*(1417), 797–801. https://doi.org/10.2109/jcersj2.121.797

Perez, M. A. (2000). Microfibers and method of making. *US Patent*, *110*, 588.

Pike, R. D. (1999). Superfine Microfiber Nonwoven Web. *US Patent*, *935*, 883.

Ravi Kumar, M. N. . (2000). A review of chitin and chitosan applications. *Reactive and Functional Polymers*, *46*(1), 1–27. https://doi.org/10.1016/S1381-5148(00)00038-9

Reneker, D. H., Chun, I., & Ertley, D. (2003). Process and Apparatus for the Production of Nanofibers. *US Patent*, *382*, 526. https://doi.org/10.1016/j.(73)

Rezaee, A., Asadikaram, G., Mirzai, M., Naimi, N., Rosa, D., & Sadegi, A. (2008). Removal of Arsenic Using Acetobacter xylinum Cellulose. *Journal of Biological Sciences*, *8*(1), 209–212. https://doi.org/10.3923/jbs.2008.209.212

Sağ, Y., & Aktay, Y. (2000). Mass transfer and equilibrium studies for the sorption of chromium ions onto chitin. *Process Biochemistry*, *36*(1–2), 157–173. https://doi.org/10.1016/S0032-9592(00)00200-4

Sajid, M., Nazal, M. K., Ihsanullah, Baig, N., & Osman, A. M. (2018). Removal of heavy metals and organic pollutants from water using dendritic polymers based adsorbents: A critical review. *Separation and Purification Technology*, *191*, 400–423. https://doi.org/10.1016/j.seppur.2017.09.011

Samatham, R., & Kim, K. J. (2006). Electric current as a control variable in the electrospinning process. *Polymer Engineering & Science*, *46*(7), 954–959. https://doi.org/10.1002/pen.20565

Sánchez-Márquez, J. A., Fuentes-Ramírez, R., Cano-Rodríguez, I., Gamiño-Arroyo, Z., Rubio-Rosas, E., Kenny, J. M., & Rescignano, N. (2015). Membrane Made of Cellulose Acetate with Polyacrylic Acid Reinforced with Carbon Nanotubes and Its Applicability for Chromium Removal. *International Journal of Polymer Science*, *2015*, 1–12. https://doi.org/10.1155/2015/320631

Sarkar, S., Deevi, S., & Tepper, G. (2007). Biased AC electrospinning of aligned polymer nanofibers. *Macromolecular Rapid Communications*, *28*(9), 1034–1039. https://doi.org/10.1002/marc.200700053

Sekine, Y., Motokawa, R., Kozai, N., Ohnuki, T., Matsumura, D., Tsuji, T., … Akiyoshi, K. (2017). Calcium-deficient Hydroxyapatite as a Potential Sorbent for Strontium. *Scientific Reports*, *7*(1), 2064. https://doi.org/10.1038/s41598-017-02269-z

Semmens, M. J., & Martin, W. P. (1988). The influence of pretreatment on the capacity and selectivity of clinoptilolite for metal ions. *Water Research*, *22*(5), 537–542. https://doi.org/10.1016/0043-1354(88)90052-8

Shen, W., Chen, S., Shi, S., Li, X., Zhang, X., Hu, W., & Wang, H. (2009). Adsorption of Cu (II) and Pb (II) onto diethylenetriamine-bacterial cellulose. *Carbohydrate Polymers*, *75*(1), 110–114. https://doi.org/10.1016/j.carbpol.2008.07.006

Sigmund, W., Yuh, J., Park, H., Maneeratana, V., Pyrgiotakis, G., Daga, A., … Nino, J. C. (2006). Processing and structure relationships in electrospinning of ceramic fiber systems. *Journal of the American Ceramic Society*, *89*(2), 395–407. https://doi.org/10.1111/j.1551-2916.2005.00807.x

Smičiklas, I. ., Milonjić, S. ., Pfendt, P., & Raičević, S. (2000). The point of zero charge and sorption of cadmium (II) and strontium (II) ions on synthetic hydroxyapatite. *Separation and Purification Technology*, *18*(3), 185–194. https://doi.org/10.1016/S1383-5866(99)00066-0

Sokkar, H. H., Abdel-Halim, E. S., Aly, A. S., & Hashem, A. (2004). Cellulosic fabric wastes grafted with DMAEMA for removal of direct dyes. *Adsorption Science and Technology*, *22*, 679–691.

Sousa, J. C. G., Ribeiro, A. R., Barbosa, M. O., Pereira, M. F. R., & Silva, A. M. T. (2018). A review on environmental monitoring of water organic pollutants identified by EU guidelines. *Journal of Hazardous Materials*, *344*, 146–162. https://doi.org/10.1016/J.JHAZMAT.2017.09.058

Srinivasan, A., & Viraraghavan, T. (2014). Oil removal in a biosorption column using immobilized M. rouxii biomass. *Desalination and Water Treatment*, *52*(16–18), 3085–3095.

Srivastava, S. K., Tyagi, R., Pant, N., & Pal, N. (1989). Studies on the removal of some toxic metal ions. Part II (removal of lead and cadmium by montmorillonite and kaolinite). *Environmental Technology Letters*, *10*(3), 275–282. https://doi.org/10.1080/09593338909384742

Taha, A. A., El-Mahmoudi, A. S., & El-Haddad, I. M. (2004). Pollution sources and related environmental impacts in the new communities southeast Nile delta, Egypt. *Emirates Journal for Engineering Research*, *9*(1), 35–49.

Tchounwou, P. B., Yedjou, C. G., Patlolla, A. K., & Sutton, D. J. (2012). Heavy

metal toxicity and the environment. *EXS*, *101*, 133–164. https://doi.org/10.1007/978-3-7643-8340-4_6

Teo, W.-E., Inai, R., & Ramakrishna, S. (2011). Technological advances in electrospinning of nanofibers. *Science and Technology of Advanced Materials*, *12*(1), 13002.

Tian, Y., Wu, M., Liu, R., Li, Y., Wang, D., Tan, J., Huang, Y. (2011). Electrospun membrane of cellulose acetate for heavy metal ion adsorption in water treatment. *Carbohydrate Polymers*, *83*(2), 743–748. https://doi.org/10.1016/j.carbpol.2010.08.054

Tseng, A. A., Notargiacomo, A., & Chen, T. P. (2005). Nanofabrication by scanning probe microscope lithography: A review. *Journal of Vacuum Science & Technology B: Microelectronics and Nanometer Structures*, *23*(3), 877. https://doi.org/10.1116/1.1926293

Viraraghavan, T., & Kapoor, A. (1994). Adsorption of mercury from wastewater by bentonite. *Applied Clay Science*, *9*(1), 31–49. https://doi.org/10.1016/0169-1317(94)90013-2

Wan, Y. Z., Huang, Y., Yuan, C. D., Raman, S., Zhu, Y., Jiang, H. J., … Gao, C. (2007). Biomimetic synthesis of hydroxyapatite / bacterial cellulose nanocomposites for biomedical applications. *Materials Science and Engineering C*, *27*, 855–864. https://doi.org/10.1016/j.msec.2006.10.002

Wang, L. K., Vaccari, D. A., Li, Y., & Shammas, N. K. (2005). Chemical Precipitation. In *Physicochemical Treatment Processes* (pp. 141–197). Totowa, NJ: Humana Press. https://doi.org/10.1385/1-59259-820-x:141

Wang, P., Li, C., Gong, H., Jiang, X., Wang, H., & Li, K. (2010). Effects of synthesis conditions on the morphology of hydroxyapatite nanoparticles produced by wet chemical process. *Powder Technology*, *203*(2), 315–321. https://doi.org/10.1016/J.POWTEC.2010.05.023

Warner, S., & Buer, A. (2001). A fundamental investigation of the formation and properties of electrospun fibers. *Materials Science*, *7*(M98-D01), 1–9.

Yeo, L. Y., Gagnon, Z., & Chang, H.-C. (2005). AC electrospray biomaterials synthesis. *Biomaterials*, *26*(31), 6122–6128. https://doi.org/10.1016/J.BIOMATERIALS.2005.03.033

Yusoff, Y. M., Salimi, M. N. A., & Anuar, A. (2015). Preparation of hydroxyapatite nanoparticles by sol-gel method with optimum processing parameters. In *AIP Conference Proceedings* (Vol. 1660, p. 070054). AIP Publishing LLC. https://doi.org/10.1063/1.4915772

Zhang, L., Ruan, D., & Gao, S. (2002). Dissolution and Regeneration of Cellulose in NaOH / Thiourea Aqueous Solution. *Journal of Polymer Science:*, *40*(14), 1521–1529. https://doi.org/10.1002/polb.10215

Zhang, Z., Li, M., Chen, W., Zhu, S., Liu, N., & Zhu, L. (2010). Immobilization of lead and cadmium from aqueous solution and contaminated sediment using nano-hydroxyapatite. *Environmental Pollution*, *158*(2), 514–519. https://doi.org/10.1016/j.envpol.2009.08.024

Zhou, D., Zhang, L., Zhou, J., & Guo, S. (2004). Cellulose/chitin beads for adsorption of heavy metals in aqueous solution. *Water Research*, *38*(11), 2643–2650. https://doi.org/10.1016/j.watres.2004.03.026